

# LA-UR-22-23925

Approved for public release; distribution is unlimited.

**Title:** LightSlingers

**Author(s):** Schmidt, Andrea Caroline  
Singleton, John  
Warner, Justin Bradley

**Intended for:** R&D100 Award entry documentation/brochure

**Issued:** 2022-04-27



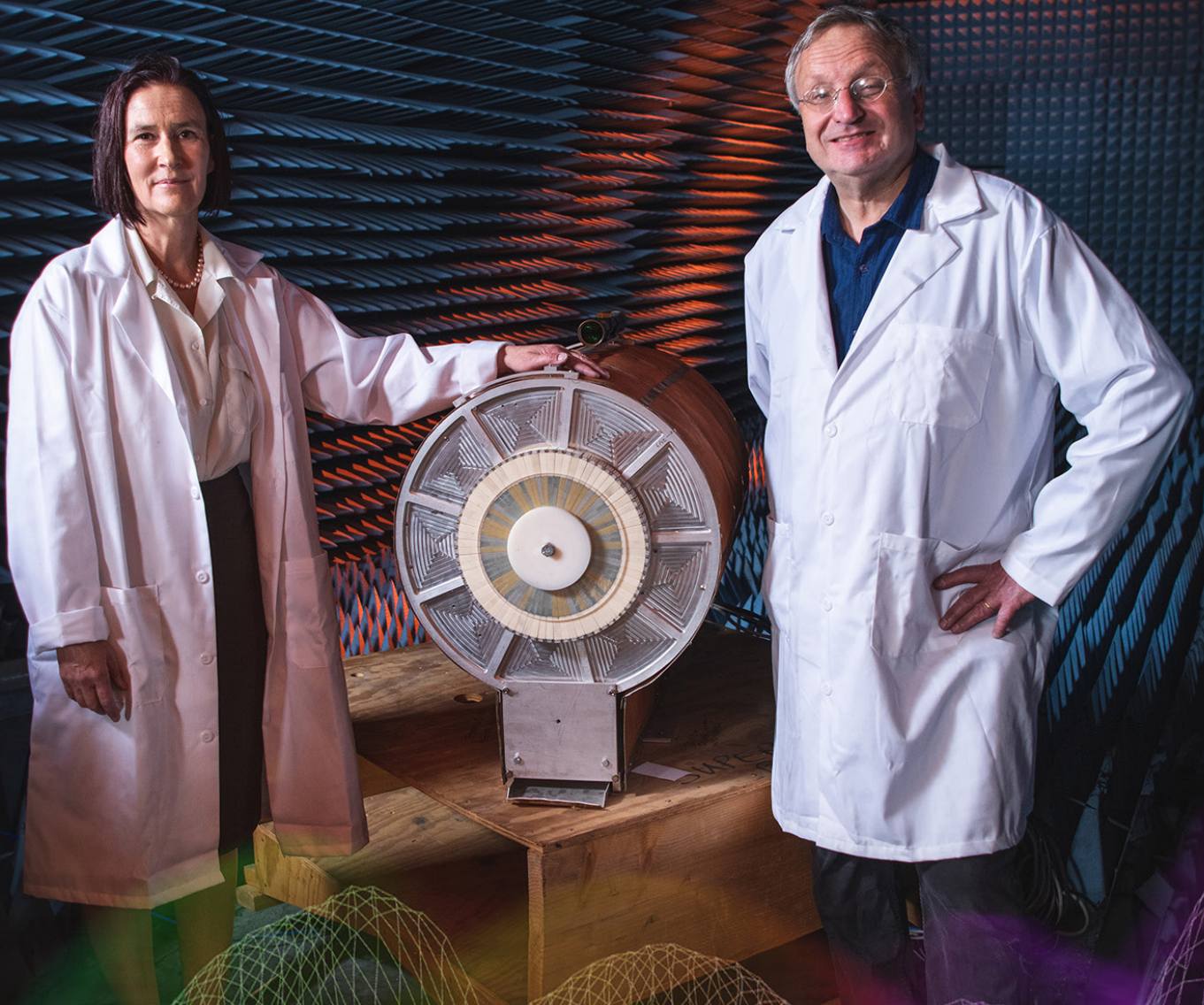
Los Alamos National Laboratory, an affirmative action/equal opportunity employer, is operated by Triad National Security, LLC for the National Nuclear Security Administration of U.S. Department of Energy under contract 89233218CNA000001. By approving this article, the publisher recognizes that the U.S. Government retains nonexclusive, royalty-free license to publish or reproduce the published form of this contribution, or to allow others to do so, for U.S. Government purposes. Los Alamos National Laboratory requests that the publisher identify this article as work performed under the auspices of the U.S. Department of Energy. Los Alamos National Laboratory strongly supports academic freedom and a researcher's right to publish; as an institution, however, the Laboratory does not endorse the viewpoint of a publication or guarantee its technical correctness.



2022 R&D 100 ENTRY

# Light*Slingers*

Antennas that generate radio waves  
from faster-than-light currents



☞ Deliver information in tightly focused wave packets to specific locations

☞ Consist of only five readily sourced components, compared to 200+ on competing antennas

☞ Can be shaped into optimized forms; conformable to surfaces; scalable

☞ Wide bandwidth from a single antenna; greater efficiency



**Los Alamos**  
NATIONAL LABORATORY



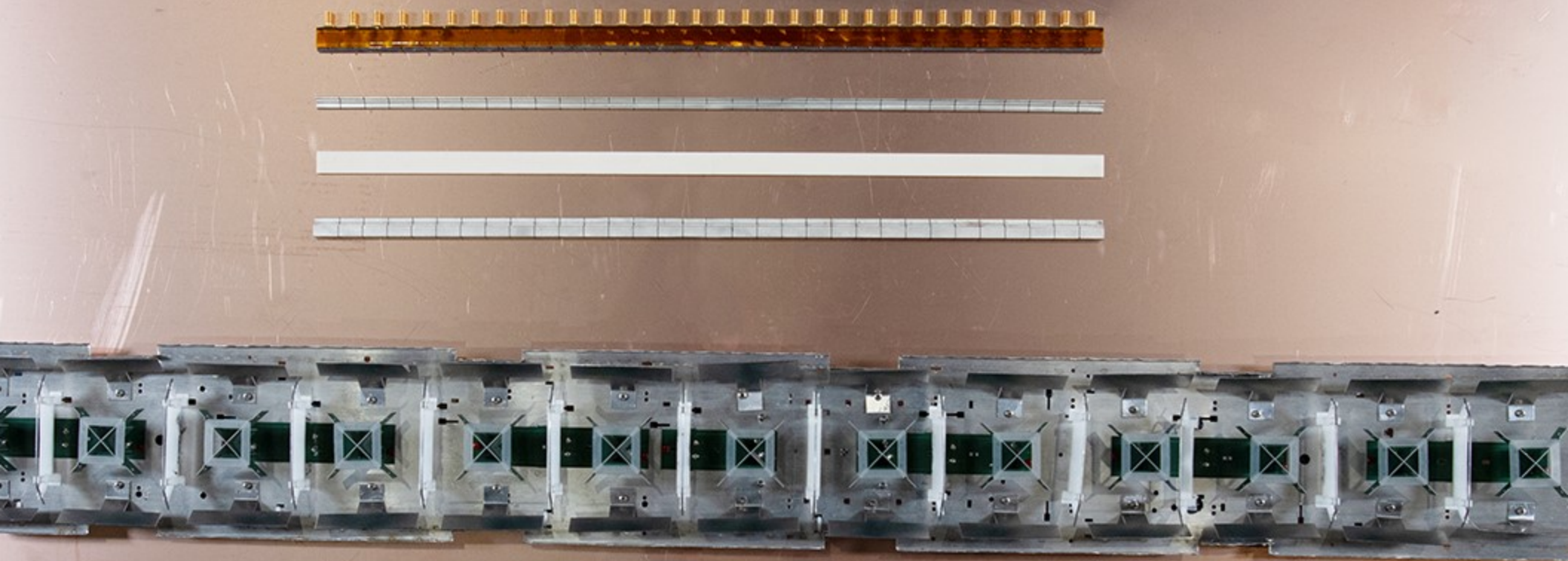


**Photo 2: Disassembled LightSlinger (above) compared with a traditional base station array (below)**





Photo 3: Two original prototype LightSlingers

## 2022 R&D 100 Awards

### **LightSlingers: Focusing information using faster-than-light sources of electromagnetic radiation.**

LA-UR-22-

#### **Category(ies)**

- |   |  |
|---|--|
| <input type="checkbox"/> Analytical/Test          | <input type="checkbox"/> Special recognition: Corporate Social Responsibility        |
| <input checked="" type="checkbox"/> IT/Electrical | <input type="checkbox"/> Special recognition: Green Tech                             |
| <input type="checkbox"/> Mechanical/Materials     | <input checked="" type="checkbox"/> Special recognition: Market Disruptor - Products |
| <input type="checkbox"/> Process/Prototyping      | <input type="checkbox"/> Special recognition: Market Disruptor - Services            |
| <input type="checkbox"/> Software/Services        |  |
| <input type="checkbox"/> Other                    |  |

#### **Name of primary submitting organization**

Los Alamos National Laboratory

#### **Product/Service Brand Name**

LightSlingers

#### **Was the product/service introduced to the market between January 1, 2021, and March 31, 2022?**

☒ Yes

☐ No

#### **If your submission is subject to regulatory approval, has the product been approved?**

☐ Yes

☐ No - *If no, the product is disqualified.*

☒ Not applicable to this product

#### **Price of Product/Service (U.S. dollars)**

One of the strengths of LightSlinger technology is that once a production line is established, each antenna could be manufactured individually in response to a bespoke specification at about the cost that an equivalent mass-produced system would incur. A prototype LightSlinger array, consisting of three identical linear LightSlingers, has already been created for a directed energy/information focusing demonstration. With this work completed, conventional industrial/economic considerations suggest that a similar mass-produced product would be approximately \$1000.

**Product Description**

LightSlingers are a novel type of directional broadband antenna capable of “slinging” tightly focused wave packets with precision toward a target location. Unlike conventional antennas, they use polarization currents, animated to faster-than-light speeds, as their emission mechanism. Sturdy, small, and versatile, they have the potential to disrupt the telecommunications market.

**Indicate the Type of Institution you Represent**

Government Laboratory

**Submitter’s Relation to Entered Product/Service**

Product Developer

**Product Photos**

Photo 1 – Cover

Photo 2 – LightSlinger/Traditional Base Array comparison

Photo 3 – Two original prototype LightSlingers

**Video Files**

## What does the product or technology do?

*“The wireless music box has no imaginable commercial value. Who would pay for a message sent to no one in particular?” -1921 (responding to calls to invest in radio)<sup>1</sup>*

In the century since this less-than-prescient prediction, the world has witnessed an explosion of broadcasting technology. Electromagnetic waves permeate the air around us and nearly every aspect of communication depends on reliable and secure signal propagation with high throughput, large capacity, and broad coverage [1]. Technologies developed for early radios still underpin modern antennas: an electric current flows along the surfaces of metal components to create electromagnetic waves that then dart across the sky [2]. The same fundamental principles have carried antenna technology through four generations of wireless technology, but as the *fifth* generation (5G) stumbles haltingly onto the market—promising to connect virtually everyone and everything—a new paradigm is needed.

In the early days of radio, the airwaves’ capacity for carrying signals probably seemed limitless; a family with an icebox could hardly imagine wifi-connected refrigerators. However, the proliferation of wireless devices has created a tsunami of data streams, driven by a seemingly endless demand for connectivity, that now threatens to overwhelm existing and near-future wireless infrastructure. The telecommunications industry acknowledges that it has for decades been overly cautious in applying inventive technologies, resulting in the current mad scramble to deploy novel multi-antenna systems that can sufficiently enhance network performance [1]. Other organizations have their own concerns. The Federal Aviation Administration (FAA) has warned that 5G frequencies could interfere with critical systems such as radio altimeters. At the same time, recent events have exposed supply chain dependencies that could limit the availability of complex electronics manufactured overseas. Nevertheless, devices hungry for bandwidth continue to multiply and it has become clear that sustaining this demand will require antennas with higher throughput, improved security, and greater ease of manufacture from locally sourced components.

---

<sup>1</sup> This quotation is attributed to un-named business associates of David Sarnoff; it was Sarnoff who relayed the quotation to the wider world. See Kovarik, Bill (2015). *Revolutions in Communication: Media History from Gutenberg to the Digital Age*. Bloomsbury Publishing. p. 314. ISBN 9781441185501.



Scientists at Los Alamos National Laboratory have developed a new type of directional broadband antenna (Figure 1) that promises to transform current methods. Known as “LightSlingers,” the technology creates a transmissible signal in an



**Figure 1.** Prototype LightSlinger under test. Photo credit: LANL

entirely new way. Instead of using a surface current of free electrons to emit electromagnetic waves, as do traditional antennas [3], LightSlingers generate them using faster-than-light *polarization currents*. Precisely timed to achieve a focusing effect akin to a sonic boom, they “sling” electromagnetic wave-packets carrying data with precision toward a location of choice. This approach grants unparalleled flexibility and confers multiple advantages over traditional wireless technologies—all while remaining backwards compatible and adaptable to commercially available couplers, feeders, and tuners:

### **Customization**

LightSlingers are 3D printable, conformable to unusual surfaces, such as the body of a vehicle, aircraft, ship, or satellite, and they can be molded into any shape without loss of performance. They can be made in bespoke forms optimized for particular applications.



**Figure 2.** (left) Researchers comparing the size of a LightSlinger antenna with a traditional base array. Both antennas operate at a similar frequency. (right) The four main, monolithic components of a LightSlinger prior to assembly. Base station antennas are typically assembled from over 200 components. Photo credit: LANL

### **Ease of construction**

A LightSlinger has just five components that can be assembled robotically: two copper-plated monolithic pieces of composite or 3D-printed plastic, one strip of alumina and an input plug, all bonded to a single circuit board. LightSlingers represent a return to simplicity in antenna manufacturing using *locally sourced components*. In contrast to other modern competitors, LightSlingers are not delicate and complex, they do not require hundreds of tiny components, and they do not need to be assembled by hand in specialized factories overseas. This ease of manufacture is important in defense applications. For example, damage control on a ship could quickly print a new antenna to replace one that was just destroyed.



## Directionality

In future incarnations of 5G and looking ahead to 6G, information must be transmitted in tightly focused beams that target precise locations (such as a room) instead of spreading data all over the neighborhood. LightSlingers achieve tightly focused beams and directionality with minimal footprint. A LightSlinger antenna the size of a paperback book could beam rapid sequences of focused signals at the same frequency to many different targets simultaneously within a local area network (Figure 3). This means it is ideally suited to exploit the underutilized, short-range millimeter wave frequency bands historically reserved for satellites and radar. These bands see little traffic due to the poor building penetration, poor performance during humid weather, and the limited range of short millimeter radio waves [4] —problems networked directional LightSlingers could overcome.

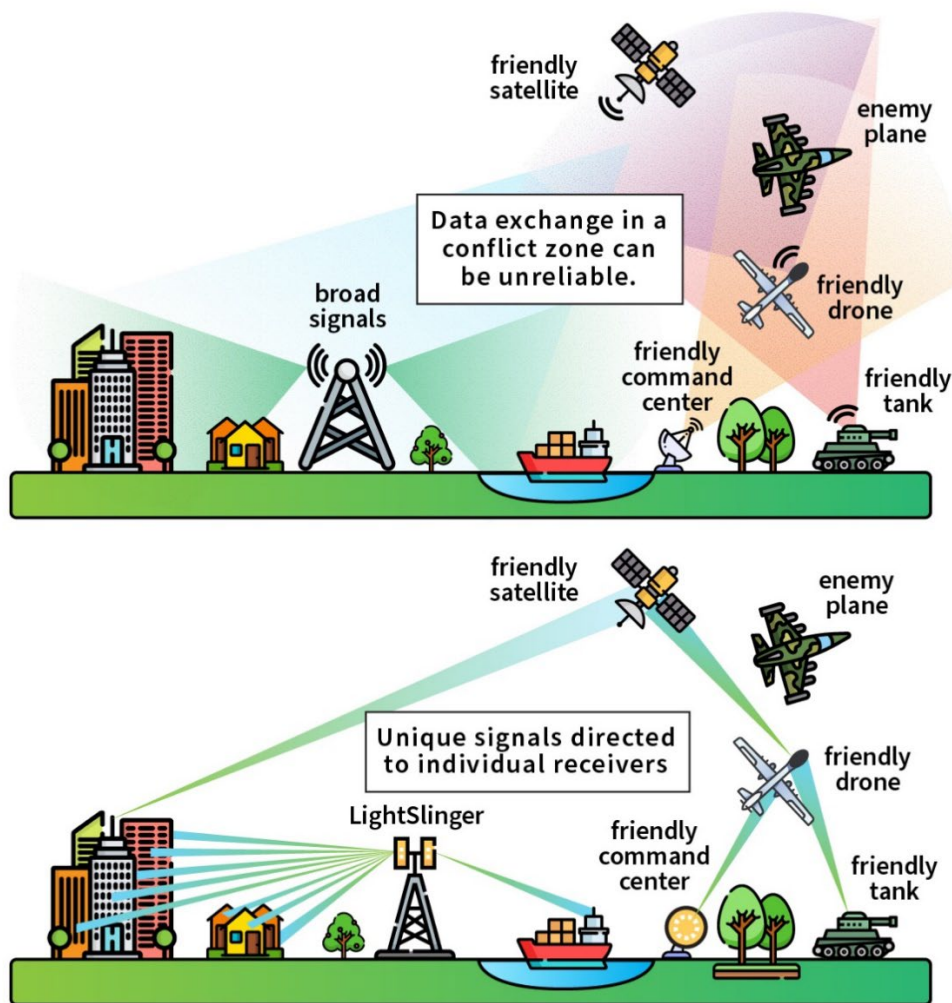


**Figure 3.** Contrast between broadly spread signals using current technology (upper) and precisely targeted information using LightSlingers in 5G and warfighter applications (lower).

## Security

As the variety of wifi-enabled devices has multiplied, so has the number of nefarious actors attempting to intercept private signals. Unlike a traditional broadcast, only the main beam from a LightSlinger contains a decipherable signal; the stray signals are so weak or scrambled as to be difficult to decipher. This capability is a critical security advantage over traditional antennas.

## Bandwidth

The Federal Communications Commission (FCC) has opened new frequency bands to address cluttered airwaves. However, to use the new frequency bands, the mobile communication industry must add new antennas to existing sites, because existing antennas can only transmit in the specific bands for which they were designed. Unfortunately, space is limited on base station sites and mobile platforms, and it is not always easy to achieve peaceful coexistence between old and new antennas on an established platform. LightSlingers solve this problem because they are intrinsically broadband, and once established, can easily take advantage of any new channels while continuing to serve existing ones.

## Efficiency

In contrast to traditional antennas, the signal from a LightSlinger is produced by a current that occupies the whole active volume of the antenna (Figure 4, top). Consequently, LightSlingers produce several percent more emitted power than a phased array (a grouping of traditional antennas networked to function as one) of the same length under the same excitation. Moreover, LightSlingers emit only “outward,” as opposed to the elements in a phased array, which also radiate backward into the antenna assembly, reducing efficiency.

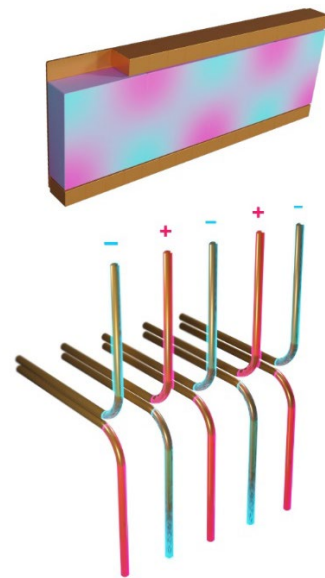


**Figure 4.** In a LightSlinger, (top) the current fills the whole volume of the dielectric. By contrast, in a conventional array made up of dipoles (bottom), the current is only present on the surfaces of metal components.

## Multiple input/multiple output (MIMO) applications

Curved (i.e., circular, spiral, or helical) LightSlingers are uniquely positioned to exploit experimental concepts that would significantly enhance the capacity of data transmission between antennas. The most efficient—and, frankly, easiest—way to save bandwidth is to establish separate data streams using the same frequency band. This process is known as MIMO

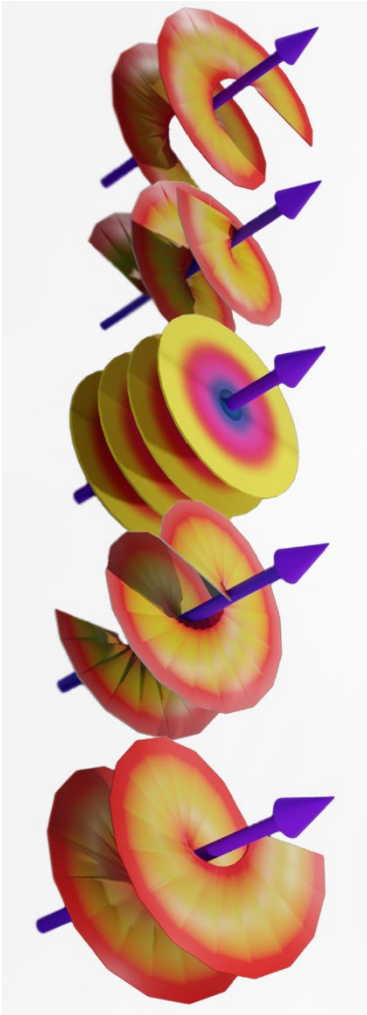


**Figure 5.** Phase fronts of five different OAM signals. A receiving antenna can be tuned to accept just one of these states and reject all of the others, allowing many different signals to be transmitted using the same wavelength.

(multiple input/multiple output) and, traditionally, requires multiple antennas emitting at the same frequency into different directions. Due to their unique emission mechanism, LightSlingers are capable of radiating helical-mode radio beams—wavefronts that are a helix—instead of typical radio waves. This allows us to take advantage of the waves' orbital angular momentum (OAM) to achieve MIMO, an approach that confers key advantages, the nuts and bolts of which are explained below.

Imagine the OAM radio beams as metal bolts and the receiving antennas as metal nuts. To get the nut (antenna) to accept the bolt (radio beam), they both require the same thread direction and thread spacing. OAM antennas throw various bolts (beams with signals) with differing thread spacings and direction at a cluster of nuts (receiving antennas) with different thread spacings and thread directions. Each nut will accept (receive) the corresponding thread (beam) and no other. Thus, a transmitting antenna can send many signals all at once, and the receiving antenna only picks up the signal to which it is tuned. Future circular LightSlingers could generate OAM-type signals with a wide variety of novel phase fronts, some of which go beyond the simple concept described above.

LightSlingers also have potential applications in countermeasure-resistant radar. With conventional radar, an aircraft that is being imaged can potentially destroy the radar installation by sending a missile on a course perpendicular to the phase fronts. Similarly, an aircraft can send back a synthesized rogue signal suggesting a reflection from elsewhere. LightSlingers can produce phase fronts that are sufficiently complex to defeat an aircraft's attempts to locate the source of the signal. Moreover, the complexity of the phase fronts makes it almost impossible to synthesize a rogue reflection. Radar using LightSlinger technology, on the other hand, has no such drawback. A LightSlinger antenna coupled with a timing system is sufficient for radar operators to locate an aircraft, given knowledge of the LightSlinger's speed and modulation pattern. As of yet, there is no commercial equivalent.

Worldwide information communication technology market spending is expected to reach \$5.8 trillion in 2023. The vast majority of humans own a smartphone, connected in a vast network of over six billion devices. The devices within these vibrant technological ecosystems depend on a constantly evolving telecommunications infrastructure that can adapt to meet the world's exponentially growing appetite for data and speed. Obviously, investment in traditional antennas has so far been well-rewarded. Still,

diminishing returns on investment and the intrinsic limitations of traditional antennas' surface current emission mechanism all but guarantee that a new technology will soon supplant the current paradigm and reap the benefits of sustained investment and optimization.

#### **Theoretical Directed Energy Applications**

LightSlinger technology has also demonstrable advantages in directed-energy applications as a ranged weapon that disrupts electronic components in hostile vehicles and incoming missiles. LightSlingers could theoretically create sufficiently focused bursts of electromagnetic waves in a particular location, without causing damage outside the target area.

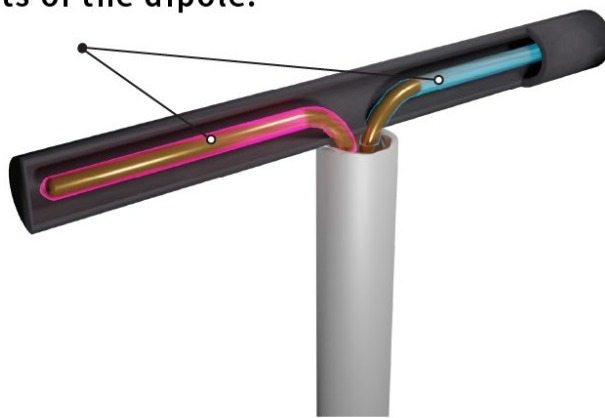
Unlike the "wireless music box" a century ago, LightSlingers' commercial value should be immediately apparent to those following the industry. Demands for bandwidth continue to skyrocket and new antenna technology is essential to realize futuristic 3D online environments such as the buzzy "metaverse." Wireless communication is a high-stakes game; whoever will build the smallest, most versatile, energy- and cost-efficient antenna will win. LightSlinger technology is setting the bar for this competition. But beyond commercial value, we believe this

five-component, secure, efficient, high-throughput antenna can help bridge the digital divide between those with access to wireless infrastructure and those without. Cheap, durable, and easy-to-manufacture antennas can grant internet access to people in developing areas who live outside the bounds of traditional wireless infrastructure. Internet is a utility that should be available to everyone. That is our loftiest hope for this technology—that LightSlingers' signal reaches everyone specifically, as well as no one in particular.

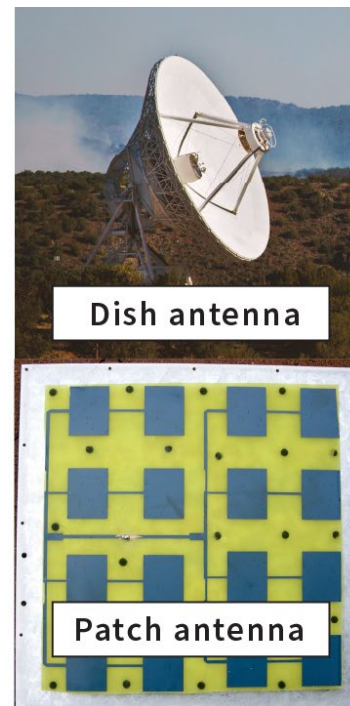
## How does the product operate? Describe the mechanism of action, theories, materials, composition, or construction.

To fully appreciate LightSlingers, we first need to understand how a traditional antenna works. Just as waves are created in water by wiggling something back and forth, an antenna creates electromagnetic waves by wiggling electrons back and forth along a conductive metal surface (Figure 6). This motion of electrons radiates invisible electromagnetic waves that travel at the speed of light until they arrive at a different, receiving antenna, disturbing that antenna's carefully arranged electrons. These electrons move, like a docked boat rising and falling with the incoming waves. Receiving equipment then translates and amplifies this signal so it can become your favorite song on the radio. The key concept to remember is that the wiggling electrons compose a *surface current* that emits the signal.

Current flows only on the surface of the metal parts of the dipole.



Dipole antenna



Dish antenna

Patch antenna

**Figure 6.** *Dipole antennas* were the most widely used class of antenna in the early days of radio and over-the-air television. They are still used as the elements in certain types of phased array and in Bluetooth systems. *Dish antennas* leverage their size and shape to transmit or receive signals in/from a particular direction. *Patch antennas* are commonly used for transmitting shorter wavelengths. Variants are used in mobile phones. Photo credit: LANL



In LightSlingers, the waves are created by an entirely different kind of current called the *polarization current* that occupies a significant fraction of the antenna's volume. This polarization current, first described in the 19<sup>th</sup> century, offers multiple advantages over surface current emission, and it has not been practically exploited as the primary emission mechanism of antennas until now. To see how the polarization current works, let's look at a prototype LightSlinger.

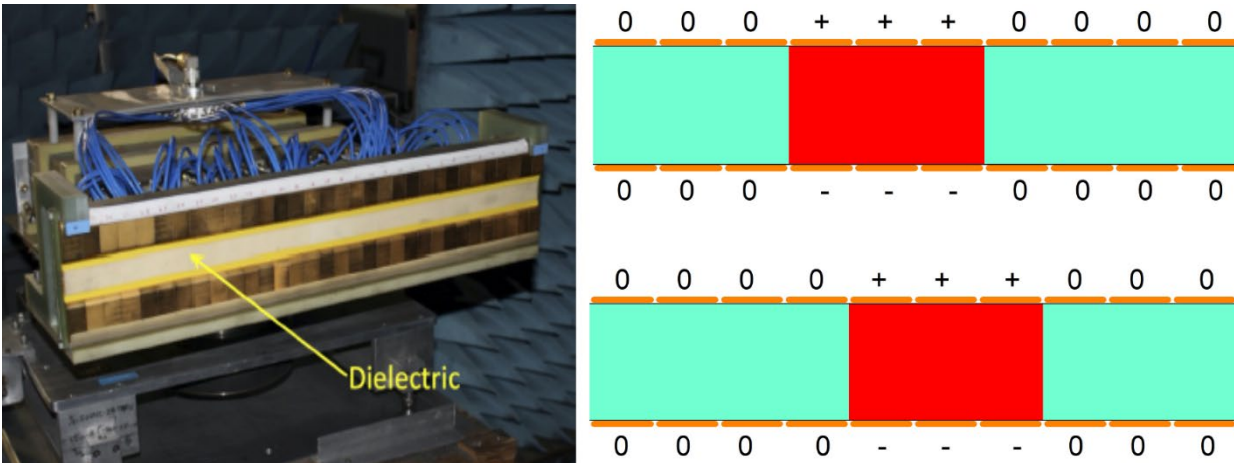


**Figure 7** (left) Front view of a prototype LightSlinger. (right) Simplified side view of a LightSlinger, showing metal electrodes (orange) above and below a strip of dielectric (light blue). “0” indicates that there is no voltage on that particular electrode; the symbols + and - indicate that a voltage is applied between those electrodes, polarizing the dielectric in between (red). By switching the voltages on the electrodes on and off, the polarized region can be made to move along the dielectric.

LightSlingers consist of an insulating material or *dielectric* (Figure 7, left) sandwiched between pairs of copper electrodes. When an electrode pair is turned on, it applies an electric field to a portion of the dielectric so that the negative and positive charges within move small distances in opposite directions, creating electrical polarization. If an adjacent electrode pair is turned on and the first switched off, the polarization moves (Figure 7, right, Figure 8). Using suitably accurate timing, the polarization can be made to move much faster than the speed of light, and in doing so emits tightly focused packets of electromagnetic radiation—the signal. The effect may sound like an exotic, laws-of-physics-breaking

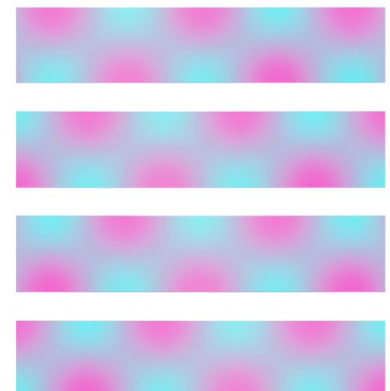


**Figure 8.** Snapshots at different times of the current moving from left to right in a LightSlinger

phenomenon, but in fact, only the disturbance moves very fast; the particles creating it are displaced only by tiny distances. The carefully timed polarization, or *metachronal pattern*, creates the signal, instead of the surface current used in a traditional antenna.

Another example of a metachronal pattern is the “stadium wave” that causes so many spilled drinks in crowded bleacher seats. Imagine that the stadium represents the dielectric and the fans and their seats represent positive and negative charges. Standing creates polarization whereas sitting represents none. When the fans stand in quick succession with precise timing, they create a fast-moving “wave” that travels around the stadium, far outpacing the movements of any one individual. In the same way, LightSlingers use carefully timed voltages applied to the electrode pairs to create faster-than light (or *superluminal*) polarization current (Figures 7 and 8). The current can be superluminal without breaking the laws of physics because it has no mass—it is just a pattern. As predicted by pioneering scientist James Maxwell in the 19th century, the moving polarization current emits electromagnetic waves just like a current of free electrons. However, unlike electrons, which are limited to subluminal speeds, a polarization current can be made to travel arbitrarily fast. Just like a supersonic airplane, a superluminal polarization current outpaces the waves that it emits (once emitted, radio waves can of course only travel at the speed of light). This capability is a key innovation of LightSlingers, and it opens up a wide vista of possible applications.



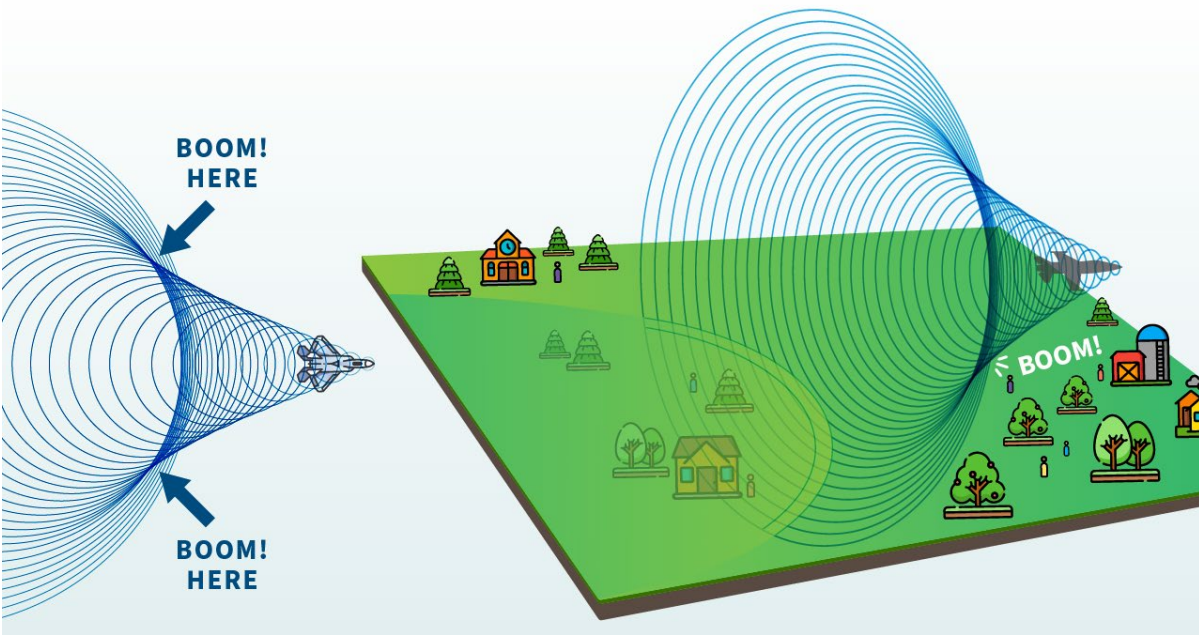


**Figure 9.** Representations of an accelerating supersonic jet creating sonic booms. The jet overtakes the waves that it emits so that they pile up to produce a localized boom.

One of the unique advantages of a source that outdistances the waves that it emits is the ability to focus the signal by leveraging an effect known in acoustics as the “sonic boom.” A sonic boom occurs when an aircraft accelerates through the sound barrier, traveling faster than the sound it produces. Sound waves that normally would turn up sequentially instead intersect (Figure 9), in essence arriving at the awe-struck observer all at once. LightSlingers achieve an analogous effect with electromagnetic waves (silently, of course). In LightSlingers, the polarization current is the “jet,” this time traveling faster than the emitted *light* waves. In this way, a LightSlinger concentrates the transmitted signal at the intended reception point; elsewhere it is weak.

With traditional antennas, shape and size determines the properties of the wave—for example tiny patches are used for high frequency cell phone signals, and large dishes are set up in the desert to capture low frequency signals from distant space phenomenon. The relationship between intended wavelength and antenna size has always influenced antenna design, but LightSlingers’ unique radiation mechanism means that designers have more freedom to innovate. Antenna size does not need to exactly correspond to wavelength, like with a traditional antenna. LightSlingers can be made in a variety of shapes and configurations, each uniquely optimized for

a particular task. Changing any one of the design parameters will—subtly or radically—alter the character of the emitted radiation. For instance,

- the speed of the polarization current sends the central lobe of the radiation in the desired direction;
- its acceleration focuses the radiation, “slinging” it towards a target;
- the dielectric shape accounts for the beam width, height of the side lobes, and the position of nulls (the direction in which no signal is emitted or detected)
- the dielectric constant (the ability of the solid to store electric energy) determines the optimal frequency band of operation.

For further details of operation, see the journal article published in *Physical Review Applied*, “Information Carried by Electromagnetic Radiation Launched from Accelerated Polarization Currents” and press materials from 2021-2022 presented in the appendix.

## Antenna Comparison Matrix

Initially, LightSlingers were developed as fundamental science models of violent astronomical phenomena. However, it was soon realized that they have the potential to be more efficient and more flexible than conventional phased arrays of a similar size. Cellular base-station antennas (BSAs) are perhaps the simplest and cheapest phased arrays available, and so are used for this comparison. The two BSAs in the table above were selected because they are widely deployed.

Parameter	LightSlinger	CommScope HBX-6516DS-VTM   2-port sector antenna, 2x 1710–2180 MHz, 65°	Huawei A26451500v06 Single-band Antenna, 1710-2690MHz
Number of components required for assembly	5	198 components made from a wide spectrum of materials including copper, aluminum, steel, polyethylene, and 35 circuit boards alone.	~200 components, presenting in numerous forms: wires, plates, coaxial cables, bent and stamped metal parts, screws (66), etc. Similar to CommScope antenna.
Comments: LightSlingers' primary competitors require the hand-assembly of hundreds of components by unskilled labor in specialized factories in China and elsewhere outside the US (this is true even for US-designed examples). By contrast, LightSlingers can be made from two copper-plated monolithic pieces of composite or 3D-printed plastic, plus a piece of alumina. At the end of a traditional antenna's useful life, the hundreds of components, made from diverse materials, make it very labor intensive to recycle. However, the very small number of components in a LightSlinger makes it easy to dismantle for recycling. The metallic plating may be chemically stripped for reuse of metals such as gold and copper. Alumina is increasingly being recycled using remelting in a furnace. From a sustainability standpoint, the composite that we use, G10, is a versatile material that provides tangible advantages over conventional materials such as aluminum, and steel; its production uses less energy, resulting in fewer carbon emissions. It has high mechanical strength, impact resistant, is chemical, fire and corrosion resistant, and a good thermal and electrical insulator. Though little recycled previously, used G10 is now being converted via pyrolysis to synthgas for resins or other hydrocarbons, with solid byproducts of pyrolysis being ground into reinforcement for low-carbon concrete.			

## Antenna Comparison Matrix (continued)

Parameter	LightSlinger	CommScope HBX-6516DS-VTM   2-port sector antenna, 2x 1710–2180 MHz, 65°	Huawei A26451500v06 Single-band Antenna, 1710-2690MHz
Bandwidth	> 0.9 GHz to 4.5 GHz	1.71 GHz to 2.18 GHz	1.71 GHz to 2.69 GHz
<p>Comments: The greater the bandwidth, the greater the capacity to transmit information. Phased arrays are limited by the spacing of the individual antennas that make up the array, which is usually about half the wavelength of the emitted radiation. To achieve broadband coverage, the current industrial state-of-the-art is to incorporate multiple phased arrays, each optimized to a particular frequency band within the same antenna assembly, leading to additional cost and complexity. LightSlingers have no such limitation: the 0.9-4.5 GHz range is based on published data (2020) for a linear LightSlinger; the upper limit of the measurement was constrained by the receiving equipment and not the LightSlinger itself. Hence, a single LightSlinger could replace a collection of phased arrays in broadband transmission. As an illustration of the contrasts in bandwidth, we have deliberately chosen a single-band antenna by CommScope for comparison. The Huawei example has more than one phased array to achieve greater coverage.</p>			
Information focusing ability	Yes	No currently known competitor	No currently known competitor
<p>Comments: An information focusing ability provides better security and less potential for interference with other signals. In most conventional antenna, selectivity of reception is achieved through the use of narrow frequency bands. In place of this, a LightSlinger employs a spread of frequencies to transmit information to a particular location; the signal is weaker and has a scrambled time dependence elsewhere. There is currently no commercial competitor capable of this application.</p>			
Variable Geometry	Yes	No known competitor	No known competitor
<p>LightSlingers can be optimized to emit a desired radiation pattern by changing the topology and material of the dielectric. Since dielectrics are easy to cut, shape or cast, novel topologies can be created using varied materials and topological optimization methods. These approaches have, so far, hardly been pursued in antenna design, primarily due to the challenges associated with the fabrication of inhomogeneous materials, limited access to analysis tools and, in traditional antennas, the almost complete absence of a topology to be optimized. There are no commercial competitors in this application.</p>			

## Antenna Comparison Matrix (continued)

Parameter	LightSlinger	CommScope HBX-6516DS-VTM   2-port sector antenna, 2x 1710–2180 MHz, 65°	Huawei A26451500v06 Single-band Antenna, 1710-2690MHz
<b>Suitable for multiple input/multiple output</b>	Yes, Experimental demonstration and simulations	No, Experimental reports of limited commercial applicability	No, Experimental reports of limited commercial applicability
Comments: Multiple input/multiple output (MIMO- see page 7) has aroused a widespread interest in telecommunications for its potential for unleashing new capacity in the severely congested spectrum of commercial communication systems.			
<b>Efficiency</b>	c.1020 percent higher	Standard	Standard
Comments: Under the same excitation, the LightSlinger produced approximately 120 percent more emitted power than a phased array of the same length, mainly because of the confining effect of the dielectric and the fact that the LightSlinger emits only “forward” (as opposed to the elements in a phased array, which also radiate backward into the antenna assembly, reducing efficiency). (see <i>Launching information from faster-than-light polarization currents</i> , Singleton, J.; Schmidt, A.C. Research Features, 138, 38 (2021))			
<b>Countermeasure-resistant radar</b>	Yes	No	No
Comments: LightSlingers can produce phase fronts that are sufficiently complex to defeat aircrafts’ attempts to locate the source of the signal. Moreover, the complexity of the phase fronts makes it almost impossible to synthesize a rogue reflection. (see page 7)			

## **Describe how your product/service improves upon competitive products or technologies.**

### **Number of components**

LightSlingers have simplicity and robustness advantages over equivalent conventional antennas. They are made from a handful of monolithic components, compared to ~200 fragile and diverse components used in commercial antennas (Figure 2). Fewer components means greater ease of manufacture and assembly, as well as additional durability.

### **Bandwidth**

The greater the bandwidth, the greater the capacity to transmit information. Phased arrays are limited by the spacing of the individual antennas (e.g., dipoles) that make up the array, which is usually about half the wavelength of the emitted radiation. This constrains the bandwidth, as can be seen from the frequency ranges of Competitors A and B. By contrast, LightSlingers use a continuous distribution of polarization current to emit radiation (Figure 7). Thus, a LightSlinger has no equivalent of the “individual antennas” that make up the phased array, so that there is much less of a bandwidth limitation. The 0.9-4.5 GHz range is based on published experimental data (2020) for a linear LightSlinger; the upper limit of the measurement was constrained by the receiving equipment and NOT the LightSlinger itself.

### **Information focusing ability**

The continuously moving volume-distributed polarization current imparts advantages over phased arrays in niche applications such as secure communications. For example, because of its ability to transmit directionally, LightSlingers is ideally suited for propagating signal in neighborhood local networks because they can beam data directly into a specific home (Figure 3), and nowhere else. This unique ability also offers enormous benefits in warfighter communications where security is paramount.

There is some concern that advances in quantum computing could reduce the effectiveness of standard encryption methods. In this scenario, LightSlingers is especially valuable because data can be transmitted directionally. LightSlingers can be configured so that there are no stray signals to intercept and decrypt. The recipient must be in the correct location to receive the signal.



## Variable geometry

LightSlingers can be built in unusual shapes (flat panels, cylinders, disks) uniquely optimized to particular situations and applications (Figure 10). For example, they can be concealed within the ceramic armor applied to a tank or unmanned ground vehicle. The size and shape of conventional antennas, on the other hand, are constrained by the wavelength they emit. Large wavelength antennas, used to transmit low frequency signals at kHz frequencies, need to be large. Small wavelength antennas, commonly found in cell phones, can be small, but they cannot transmit longer wavelengths. LightSlingers are around 25 percent smaller than equivalent phased arrays, freeing up space on cell towers and other areas where the technology could be deployed.



**Figure 10.** LightSlingers can be made in a wide variety of shapes and sizes, each optimized to a particular application. LightSlingers have been extensively tested in anechoic chambers and in the field, using both the facilities of commercial companies and government laboratories. Photo credit: LANL

**Efficiency**

Under the same excitation, the LightSlinger produced approximately 10-15 percent more emitted power than a phased array of the same length, mainly because of the confining effect of the dielectric and the fact that the LightSlinger emits only “forward” (as opposed to the elements in a phased array, which also radiate backward into the antenna assembly, reducing efficiency).



## **Describe the limitations of your product/service.**

### **Manufacturing inertia**

The chief hurdle for widespread adoption of LightSlinger technology may involve its construction. The construction method for LightSlingers involves 3D printing or CNC milling of a small number of monolithic components (Figure 2, right), followed by bonding them to a circuit board. This is completely different from techniques used by industry to make conventional antennas. Conventional antennas are almost always assembled from large numbers of small components by hand using unskilled labor. The electrical-engineering community may be resistant to change if it believes existing technology is adequate; industry often prefers to stick with what it knows. Even though a LightSlinger production line would be easy to set up for a company already involved in bespoke PCB design and production, there may be a “why bother when we can do it the old way?” attitude. However, as 3D printing becomes more widespread, LightSlingers stand to gain additional production advantages, as they are the only antennas capable of being produced in this much less labor-intensive way.

### **Specialized applications are technologically immature**

The second limitation—which might in fact turn out to be an opportunity—is that even though LightSlingers are already excellent replacements for conventional antennas, many of their potential applications are not yet technologically mature. For example, broadband information focusing, directed energy, and the generation of complex phase fronts are relatively new, ongoing areas of research. Some of these applications are just starting to be considered for the later incarnations of 5G. For LightSlinger technology to become widespread, low-volume, high-margin applications will probably be needed to demonstrate feasibility and size, weight, power and robustness advantages to a wider audience. These will likely come from the defense industry, similar to how LCD displays were developed in parallel by industry (e.g., RCA Princeton, NJ) and secretive government laboratories (e.g., RSRE Malvern, UK).

## Summary

Every antenna since the discovery of radio has used, in one form or another, the current density of free electrons as their radiative mechanism. For years, this approach was sufficient, though not without drawbacks. As connectivity came to define modern life, frequency bands became overloaded, and as devices grew in complexity, manufacture of their fragile parts moved overseas. Only a new paradigm in antenna technology can keep pace with the endless proliferation of wireless devices.

Researchers at Los Alamos National Laboratory have developed LightSlingers, a leap forward in antenna design that promises to simultaneously declutter and secure the airwaves. LightSlingers uses the “other” radiative mechanism—the polarization current—creating, in effect, an entirely new class of antenna with myriad benefits. LightSlingers offer better coverage, efficiency, bandwidth, and security than traditional antennas or phased arrays, all in a sturdier package with far fewer components. Further, they have no geometry requirements—a LightSlinger antenna can be any shape and molded into any device. On 5G local neighborhood networks or the battlefield, LightSlingers are ready to make waves.

## **Appendix A: Support Letters**

**1. Martyn Chamberlain MA D Phil FInst P**

- *Emeritus Professor of Physics, Durham University UK*

**2. Edl Schamiloglu, Ph.D.**

- *Distinguished Professor and Associate Dean for Research and Innovation,*
- *University of New Mexico School of Engineering, Director,*
- *DEC@UNM (UNM's Directed Energy Center),*
- *NSF ERVA Executive Committee Member – <https://www.ervacommunity.org>*

**3. Alicia Kim, Ph.D.**

- *Jacobs Scholar Chair Professor*
- *Structural Engineering Department, University of California San Diego*

## Appendix B.1 – References

- 1) Guo, Jay Y. and Ziolkowski, Richard W., *Advanced Antenna Array Engineering for 6G and Beyond Wireless Communications*, IEEE Press and John Wiley & Sons, Inc., 2022.
- 2) Balanis, Constantine A., *Antenna Theory and Design*, Third Edition, John Wiley & Sons, Inc., 2005.
- 3) Volakis, John L., *Antenna Engineering Handbook*, Fifth Edition, McGraw-Hill Education, 2019.
- 4) Nandi, D. and Maitra, A., “The Effects of Rain on Millimeter Wave Communication for Tropical Region,” 2019 URSI Asia-Pacific Radio Science Conference (AP-RASC), 2019, pp. 1-3, doi: 10.23919/URSIAP-RASC.2019.8738591

## Appendix B.2 – Additional supporting materials

- 1) Singleton, J.; Schmidt, A.C. *Launching information from faster-than-light polarization currents*, Research Features, 138, 38 (2021).
- 2) Singleton, J.; Schmidt, A.C.; Bailey, C.B.; Wigger, J.M.; Krawczyk, F. *On the Information Carried by Electromagnetic Radiation Launched from Accelerated Polarization Currents* Physical Review Applied, 14, 064046 (2020)
- 3) Mullane, L., “Smaller, more versatile antenna could be a communications game-changer,” 2022. <https://discover.lanl.gov/news/0323-lightslinger> accessed 03/24/2022
- 4) Carlson, Erika K., “Emitting Radio Waves with Polarization Currents,” Physics Magazine, <https://physics.aps.org/articles/v13/s160> accessed 03/23/2022
- 5) Schmidt, Andrea and Singleton, John. “Meet the LightSlingers” Presentation (2022)
- 6) “Solving 5G Antenna Design Challenges.” Digi International. October 23, 2020.

## Related Patents

- 1) Singleton, John; Earley, Lawrence M.; Krawczyk, Frank L.; Potter, James M.; Romero, William P.; and Wang, Zhi-Fu. Superluminal antenna, U.S. Patent No. 9,948,011 (February 2012, reissued April 2018).
- 2) Krawczyk, Frank L.; Singleton, John; Caroline Schmidt, Andrea. Continuous antenna arrays, U.S. Patent, filed August 2018 [USSN 62/721,031].
- 3) Singleton, John and Caroline Schmidt, Andrea. “Antenna and transceiver for transmitting a secure signal,” U.S. Patent No. 9,722,724 (August 2017).
- 4) Singleton, John; Caroline Schmidt, Andrea; Krawczyk, Frank L. “Dielectrically boosted very low frequency antenna,” US Patent number No 10,992,020 (April 2021)

## **Principal investigator(s) from each of the submitting organizations**

PI name: Andrea Schmidt

Title: Lead Engineer

Organization: Los Alamos National Laboratory

Email: [aschmidt@lanl.gov](mailto:aschmidt@lanl.gov)

Phone: 505.606.1457

PI name: John Singleton

Title: Lead Scientist

Organization: Los Alamos National Laboratory

Email: [jsingle@lanl.gov](mailto:jsingle@lanl.gov)

Phone: 505.667.4404

## **Full development team member(s)**

Team member name: Frank Krawczyk

Title: Engineer

Organization: Los Alamos National Laboratory (retired)

Team member name: Kimberley Nichols

Title: Engineer

Organization: Los Alamos National Laboratory (former)

Team member name: Connor Bailey

Title: Student

Organization: Los Alamos National Laboratory

Team member name: James Wigger

Title: Student

Organization: Los Alamos National Laboratory

Team member name: Helen Lu

Title: Student

Organization: Los Alamos National Laboratory

## **Marketing and media information**

**Contact person to handle all arrangements on exhibits, banquet, and publicity.**

First name: Janet  
Last name: Mercer-Smith  
Title: R&D 100 Leader  
Organization: Los Alamos National Laboratory  
Email: mercer-smith\_janet@lanl.gov  
Phone: 505-665-9574

**Contact person for media and editorial inquiries.**

First name: Janet  
Last name: Mercer-Smith  
Title: R&D 100 Leader  
Organization: Los Alamos National Laboratory  
Email: mercer-smith\_janet@lanl.gov  
Phone: 505-665-9574

**For a published list of commercialization opportunities please visit:**

<https://www.lanl.gov/projects/feynman-center/index.shtml>

**Company logo**



**LANL LinkedIn profile URL**

<https://www.linkedin.com/company/los-alamos-national-laboratory>

**LANL Twitter handle**

<https://twitter.com/LosAlamosNatLab>

**LANL Facebook page URL**

<https://www.facebook.com/LosAlamosNationalLab>

**LANL Instagram URL**

<https://www.instagram.com/losalamosnatlab/>

Friday, 15 April 2022

Paul J. Heney,  
Vice President,  
Editorial Director,  
R&D World  
United States of America.

*By Email*

Dear Mr Heney,

**Letter of Support: *Lightslingers* R & D 100 Nomination 2022**

It is a genuine pleasure to write in support of this innovative, elegant, and timely Project that is based on previously neglected, but intellectually sound, ideas; and which will undoubtedly result in a wealth of new products and services that are of a highly significant and economically valuable nature. Moreover, the *Lightslingers* Team have already demonstrated in practice the great scientific and technological potential of their work from the results achieved so far. This puts the *Lightslingers* Team in an ideal position to accomplish a radical transformation in the way that transmissible electromagnetic (EM) signals may be generated by antennas, with consequent substantial advantages accruing in a variety of practical applications.

In their Proposal they list a number of currently foreseen areas, where the novel antennas they have developed may be exploited advantageously. These include: secure high-bandwidth 5G communications systems; aircraft radar location methods that guarantee the safety of ground personnel; defence scenarios that require powerful and localised beams of directed energy; and the laboratory-based modelling of astrophysical phenomena. In addition to this remarkable list, I suspect that the physical principles which are deployed in their antennas (and which differ markedly from those of conventional arrangements) will also encourage a host of other uses, such as fundamental and applied studies of condensed and plasma-phase matter requiring the interrogation of dangerous materials, or materials in hard-to-reach locations (e.g., radioactive substances, plasmas and secreted explosives.)

For your information, I am now a fully retired Academic who has spent many years in the development and application of devices and systems that operate in the millimetre-wave and terahertz regions of the EM spectrum. So far as I am aware, the work that the *Lightslingers* Group have undertaken represents the first genuine application of the idea (rather hesitantly proposed by the 19<sup>th</sup> C. Physicist J.C. Maxwell) that a full description of EM behaviour in materials requires a proper recognition of the role of so-called polarization currents. Moreover, the Group's recent

*Martyn Chamberlain MA D Phil FInst P,  
Emeritus Professor of Physics, Durham University UK.  
Email: martyn.chamberlain@outlook.com*

demonstration that subtle manipulations of those currents can generate intense, directed beams of EM energy represents a remarkable result in a 'pure physics' category all of its own. However, I believe that the 'best is yet to come' when the full potential of their discoveries is realised in the design and manufacture of polarization current antennas carried out on a full commercial basis.

From my past involvement in a variety of research programmes (funded by UK national and European Community sources) I am particularly aware of the need to realise telecommunications systems of which the 'Fifth Generation' may be only the beginning. This implies, of course, a push towards higher frequency operation and the development of strategies to ensure information is conveyed with minimum errors and is received by the intended recipients alone. The novel approach of the *Lightslingers* Group will ensure that these essential requirements are satisfied in an efficient, elegant and economical fashion.

As I understand it, the R&D 100 Awards Programme is a highly prestigious award that recognizes *inter alia* the most promising new products that have recently been developed and have already been introduced to the market. The *Lightslingers* activity clearly matches these criteria perfectly. The overwhelming advantages that their product(s) will have, of course, stem from the underlying 'enabling physics' that is involved. From my perspective, a brief 'lay summary' of those advantages is that: (a) unlike the traditional antenna, EM radiation from the superluminal (faster-than-light) source originates from the entire volume of the generating material (and not, as in conventional antennas, from just its conducting surface); (b) the link between antenna size and operating wavelength that is present in conventional antennas is broken for the superluminal source, so that the beam characteristics and operating frequency are determined by the shape and nature of the dielectric material within the device; and (c) , as a consequence of the previous properties, it is possible to design an antenna that delivers intense radiation, with great security and focus, from what seems like an indirect source. In consequence, powerful sources that operate optimally at a chosen EM wavelength (or range of wavelengths) may be designed with entirely novel beam characteristics and which permit great simplification in systems design and manufacture.

A very good example of this last point, clearly mentioned in the Proposal, is the replacement of multi-component phased array systems (in conventional broadband systems) with paperback-book sized units that could be fabricated with minimum 'watchmaker' skills and, indeed, are potentially amenable to speedy robotic construction. This is a particularly important point, as such a 'return to simplicity' implies that companies across the world will be less directly dependent on complex semiconductor chips that may not be manufactured locally, thereby reducing transportation costs and with less environmental impact. Moreover, their approach should also lead to rapid deployment of manufactured systems, with all the benefits this implies.

The Proposal lists a number of applications where the *Lightslingers* antennas offer considerable advantages over what is currently available using traditional technology. The characteristic features of the superluminal polarization current devices and systems (e.g., Directionality, Ease of Construction, Customization, Security, Efficiency, Bandwidth, and the use of Orbital Angular Momentum to foil attempts at signal location) are enormously important to End Users across the various application areas proposed. To comment on just one of those areas, I have no doubt whatsoever that these features and advantages will be invaluable in the realisation of new types of modestly priced and simply constructed secure telecommunications networks, in particular for secure 'backhaul' operation. So great is the current international need for such systems, that it is

*Martyn Chamberlain MA D Phil FInst P,  
Emeritus Professor of Physics, Durham University UK.  
Email: martyn.chamberlain@outlook.com*



hard to see how the efforts of the *Lightslingers* Team (in this application area alone) would not be rapidly taken up for manufacture by interested companies worldwide. Nomination for an award under the R&D 100 Awards Programme will, without doubt, ensure that the Team's efforts are recognized across the wider community and that manufacturing programmes begin promptly.

There will, of course, be many new challenges and opportunities as the Team takes forward the *Lightslingers* concept into the marketplace. I believe the applicants are fully aware of these matters, and the final page of the Proposal text carefully and realistically identifies two specific possible impediments. In that context, they rightly note that the optimisation of 3D printing methods for antenna construction is still in its infancy: but I see no cogent reason why this approach (which is already being adopted in some European programmes for automobile collision-avoidance radar systems) should not be deployed here. Looking further ahead, the identification of new dielectric materials (for higher frequency operation), and the demonstration of efficient receiver antennas using exotic signal phase and polarization control, may be two new and fruitful areas which build on the current state technology, and which may reap considerable benefits in the future.

In my opinion, the present *Lightslingers* Proposal is brimming with exciting and well thought-through ideas. Moreover, the Team have admirably demonstrated already that they can begin to realise the practical relevance of the abstract concepts, advanced by Maxwell so long ago, that underpin these ideas. The benefits to industry, civil society and research progress across the international community will be profound.

I therefore offer my enthusiastic support to the *Lightslingers* Team with their present Application to your Programme; and I look forward to their considerable future commercial success, which gaining an Award would undoubtedly encourage.

Yours sincerely,



J M Chamberlain



## ENGINEERING

Associate Dean for Research and Innovation  
 School of Engineering  
 MSC01 1140  
 1 University of New Mexico  
 Albuquerque, NM 87131-0001 USA  
<http://engineering.unm.edu/research/associate-dean-for-research.html>  
 (505) 277-6095, [edls@unm.edu](mailto:edls@unm.edu)

April 14, 2022

Paul J. Heney  
 Vice President  
 Editorial Director  
 R&D World

### RE: Letter of Support for LANL R&D 100 Entry

Dear Mr. Heney,

I am very pleased to provide my strong support for Los Alamos National Laboratory's (LANL's) selection of the LightSlingers invention as a nominee for an R&D 100 award. Congratulations to the LightSlingers Team! This is a well-deserved honor!

I am very familiar with the LightSlingers technology's historical development. I had the honor to serve as Chair of Dr. Andrea Schmidt's Ph.D. committee at the University of New Mexico (UNM) and I am intimately familiar with the arduous path of the theoretical development and the experimental demonstration of the LightSlingers technology.

LightSlingers are a new class of directional broadband antennas capable of radiating tightly focused wave packets with precision toward a receiving location. Unlike conventional antennas driven by surface currents, LightSlingers use polarization currents, switched to faster-than-light speeds, as their radiative mechanism (the radiated energy still travels at the speed of light). They are sturdy, small, versatile, and they have the potential to disrupt the telecommunications market.

The LightSlingers technology has several novel features that make it attractive to the telecommunications market and for other applications, such as in defense. I cite several of these below.

- **High Directionality** – In future incarnations of 5G and future 6G now under consideration, information must be transmitted in tightly focused beams that target precise locations instead of wasting energy by spreading data throughout a region. LightSlingers achieve tightly focused beams with high directionality and minimal footprint.
- **Simplicity** – A LightSlingers antenna has just five components that can be assembled robotically: two copper-plated monolithic pieces of composite or 3D-printed plastic, one strip of alumina and an input plug, all bonded to a single circuit board. LightSlingers can be additively manufactured and, thus, reproduction is quick, simple, and inexpensive.
- **Customizable** – LightSlingers can be produced using additive manufacturing. They can be made to be conformable to unusual surfaces, such as the body of a vehicle, aircraft, ship, or satellite, and they can be molded into any shape without loss of performance.
- **Secure Communications** – Unlike traditional antennas, only the main beam from a LightSlingers antenna contains a decipherable signal; the stray signals are so weak or scrambled as to be difficult to decode.
- **Efficiency** – The signal from a LightSlingers antenna is produced by a polarization current that occupies the whole active volume of the antenna. Therefore, LightSlingers produce several percent more emitted

## ENGINEERING

power than a phased array (as an example) of the same length under the same excitation. Moreover, LightSlingers emit only in the forward direction, as opposed to the elements in a phased array, which also radiate back lobes and side lobes, reducing efficiency.

- **Bandwidth** – The communications industry uses different antennas to support different frequency bands. However, because of the limited space at base station antenna sites and in mobile platforms, the coexistence of these different antennas poses serious challenges. LightSlingers are intrinsically broadband so that a single antenna may replace several conventional antennas in a system.
- **Orbital Angular Momentum** – Orbital angular momentum (OAM) is an experimental concept that is of great interest in the quest to enhance the capacity of radio links between two antennas. OAM uses helical-mode radio beams, which are characterized by a wavefront that is a helix. To enhance capacity, each individual channel is allocated a different helical mode light beam with distinct angular variations of phase, all of which could potentially be emitted by the same antenna. Future circular LightSlingers could be used for such applications.
- **Defense Applications** – LightSlingers have potential applications in countermeasure-resistant radars. In conventional radars, an aircraft that is being imaged can potentially destroy the radar installation by sending a missile on a course perpendicular to the phase fronts. Similarly, an aircraft can send back a synthesized rogue signal suggesting a reflection from elsewhere. LightSlingers can produce phase fronts that are sufficiently complex to defeat an adversary's attempts to locate the source of the signal. Moreover, the complexity of the phase fronts makes it almost impossible to synthesize a rogue reflection. Radar using LightSlingers technology, on the other hand, has no such drawback. Furthermore, the LightSlingers technology can also have applications in directed energy as a nonlethal weapon that disrupts electronic components in an adversary's vehicles and incoming missiles. LightSlingers could, in principle, create sufficiently focused bursts of electromagnetic energy in a particular location from a considerable distance, without causing damage outside the target area.

It is for these reasons that I strongly support LANL's selection of the LightSlingers Team's technology as a nominee for a prestigious international R&D 100 Award. The fruits of this over two-decade-old research and development effort clearly can be a disruptor in future 5G and 6G telecommunications systems, as well as in the defense sector.

I have attached my brief bio for your perusal.

Respectfully yours,



Edl Schamiloglu

Distinguished Professor and Associate Dean for Research and Innovation  
University of New Mexico School of Engineering  
Director, DEC@UNM (UNM's Directed Energy Center)  
Special Assistant to the Provost for Laboratory Relations  
NSF ERVA Executive Committee Member – <https://www.ervacommunity.org>

### Schamiloglu Bio

Edl Schamiloglu was born in The Bronx, NY in 1959. He received the B.S. degree from the Applied Physics and Applied Mathematics Department at Columbia University, NY, in 1979; he received the M.S. degree in Plasma Physics from Columbia University in 1981; he received the Ph.D. degree in Engineering (minor in Mathematics) from Cornell University, Ithaca, NY, in 1988 (dissertation advisor David A. Hammer, J.C. Ward Jr. Professor of Nuclear Energy Engineering). He joined the University of New Mexico (UNM) as Assistant Professor in 1988 and he is currently Distinguished Professor of Electrical and Computer Engineering and Associate Dean for Research and Innovation in the School of Engineering. He is also the *Special Assistant to the Provost for Laboratory Relations*. He lectured at the U.S. Particle Accelerator School (Harvard University in 1990 and at MIT in 1997). He coedited *Advances in High Power Microwave Sources and Technologies* (IEEE Press/Wiley, New York, NY, 2001) (with R.J. Barker), he has coauthored *High Power Microwaves, 3<sup>rd</sup> Ed.* (CRC Press, Boca Raton, FL, 2016) (with J. Benford and J. Swegle), and he is coediting *Advances in High Power Microwave Sources and Technologies using Metamaterials* (with J.W. Luginsland, J.A. Marshall, and A. Nachman) (IEEE Press/Wiley, New York, NY, 2021). He has coauthored over 180 refereed journal papers, 275 reviewed conference papers, and 8 patents. His publications have been cited over 8500 times (h-index=38, i10-index=143). He has been PI on over \$40M of contracts and grants at UNM.

Professor Schamiloglu is a Fellow of the IEEE, a Fellow of the American Physical Society, and an EMP Fellow (sponsored by the Summa Foundation). He was awarded the 2013 IEEE Nuclear and Plasma Sciences Society's Richard F. Shea Distinguished Member Award "For outstanding contributions to the IEEE Nuclear and Plasma Sciences Society through its Pulsed Power Science and Technology and Plasma Science and Applications Technical Committees," the 2014 IEC '1906 Award' "For his valuable technical contributions to SC77C projects and specifically for his technical contributions with respect to HPEM source technologies to support the standardization of test techniques for HPEM/IEMI," the 2015 IEEE NPSS PPST Peter Haas Award "For research in the area of pulsed power, beams, and microwaves, and for his dedicated service to the current and future pulsed power community through his leadership and educational endeavors," the 2017 UNM Senior Faculty Research Excellence Award, and the 2019 (inaugural) IEEE NPSS Magne "Kris" Kristiansen Award "For outstanding contributions in experimental nuclear and plasma science."

**Updated April 14, 2022**



### Schamiloglu Bio

Edi Schamiloglu was born in The Bronx, NY in 1959. He received the B.S. degree from the Applied Physics and Applied Mathematics Department at Columbia University, NY, in 1979; he received the M.S. degree in Plasma Physics from Columbia University in 1981; he received the Ph.D. degree in Engineering (minor in Mathematics) from Cornell University, Ithaca, NY, in 1988 (dissertation advisor David A. Hammer, J.C. Ward Jr. Professor of Nuclear Energy Engineering). He joined the University of New Mexico (UNM) as Assistant Professor in 1988 and he is currently Distinguished Professor of Electrical and Computer Engineering and Associate Dean for Research and Innovation in the School of Engineering. He is also the *Special Assistant to the Provost for Laboratory Relations*. He lectured at the U.S. Particle Accelerator School (Harvard University in 1990 and at MIT in 1997). He coedited *Advances in High Power Microwave Sources and Technologies* (IEEE Press/Wiley, New York, NY, 2001) (with R.J. Barker), he has coauthored *High Power Microwaves, 3<sup>rd</sup> Ed.* (CRC Press, Boca Raton, FL, 2016) (with J. Benford and J. Swegle), and he is coediting *Advances in High Power Microwave Sources and Technologies using Metamaterials* (with J.W. Luginsland, J.A. Marshall, and A. Nachman) (IEEE Press/Wiley, New York, NY, 2021). He has coauthored over 180 refereed journal papers, 275 reviewed conference papers, and 8 patents. His publications have been cited over 8500 times (h-index=38, i10-index=143). He has been PI on over \$40M of contracts and grants at UNM.

Professor Schamiloglu is a Fellow of the IEEE, a Fellow of the American Physical Society, and an EMP Fellow (sponsored by the Summa Foundation). He was awarded the 2013 IEEE Nuclear and Plasma Sciences Society's Richard F. Shea Distinguished Member Award "For outstanding contributions to the IEEE Nuclear and Plasma Sciences Society through its Pulsed Power Science and Technology and Plasma Science and Applications Technical Committees," the 2014 IEC '1906 Award' "For his valuable technical contributions to SC77C projects and specifically for his technical contributions with respect to HPEM source technologies to support the standardization of test techniques for HPEM/IEMI," the 2015 IEEE NPSS PPST Peter Haas Award "For research in the area of pulsed power, beams, and microwaves, and for his dedicated service to the current and future pulsed power community through his leadership and educational endeavors," the 2017 UNM Senior Faculty Research Excellence Award, and the 2019 (inaugural) IEEE NPSS Magne "Kris" Kristiansen Award "For outstanding contributions in experimental nuclear and plasma science."

**Updated March 09, 2022**



April 11, 2022

Paul J. Heney, VP,  
Editorial Director,  
R&D World

Dear Mr Heney,

I am delighted to write this letter in support of LightSlingers. When I first came across this superluminal antenna concept, it was immediately clear that this was a ground-breaking innovation with unprecedented potential and applications. Now in 2022, with the digital transformation of engineering being well under way and the 6G networks set to launch in 2028, LightSlingers represent a particularly timely innovation that will help to enable the hyper-connected future. The recent Samsung 6G vision report identifies Orbital Angular Momentum (OAM) being one of the most promising concepts in enabling antenna technology; LightSlinger technology represents its practical demonstrator.

In the hyper-connected future of 6G networks, which is currently under development, humans and everything will be connected to provide an ultimate multimedia experience, by bringing communications together with state of the art technologies such as sensing, imaging and artificial intelligence (AI). This will enable truly immersive extended reality (XR), with mobile holograms and digital twins of all objects and systems. This means a huge amount of data exchange. Since the LightSlinger concept partially decouples antenna size, shape and wavelength, it is much more agile than traditional antennas and offers unprecedented opportunities to integrate antennas with the existing systems. This is a highly significant advance also in the context of the current engineering revolution. Across all engineering disciplines from aerospace to civil infrastructure, digital transformation is taking place. The ultimate aim is to create a digital twin or digital replica of an engineered system such that system behaviour, including “unintended consequences”, is predicted and mitigated against. Sensor information continuously updates the digital twin to enable virtual testing and qualification. Such connected systems necessitate continuous data transfers between the physical asset and its digital model, essentially requiring everything to have integrated antennas.

In my research in engineering optimization for multifunctional and complex systems, the current focus of research is integrating multiphysics functionalities into a system, as it often leads to one or more order of magnitude improvement in the system performance. Given the limited resources and energy in today’s environment, there is an increasing demand for multifunctional systems. For example, instead of an electrical vehicle with batteries in a pack protected by a load carrying structure with a separate thermal management system, we build in the load carrying and thermal management functionalities into a battery pack structure, thereby reducing the overall weight of the battery system by over 50%. The LightSlinger is ideal for this trend in engineering, as such an antenna can be elegantly integrated into the structure of an overall system. I believe this is a disruptive and timely invention where its customizability can be fully exploited for countless applications and systems. I am personally very excited by this new branch of engineering and the research opportunities that the LightSlingers bring.



Recent problems in global supply chains have significantly disrupted high-tech industries. In the highly competitive international landscape of the future communication industry, it is imperative that similar problems do not impede developments. The LightSlinger concept is ideal in this regard; it is customizable and can be fabricated in small to midscale additive manufacturing facilities and/or from a small number of locally sourced components and materials, greatly reducing the reliance on the assembly of large numbers of parts by cheap and untrained labor that common in the traditional antenna manufacturing industry. Therefore, this is an extremely important technology that can provide substantial advantage as the global market moves forward. This is the reason why I strongly believe that the LightSlinger is the perfect candidate for the R&D 100 Awards.

It is clear that LightSlingers have substantially more potential than has been demonstrated so far. Traditional antennas have been designed as separate (sub)system(s). This novel antenna concept opens up a new field of engineering, tailoring antennas into a multifunctional system. While there are challenges ahead, my research expertise sees no fundamental scientific obstacles in developing a model-based topology and shape optimization method for LightSlingers and extending it further to make them parts of a multifunctional system. With this evolving field of engineering, I feel sure that LightSlingers can secure a concrete and unique advantage in the global market. I would like to congratulate the team in helping to bring forward and enable the hyper-connected XR future.

Sincerely,

A handwritten signature in black ink, appearing to read "H Alicia Kim", followed by a long horizontal line.

H Alicia Kim, Ph.D.  
Jacobs Scholar Chair Professor  
Structural Engineering Department  
University of California San Diego  
Alicia@ucsd.edu



# Launching information from faster-than-light polarization currents

Although Einstein's theories place a universal speed limit on all objects in the universe, the same rules don't necessarily apply to sequentially moving disturbances which don't carry any mass. A team of researchers at Los Alamos National Laboratory led by Dr John Singleton in collaboration with Dr Andrea Schmidt, shows how polarization currents, carried by the relative displacement of charged particles within specialised antennas, can be used to generate bright bursts of light – emulating more familiar behaviours displayed by sound waves. The discoveries of the research team could lead to new innovations in wireless communications networks; and may also shed new light on a long-standing astronomical mystery.

If you've ever witnessed an aeroplane accelerating to supersonic speeds, it would have been hard to miss the intense burst of sound it created as it crossed the sound barrier. Known as a 'sonic boom,' this dramatic effect arises when the sound waves emitted by an accelerating plane can no longer keep pace with the plane itself. "As the plane overtakes the sound waves that it creates, they pile up behind it," Dr Singleton from the Los Alamos National Laboratory explains. "Then, the noise that was made by the plane over seconds of its flight path hits a well-placed observer all at once."

At first sight, analogous behaviour using electromagnetic waves, which are conventionally emitted by moving electrically charged particles, appears to be strictly forbidden. As Einstein famously pointed out, his Special Theory of Relativity imposes a universal speed limit – the speed of light – that can never be reached by any object that carries mass. This means that the electromagnetic waves emitted by a charged particle – which themselves carry zero mass – will

always move faster than the particle itself. As a result, it seems impossible that these waves could somehow form an 'electromagnetic boom,' in which they pile up to form a sudden, intense burst of light. However, it turns out that this problem can be overcome using collections of particles, rather than a single one.

### THE ELECTROMAGNETIC STADIUM WAVE

To understand this line of reasoning, we first need to look at the microscopic processes which play out within ionic solids and plasmas: the latter are extremely hot fluids in which atoms are stripped of their outer electrons. If an electric field is applied to a portion of one of these systems, the negative and positive charges within that part will move small distances in opposite directions, creating what is known as *polarization*. If a second electric field is then applied to an adjacent bit of the solid or plasma and the first field is turned off, the polarization moves. Using suitably accurate timing, the polarization can be made to move



much faster than the speed of light. "We have easily achieved 100 times the speed of light in one of our antennas, or, for Trekkies, between warp factor 4 and 5," says Singleton.

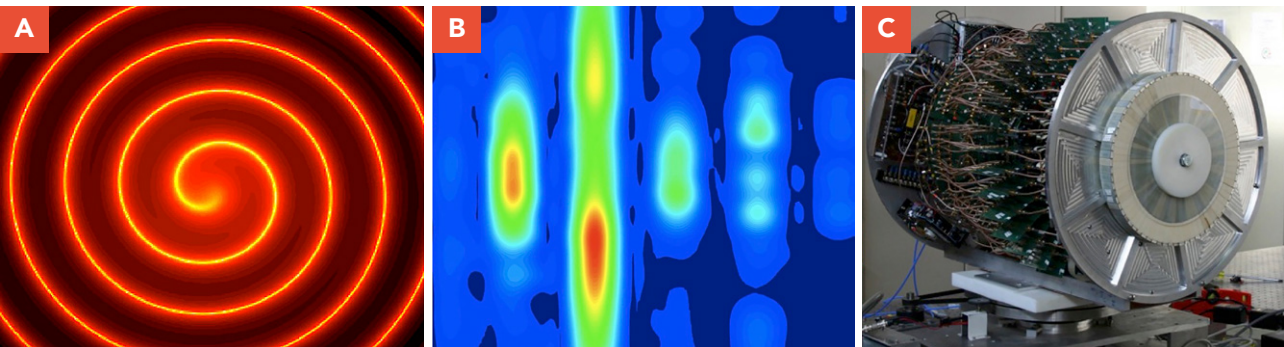
The effect may sound like an exotic phenomenon, but in fact, only the disturbance moves very fast; the particles creating it are displaced only tiny distances. "It's like a stadium wave at a football match, where slowly moving people stand up and sit down," Dr Schmidt illustrates. "If their timing is good enough, a wave rolls round the stadium at high speed, even if the people making it hardly budge from their places."

As predicted by Maxwell in the 19th century, the moving polarization, or polarization current, emits electromagnetic waves. We therefore have a source of radiation that travels faster than the waves that it emits without breaking any laws of physics. (Of course, the electromagnetic waves emitted can

As predicted by Maxwell in the 19th century, the moving polarization, or polarization current, emits electromagnetic waves.

only travel at the speed of light.) For the Los Alamos National Laboratory research team, such a setup presented some fascinating opportunities.

**A NEW TYPE OF ANTENNA**  
Conventional antennas involve electrical currents that are made up of electrons. "Travelling faster than the speed of light is impossible



(A) The spiral 'electromagnetic boom' produced by a large circular antenna, as predicted by Andrea Schmidt; (B) An example of the detector signal plot, demonstrating the 'information focusing' effect; (C) A circular antenna built at the Los Alamos National Laboratory.





for electrons because they have mass,” explains Dr Singleton. “But no such speed limit applies to polarization currents.” Faster-than-light polarization currents can also be made to accelerate or decelerate in a very controllable way, meaning that electromagnetic analogues of many interesting focusing effects, including some previously known from acoustics, can now be achieved.

Starting from theoretical simulations, Schmidt, Dr Frank Krawczyk, and Singleton designed and built a specialised antenna rather like a linear accelerator (for polarization currents) at Los Alamos National Laboratory. Faster-than light polarization currents on which a simple, repeated ‘message’ was encoded were sent along this antenna using a carefully controlled acceleration scheme designed to focus the emitted radiation in an unusual way.

**CONVEYING SECURE MESSAGES**

The key ingredient of the acceleration scheme is that the component of the polarization current’s velocity in the direction of a chosen target point is always exactly the speed of light as it travels along the antenna. If we substitute sound for light, this is similar to the conditions for getting a ‘super boom’ in acoustics. However, “rather than aiming for an ‘electromagnetic boom’, we showed that the message encoded on the polarization current is received strong and understandable only at the target point,” Dr Singleton describes. “At all other places, the radio waves are weak and scrambled.”

The antenna could be used to spray bursts of information to specific locations in its surroundings, ensuring that the message remained very difficult to decode at all other points. For example, the team noted that such behaviour could be useful for neighbourhood 5G networks – which are planned to wirelessly transmit signals to specific target buildings. Using such an antenna would ensure that your neighbours would not be able to see what you ordered on Amazon.

In such a system, messages or data would be encoded as specially-shaped polarization currents



A pulsar (pulsating radio source) is a highly magnetized rotating compact star that emits very sharp pulses of electromagnetic radiation.

**These antennas could one day provide a reliable basis for enhancing the security of communications networks.**

which would be accelerated along the antenna – producing clear electromagnetic signals at highly specific target locations. As a result, these antennas could one day provide a reliable basis for enhancing the security of communications networks.

**EXPLAINING AN ASTRONOMICAL MYSTERY**

Elsewhere, Dr Singleton proposes that the bursts of light produced by faster-than-light polarization currents could explain a phenomenon that has long remained something of a mystery to astronomers. Pulsars are rapidly-rotating, highly magnetic remains of stars born in supernova explosions. Intriguingly, these objects transmit distinctive pulses with the same period as that of the star’s rotation.

“There have been previous attempts to explain these incredibly sharp pulses using faster-than-light polarization currents driven by the intense magnetic field as it whirls through the pulsar’s

plasma atmosphere,” Dr Singleton describes. “However, we have shown that there are fundamental mathematical problems with those prior theoretical attempts. Instead, it now seems likely that pulsars work in a very similar way to the demonstration antenna in our paper. One could even say that we have a ground-based pulsar here.” The ability to play with an experimental ‘pulsar’ in one’s own lab could help to solve the long-standing mystery as to why the equivalent astronomical objects shine in the way that they do.

Through their future research, the Los Alamos National Laboratory researchers will now aim to explore this fascinating effect in more detail; and to design more advanced antennas, capable of generating specially-shaped polarization currents even more accurately. Together, these efforts could soon lead to groundbreaking new insights into an effect which seems at first glance to defy Einstein’s robust descriptions of how the universe works.

Behind the Research



Dr John Singleton



Dr Andrea C. Schmidt

E: [jsingle@lanl.gov](mailto:jsingle@lanl.gov) T: +1-505-667-4404 E: [aschmidt@lanl.gov](mailto:aschmidt@lanl.gov)  
W: [MagLab Staff -John Singleton, maglabdata \(nationalmaglab.org\)](mailto:MagLab Staff -John Singleton, maglabdata (nationalmaglab.org))

Research Objectives

Dr John Singleton and Dr Andrea Schmidt’s research explores novel phenomena in electromagnetism. Their current research could lead to new innovations in wireless communications networks.

Detail

John Singleton  
National High Magnetic Field Laboratory  
MPA-MAGLAB, TA-35, MS-E536  
Los Alamos National Laboratory  
Los Alamos NM 87545, USA

**Bio**  
John Singleton researches condensed-matter physics and electrical engineering at the National High Magnetic Field Laboratory’s pulsed-field facility. Prior to this, he taught, and ran a large research group at Oxford University; he still holds a visiting professorship there. He has over 500 publications, including a text book; his h-index is 58.

Following a successful career as a linguist, **Andrea Schmidt** commenced a pioneering 15-year-long experimental and theoretical study of superluminal antennas, in parallel completing BS and MS degrees in Mathematics and a PhD in Electrical Engineering. She currently works in the Space and Remote Sensing Group at Los Alamos National Laboratory.

**Funding**  
The experiments and calculations are supported by Los Alamos National Laboratory LDRD Projects 20200285ER and 20180352ER.

Additional support from LANL FY17 Pathfinder Fund Call for Technology

Demonstration, PADGS:16-036. Much of this work is performed at the National High Magnetic Field Laboratory, USA, which is supported by NSF Cooperative Agreements DMR-1157490 and DMR-1644779, the State of Florida, and US DoE. JS also acknowledges a Visiting Professorship from the University of Oxford that enables some of the calculations.

**Collaborators**  
• Kim Nichols ([knichols@lanl.gov](mailto:knichols@lanl.gov))  
• **Previous students:** Connor Bailey, James Wigger  
• **Recently retired:** Frank Krawczyk

References

Singleton, J. Schmidt, A.C. Bailey, C. Wigger, J. and Krawczyk, F. (2020). Information carried by electromagnetic radiation launched from accelerated polarization currents. *Physical Review Applied*, 14(6), p.064046. doi:10.1103/PhysRevApplied.14.064046

Schmidt, A.C. Theoretical and Experimental Studies of the Emission of Electromagnetic Radiation by Superluminal Polarization Currents PhD dissertation (2020) [www.digitalrepository.unm.edu/ece\\_etds/497/](http://www.digitalrepository.unm.edu/ece_etds/497/)



Personal Response

**How difficult would it be to implement this technique in real 5G networks?**


“ The polarization current antennas are fully scalable, and for 5G could be constructed in the form of a two-dimensional array about the size of a paperback book. Such a device would be suitable for beaming focused signals in many different directions without the need to physically rotate the antenna. Moreover, in contrast to conventional phased arrays, which tend to be hand-assembled from literally tens of tiny metal components, the superluminal antenna arrays are very robust and monolithic; they can be simply constructed using CNC milling and 3D printing techniques.”

# Information Carried by Electromagnetic Radiation Launched from Accelerated Polarization Currents

John Singleton<sup>1,\*</sup>, Andrea C. Schmidt<sup>1,†</sup>, Connor Bailey<sup>1</sup>, James Wigger<sup>1</sup> and Frank Krawczyk<sup>2</sup>

<sup>1</sup>*National High Magnetic Field Laboratory, MPA-MAGLAB, MS-E536, Los Alamos National Laboratory, Los Alamos, New Mexico 87545, USA*

<sup>2</sup>*Accelerators and Electrodynamics, AOT-AE, MS-H851, Los Alamos National Laboratory, Los Alamos, New Mexico 87545, USA*

 (Received 3 June 2020; revised 29 September 2020; accepted 9 November 2020; published 15 December 2020)

We show experimentally that a continuous, linear, dielectric antenna in which a superluminal polarization-current distribution accelerates can be used to transmit a broadband signal that is reproduced in a comprehensible form at a chosen target distance and angle. The requirement for this exact correspondence between broadcast and received signals is that each moving point in the polarization-current distribution approaches the target at the speed of light at all times during its transit along the antenna. This results in a one-to-one correspondence between the time at which each point on the moving polarization current enters the antenna and the time at which *all* of the radiation emitted by this particular point during its transit through the antenna arrives simultaneously at the target. This has the effect of reproducing the desired time dependence of the original broadcast signal. For other observer-detector positions, the time dependence of the signal is scrambled, due to the nontrivial relationship between emission (retarded) time and reception time. This technique represents a contrast to conventional radio transmission methods; in most examples of the latter, signals are broadcast with little or no directivity, selectivity of reception being achieved through the use of narrow frequency bands. In place of this, the current paper uses a spread of frequencies to transmit information to a particular location; the signal is weaker and has a scrambled time dependence elsewhere. We point out the possible relevance of this mechanism to 5G neighborhood networks and pulsar astronomy.

DOI: [10.1103/PhysRevApplied.14.064046](https://doi.org/10.1103/PhysRevApplied.14.064046)

## I. INTRODUCTION

Though the subject has been studied for over a century [1–3], in the past 20 years there has been renewed interest in the emission of radiation by polarization currents that travel faster than the speed of light *in vacuo* [4–10]. Such polarization currents may be produced by photoemission from a surface excited by an obliquely incident, high-power laser pulse [4–8]. Alternatively, in *polarization-current antennas*, they are excited by the application of carefully timed voltages to multiple electrodes on either side of a slab of a dielectric such as alumina [9–15]. To illustrate these emission mechanisms, we write the third and fourth Maxwell equations [16–19] in the following form:

$$\nabla \times \mathbf{E} + \frac{\partial \mathbf{B}}{\partial t} = 0, \quad (1)$$

$$\nabla \times \mathbf{H} - \varepsilon_0 \frac{\partial \mathbf{E}}{\partial t} = \mathbf{J}_{\text{free}} + \frac{\partial \mathbf{P}}{\partial t}. \quad (2)$$

Here  $\mathbf{E}$  is the electric field,  $\mathbf{H}$  is the magnetic field,  $\mathbf{B} [= \mu_0(\mathbf{H} + \mathbf{M})]$  is the magnetic flux density,  $\mathbf{M}$  is the magnetization,  $\mathbf{P}$  is the polarization (i.e., the dipole moment per unit volume), and  $\mathbf{J}_{\text{free}}$  is a current density of mobile charges. The terms on the left-hand side of both expressions are coupled equations that describe the propagation of electromagnetic waves [16,18], whereas the terms on the right-hand side of Eq. (2) may be regarded as *source terms* [17,19]. The current density  $\mathbf{J}_{\text{free}}$  of free charges (usually electrons) is used to generate electromagnetic radiation in almost all conventional applications such as phased arrays and other antennas [17], synchrotrons [20], light bulbs [18] etc. By contrast, the emission mechanisms mentioned above employ the polarization current density,  $\partial \mathbf{P} / \partial t$ , as their source term [9–15].

In this paper, we use an experiment to study the information conveyed in the signals broadcast by such polarization currents when they are accelerated. We find that a time-dependent amplitude modulation is reproduced exactly in the received signal only when the detecting antenna is close to a particular set of points, the position of which is related to details of the acceleration. At other points, the signal is scrambled. The result has implications for

\*jsingleton@lanl.gov

†aschmidt@lanl.gov



communication applications and for astronomical observations of objects such as pulsars.

The paper is organized as follows. Section II gives a brief introduction to the type of polarization-current antenna used in this work, and how the polarization current within it is animated and accelerated; as the antennas may not be familiar to the general reader, additional detail is given in the Supplemental Material [21]. Section III gives an account of the acceleration scheme for transmitting information to particular locations. Sections IV and V describe an experimental proof of concept of the effect carried out within a 6.5-m rf anechoic chamber. Finally, Sec. VI discusses the implications of this observation for communications and astronomy.

## II. POLARIZATION-CURRENT ANTENNAS

In both dielectric resonator antennas (DRAs) [22] and polarization-current antennas (PCAs) dielectrics play a major role in the emission mechanisms. However, the two antenna types function in completely different ways; DRAs essentially use the dielectric to boost the effective size (and hence the efficiency) of a small antenna [22], whereas in PCAs, the dielectric hosts a moving, volume-distributed polarization current [9–15]. Consequently, PCAs usually consist of a continuous strip of a dielectric such as alumina with electrodes on either side [Fig. 1(a)]. Each electrode pair and the dielectric in between is referred to as an *element*; the elements are supplied independently with a voltage difference,  $V = V_U - V_L$ , where  $U$  and  $L$  refer to upper and lower electrodes. This produces polarization  $\mathbf{P}$  in the dielectric. By changing  $V_U - V_L$  on a series of elements, the polarized region is moved [Figs. 1(a) and 1(b)]; owing to the time dependence imparted by movement, a polarization current,  $\partial\mathbf{P}/\partial t$  is produced, and will, under the correct conditions, emit electromagnetic radiation [2,3,9–15].

PCAs are usually run by moving a continuous polarization current along the dielectric [12–15]. This is accomplished by applying phase-shifted time-dependent signals to the elements [21]. A simple example is given in Fig. 1(c), where the upper (green) trace shows  $[V_U - V_L]_j = \sin[\omega(t - j\Delta t)]$  versus  $j$ , where  $j$  labels the antenna element,  $\omega$  is an angular frequency,  $t$  is time and  $\Delta t$  is a time increment, at  $t = 0$ . The lower (red) trace shows  $[V_U - V_L]_j$  at a later time; the effect of the time increments is to move the “voltage wave” and hence the induced polarization at a speed  $v = a/\Delta t$ , where  $a$  is the distance between element centers. Acceleration is introduced by varying  $\Delta t$  along the antenna’s length. Further details and typical emission properties are given in the Supplemental Material [21].

The practical antenna used in the experiments below is shown in Fig. 2(a); it has 32 elements spanning a total length of 0.64 m, and the dielectric is alumina

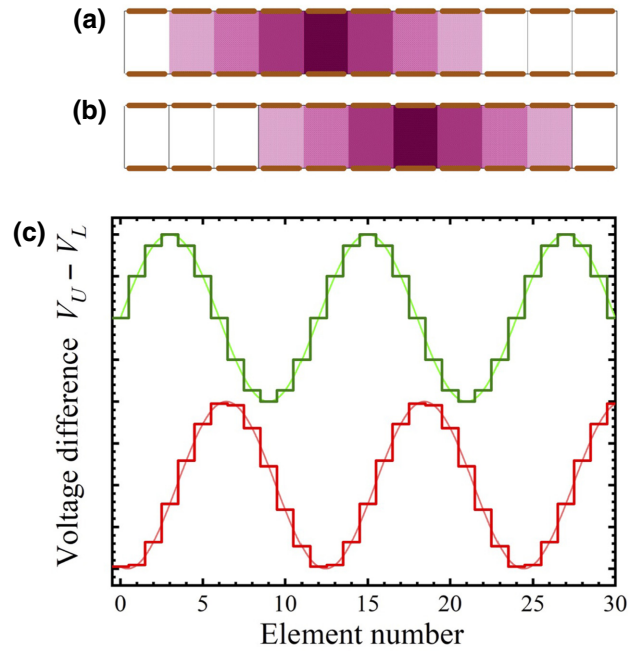


FIG. 1. (a) Polarization-current antennas (PCAs) consist of a continuous series of elements made of a dielectric (white) sandwiched between pairs of electrodes (orange). The dielectric is polarized by applying a voltage difference  $V_U - V_L$  between upper ( $U$ ) and lower ( $L$ ) electrodes; this is shown schematically for seven elements, the shading density representing the polarization strength. (b) The  $V_U - V_L$  shown in (a) are applied to elements two further to the right, moving the polarized region. (c) The upper (green) trace shows  $[V_U - V_L]_j = \sin[\omega(t - j\Delta t)]$  versus  $j$ , where  $j$  labels the antenna element,  $\omega$  is an angular frequency,  $t$  is time, and  $\Delta t$  is a time increment, at  $t = 0$ . The lower (red) trace (offset vertically for clarity) shows  $[V_U - V_L]_j$  at  $t = \frac{103}{180} (2\pi/\omega)$ ; the effect of the timing differences is to move the “voltage wave” (and the induced polarization) along. In practice, fringing effects round off the stepped voltages, leading to a smoother waveform (fine lines).

( $\epsilon_r \approx 10$ ). The elements are fed via a 32-way splitter and 32 mechanical delay lines [Fig. 2(b)] which are adjusted to produce time differences  $\Delta t$  [14]. Note that in these antennas, the polarization current fills the entire dielectric; it is a continuously moving source of radiation that emits from an extended volume, rather than at a series of points or lines (as in a phased array). Despite the discrete nature of the electrodes, simulations of our antennas performed with off-the-shelf electromagnetic software packages such as Microwave Studio show that fringing fields of adjacent electrode pairs lead to a voltage phase that varies slightly under the electrode [23]; i.e., the phase is more smoothly varying along the length of the antenna than the discrete arrangement of electrodes suggests [21,24]. This is represented by the smoother curves in Fig. 1(c).

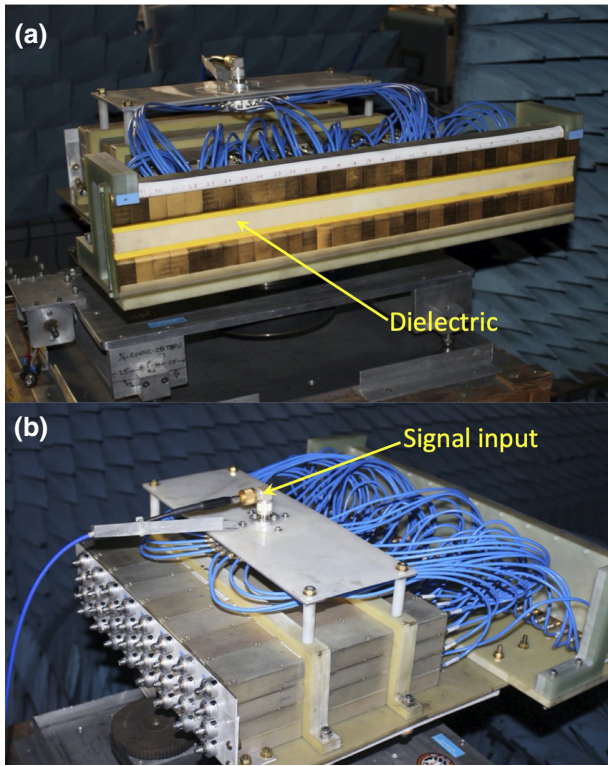


FIG. 2. (a) Front view of the passive antenna used in the demonstration experiment mounted on its turntable in the anechoic chamber. It has 32 elements spanning a total length of 0.64 m. The label indicates the cream-colored dielectric (alumina) that hosts the volume-distributed moving polarization current responsible for the emission of radio waves from the antenna. (b) Rear view of the antenna showing the 32-way splitter feeding 32 independent ATM P1214 mechanical phase shifters. The dials for adjusting the phase are visible on the lower left of the picture. The signal input on the top of the 32-way splitter is labeled.

### III. CONCEPT: ACCELERATION AND FOCUSING

We now consider an antenna containing a “wavepacket” of polarization current that has finite extent in both space and time; it moves on a linear trajectory and accelerates. Figure 3(a) shows a plan view of the antenna’s dielectric of length  $2y_0$  with its center at  $(0, 0, 0)$  lying along the Cartesian  $y$  axis. As in the experimental antennas [13–15] [Fig. 2(a)] the dielectric has rectangular cross section; its depth  $2x_0$  (extent in the  $x$  direction) and height  $2z_0$  (extent in the  $z$  direction) are symmetrical about the  $y$  axis; both  $x_0$  and  $z_0$  are  $\ll y_0$ .

A target is chosen in the  $(x, y)$  plane at a distance  $R_0$ ; the angle  $\Psi_0$  “off boresight” describes the target’s azimuthal position. As everything of interest lies in the  $(x, y)$  ( $z = 0$ ) plane, for convenience we drop the Cartesian  $z$  coordinate for the time being. Thus, the target is at  $(X_0, -Y_0)$ , where

$$X_0 = R_0 \cos \Psi_0 \quad \text{and} \quad |Y_0| = R_0 \sin \Psi_0. \quad (3)$$

Consider a point in the polarization current that is moving through the dielectric along the  $y$  axis; the instantaneous distance  $r$  between the point at  $(0, y)$  and the target at  $(X_0, Y_0)$  is given by

$$r^2 = X_0^2 + (Y_0 + y)^2. \quad (4)$$

The point is made to move in such a way that the component of its velocity towards the target is always  $c$ , the speed of light in the surrounding medium (assumed to be vacuum), that is  $(dr/dt) = -c$ , where  $t$  is the time. Differentiating Eq. (4) with respect to  $t$ , inserting the above value for  $(dr/dt)$  and rearranging, we obtain the point’s velocity along  $y$ :

$$\frac{dy}{dt} = -c \frac{[X_0^2 + (Y_0 + y)^2]^{1/2}}{Y_0 + y}. \quad (5)$$

Integrating Eq. (5), and assuming that the point commences its journey along the antenna at  $y = y_0$  and time  $t = 0$ , we obtain a relationship between the point’s position  $y$  and time  $t$ :

$$t = \frac{1}{c} \left\{ [X_0^2 + (Y_0 + y_0)^2]^{1/2} - [X_0^2 + (Y_0 + y)^2]^{1/2} \right\}. \quad (6)$$

We now consider a detector placed at a general point  $P$  with coordinates  $(X, -Y)$  in the  $(x, y)$  plane. The radiation emitted by the point as it travels along the antenna will reach  $P$  at a time  $t_P$  given by

$$\begin{aligned} t_P &= t + \frac{1}{c} [X^2 + (Y + y)^2]^{1/2} \\ &= \frac{1}{c} \left\{ [X_0^2 + (Y_0 + y_0)^2]^{1/2} - [X_0^2 + (Y_0 + y)^2]^{1/2} \right. \\ &\quad \left. + [X^2 + (Y + y)^2]^{1/2} \right\}. \end{aligned} \quad (7)$$

It should be obvious that if, *and only if*,  $X = X_0$  and  $Y = Y_0$ , then  $t_P$  is a constant. For all other choices of detector position,  $t_P$  is a function of  $y$  and therefore of  $t$ .

This situation is illustrated in the first two columns of Fig. 4. The intended target  $(X_0, -Y_0)$  is at  $R_0 = 5$  m from the antenna center and at  $\Phi_0 = 15^\circ$  [Fig. 4, row (a), left column]; if the detector  $P$  is placed *exactly* at this position, then  $t_P = \text{constant}$  [row (a), center column]. The constant here is the transit time of light from  $y = y_0$ , the place at which the point source enters the antenna at  $t = 0$ , to the target; subsequently the accelerated motion of the point source along the antenna exactly compensates for the changing point-to-target distance. If, on the other hand, the detector position  $P$  is not at  $(X_0, -Y_0)$  [Fig. 4, rows (b) and (c)], then  $t_P$  is a function of  $t$ .

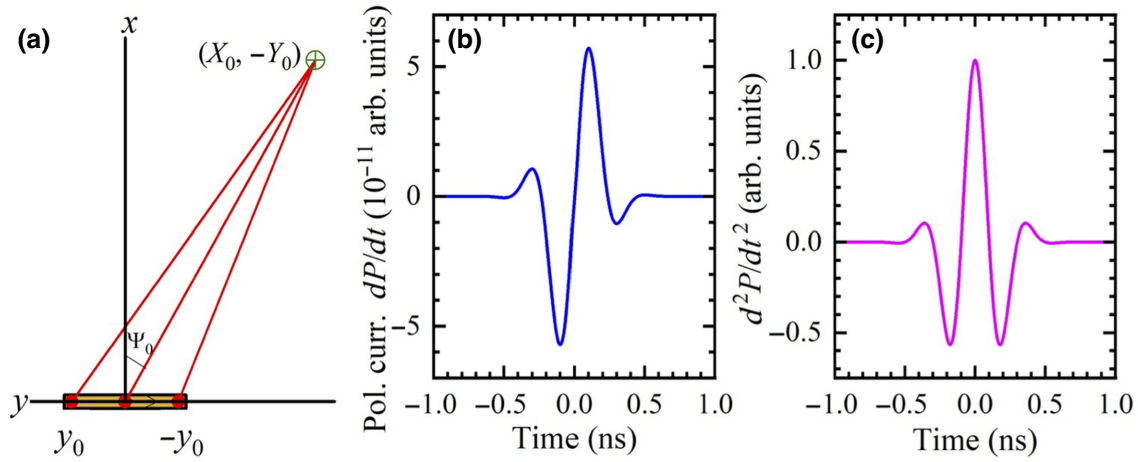


FIG. 3. (a) Experimental concept. An element of polarization current (red) moves along the dielectric antenna (dark yellow shading) such that the component of its velocity in the direction of the target [green cross at  $(X_0, -Y_0)$ ] is always  $c$ , the speed of light. The center of the antenna is at  $(0, 0)$ . (b) Notional time dependence of the polarization current  $dP/dt$  sent along the antenna. (c) Derivative of the curve shown in (b) with respect to time  $t$ . The “arbitrary units” in (c) are equivalent to those in (b), the large scaling occurring because of the fast time dependences.

Next, rather than a single point, we consider the movement of the whole time-dependent polarization-current waveform along the antenna [25]. The imposed motion is such that *each* point within the waveform is accelerated as described above; i.e., as it traverses the antenna, such a point always has a velocity component  $c$  in the direction of the target. Referring to the discussion of Eq. (7) above,

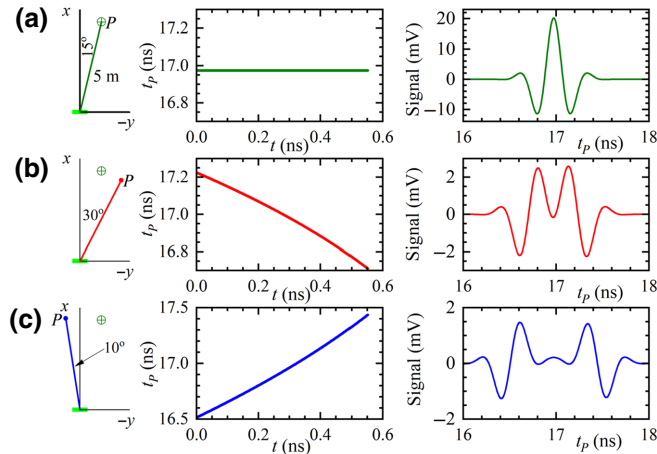


FIG. 4. Each row shows the effect of moving the detector to positions  $P$  5 m from the antenna center (light green). In each row, the left panel gives position  $P$ , the center shows the arrival time  $t_p$  of radiation emitted at time  $t$  by a point accelerating along the antenna, and the right is the signal detected due to the polarization current of Fig. 3(b) being accelerated along the antenna. In all cases, the target (green cross) is 5 m from the antenna center at an angle of  $15^\circ$  to the  $x$  axis. Row (a): detector at target position. Row (b): detector placed on a line making an angle of  $30^\circ$  with the  $x$  axis. Row (c): detector placed  $10^\circ$  to the other side of the  $x$  axis.

all radiation emitted by this point as it moves along the antenna will arrive at the target at a time given by  $t_p =$  (time that point enters the antenna at  $y = y_0$ ) + (transit time of light from  $y = y_0$  to the target). Therefore, there is a one-to-one correspondence between the time at which each point on the moving waveform enters the antenna and the arrival time at the target of the radiation emitted by this particular point as it traverses the antenna.

To show how this affects the received radiation, we send the waveform shown in Fig. 3(b) along the antenna with the constraint that each point on the waveform obeys the acceleration scheme described by Eqs. (3) and (6); as before  $\Phi_0 = 15^\circ$  and  $R_0 = 5.0$  m. The resulting signals (proportional to the  $E$  field) for the detector positions given in the first column of Fig. 4 are shown in the third column of the same figure; the Supplemental Material describes how such calculations are carried out [21,24]. At the target angle and distance [Fig. 4, row (a)], the detected signal reproduces the shape of the time derivative of the polarization-current waveform [Fig. 3(c)] exactly. Away from the target position [Fig. 4, rows (b) and (c)], the detected signal is much smaller and has altered frequency content and shape.

First, why is the time derivative of the polarization current reproduced? The calculations in the Supplemental Material show that [21,24] the magnetic vector potential  $\mathbf{A}$  resulting from each volume element of the antenna is proportional to the polarization current within that element [Supplemental Material, Eq. (8) [21]]. The corresponding  $E$  field is proportional to the derivative of  $\mathbf{A}$  with respect to time [18]. Therefore, it is the *electric field* launched from the antenna that is reproduced at, and only at, the target point.



The idea is illustrated in more detail in Fig. 5; (a) shows the launched  $E$  field [ $\propto (d^2P/dt^2)$ ] at three different times indicated by different colors during its transit through the antenna. Figure 5(b) shows the corresponding detected  $E$  field at the target point. The colored lines linking the curves in Figs. 5(a) and 5(b) illustrate the principle that radiation from a particular point on the traveling waveform *always arrives at the same time at the target*. Thus, features in the launched  $E$  field are *reinforced* at the target in the correct time sequence. In other words, the time dependence of the emission of the whole waveform is reproduced at the target [compare Figs. 3(c) and 4(a)] whereas elsewhere, it is scrambled [Figs. 4(b) and 4(c)].

Figure 5(c) illustrates the same principle using Huyghens wavelets. The colored dots represent the positions of a particular point on the polarization-current waveform at different times during its transit of the antenna; semicircles of the same color represent the corresponding emitted Huyghens wavelets, arriving at the target (orange diamond) simultaneously. At other locations, the Huyghens wavelets arrive at different times, so that the signal becomes scrambled.

For the experimental demonstration below, we need to describe a polarization-current waveform that possesses the

required motion for the above focusing effects. To do this, we write [25]

$$\frac{\partial \mathbf{P}}{\partial t} = \mathbf{f}(y, t) = \mathbf{f}[t - p(y)], \quad (8)$$

where  $\mathbf{f}$  is a vector function of time  $t$  and the function  $p(y)$ . Constant phase points are represented by  $t - p(y) = \text{constant}$ ; differentiating this with respect to  $t$  results in

$$1 = \frac{dp}{dt} = \frac{dp}{dy} \frac{dy}{dt}. \quad (9)$$

Substituting from Eq. (5) and integrating, we obtain

$$p(y) = -\frac{[X_0^2 + (Y_0 + y)^2]^{1/2}}{c}. \quad (10)$$

Equations (8) and (10) describe the required extended polarization-current waveform, all of the points within which approach the target at a speed of  $c$ .

Finally, note that we have only treated a time-domain focus in the  $(x, y)$  plane. In fact the criterion for focusing—that points in the polarization-current distribution approach the observer-detector at the speed of light along their entire path though the antenna—is fulfilled on a *semicircle* of points around the antenna (our antennas are designed not to emit from their rear surfaces [14] that extends in the  $y$  and  $z$  directions, with a radius  $(y^2 + z^2)^{1/2} = Y_0$ ). However, in a proof-of-concept demonstration experiment, moving the observer-detector away from  $z = 0$  complicates matters, as the radiation's  $E$  field is no longer vertically polarized; there is an additional component polarized parallel to  $y$  (this may be deduced from the calculations in the Supplemental Material [21]; for more details see Chapter 7 of Ref. [24]). In the next implementation of this concept, the single antenna discussed in the present paper is replaced by an array of linear antennas configured to allow full three-dimensional  $(x, y, z)$  control of the information focus point, along with minimization of the parasitic  $y$  polarization of the  $E$  field [26].

#### IV. EXPERIMENTAL DEMONSTRATION

The antenna shown in Fig. 2 is used for the experimental demonstration. It is mounted on a powered turntable (vertical rotation axis) with an azimuthal angular precision of  $\pm 0.1^\circ$ . A Schwarzbek-Mess calibrated dipole at the same vertical height is used to receive the vertically polarized transmitted radiation; this is mounted on a TDK plastic tripod on rails that allows it to be moved to different distances without changing the height or angular alignment of the equipment. The entire system is in a  $5.8 \times 3.6 \times 3.6 \text{ m}^3$  metal anechoic chamber

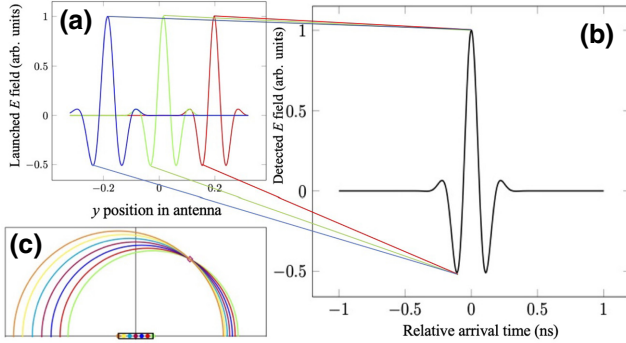


FIG. 5. (a) Launched  $E$  field [ $\propto (d^2P/dt^2)$ ], corresponding to a polarization current similar to that in Fig. 3(b), at three different times (denoted by red, green, and blue curves) during its transit along the antenna; note that the waveform “stretches out” due to the acceleration parameterized by Eqs. (3) and (6). (b) The corresponding detected  $E$  field at the target point; colored lines linking (a),(b) show schematically the principle that radiation from a particular point on the traveling waveform arrives at the same time at the target. This is because the acceleration compensates exactly for the different distances between source point and detection locations [see Eq. (7) *et seq.*]. Hence, features in the launched  $E$  field are reinforced in the correct time sequence in the detected signal. (c) The same principle is illustrated using Huyghens wavelets; colored dots in the antenna (dielectric outlined by black lines) represent the positions of a particular point on waveform (a) at different times during its transit of the antenna; semicircles of the same color show corresponding emitted Huyghens wavelets arriving at the focus point (orange diamond) simultaneously.

completely lined with ETS-Lindgren EHP-12PCL pyramidal absorber tiles.

Signals received by the dipole are sent either to a Hewlett-Packard HP8595E spectrum analyzer to monitor power at a chosen frequency, or to a Mini-Circuits TVA-82-213A broadband amplifier that allows the time-dependent voltage to be viewed and/or digitized using a Tektronix TDS7404 digital oscilloscope. Care is taken to ensure that the cables used are shielded from the radiation within the anechoic chamber and that secondary-path signals are approximately 60 dB less than direct radiation from antenna to dipole.

The description in Sec. III is framed in terms of a traveling wavepacket. However, detecting a single pulse, especially if it contains a spread of frequencies, presents technical difficulties in a facility where only low power levels are permitted. Instead, we choose to transmit and detect what is in effect a train of wavepackets. This forms a continuous broadband signal with a distinctive shape, based on a mixture of harmonics of 0.90 GHz and synthesized by mixing outputs from phase-locked TTI TGR6000 and Agilent N9318 function generators. The synthesized signal is sent to a Mini-Circuits TVA-82-213A amplifier, the output of which drives a 32-way splitter feeding 32 independent ATM P1214 mechanical phase shifters [Fig. 2(b)]. The latter are used to set the time delays of the signals sent to each antenna element, reproducing the above acceleration scheme. To keep the “information focus” well within the anechoic chamber,  $X_0 = 3.03$  m and  $Y_0 = 0.64$  m are chosen, yielding target distance  $R_0 = 3.09$  m and azimuthal angle  $\Phi_0 = 11.9^\circ$ .

The time dependence of the broadcast waveform is recorded by placing the receiver dipole 10 mm in front of the 16th element of the antenna and observing the signal on the oscilloscope. As long as the shortest emitted wavelength is much larger than the distance from the dielectric to the detector, the calculations described in the Supplemental Material [21] can be used to show that the  $E$  field thus detected by the dipole is, to a good approximation,  $\propto \partial^2 \mathbf{P} / \partial t^2$ , where  $\mathbf{P}$  is the polarization passing the point in the dielectric closest to the detector antenna. Hence, an analog of Fig. 3(c) for the experimental wavetrain is captured; moreover, any frequency-dependent artefacts are the same in the measurements of the broadcast and received signals, making a comparison analogous to that between Fig. 3(b) and the third column of Fig. 4 simpler.

The waveform used for the experiments is selected by adjusting the outputs of the two signal generators and is shown in Fig. 6(a). It is chosen because (i) it has a distinctive time-dependent shape (e.g., the double peak followed by two differing minima, one relatively broad) and (ii) an easily recognized “triangular” Fourier spectrum [Fig. 6(b)]. These traits aid in the rapid location of ranges of distance and azimuthal angle over which the broadcast signal is reproduced.

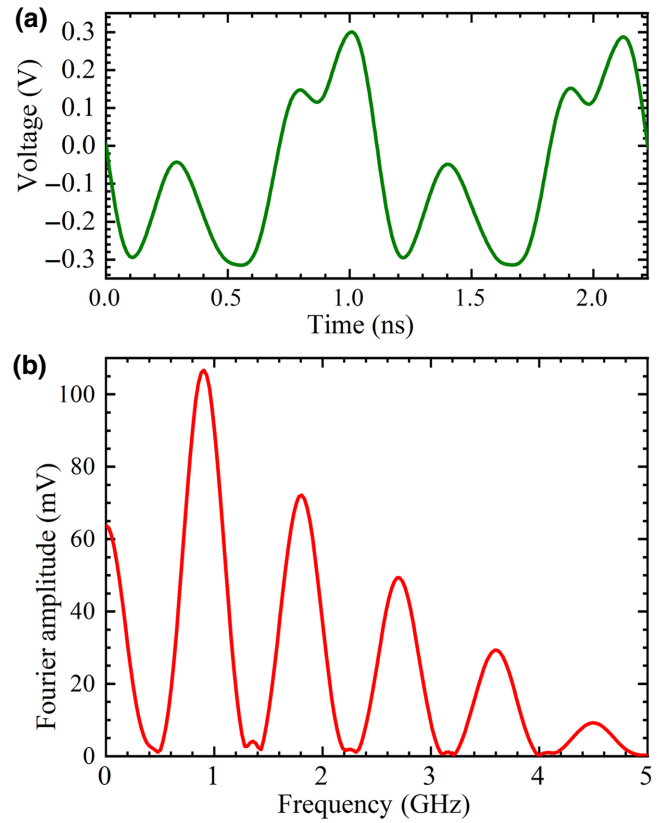


FIG. 6. (a) Voltage measured by placing the dipole receiver 10 mm in front of the 16th antenna element as a function of time; in effect, this is the desired transmitted signal. (b) Fourier transform of the waveform in (a). Note the distinctive “triangular” pattern of harmonics of 0.9 GHz.

## V. RESULTS

Preliminary surveys are carried out by sweeping the transmitter azimuthal angle at closely spaced distances around the expected  $R_0$  whilst carefully observing the received signal on the oscilloscope or spectrum analyzer. Slight phase-setting errors result in actual target coordinates  $R_0 \approx 3.00$  m and  $\Phi_0 \approx 11.6^\circ$  (cf. planned values of 3.09 m and  $11.9^\circ$ ).

Once this “focus” is established, the transmitter-to-receiver distance is fixed at 3.0 m and the oscilloscope trace of the received signal recorded for several fixed azimuthal angles spaced by approximately  $1^\circ$ . The results of this procedure are shown in Fig. 7. On comparing with Fig. 6(a), it is clear that the broadcast signal (double peak, narrower than wider minimum) is only reproduced faithfully at an azimuthal angle of  $11.6^\circ$  (orange, thicker curve). The time-dependent signals for angles  $12.8^\circ$  and  $10.5^\circ$  show distinct differences from the broadcast waveform; one only has to move a few more degrees away from  $\Psi_0$  and any resemblance to the broadcast signal is lost.

This picture is confirmed by Fourier transforms of the oscilloscope data [Fig. 8(a)]. At an angle of  $11.6^\circ$  (red

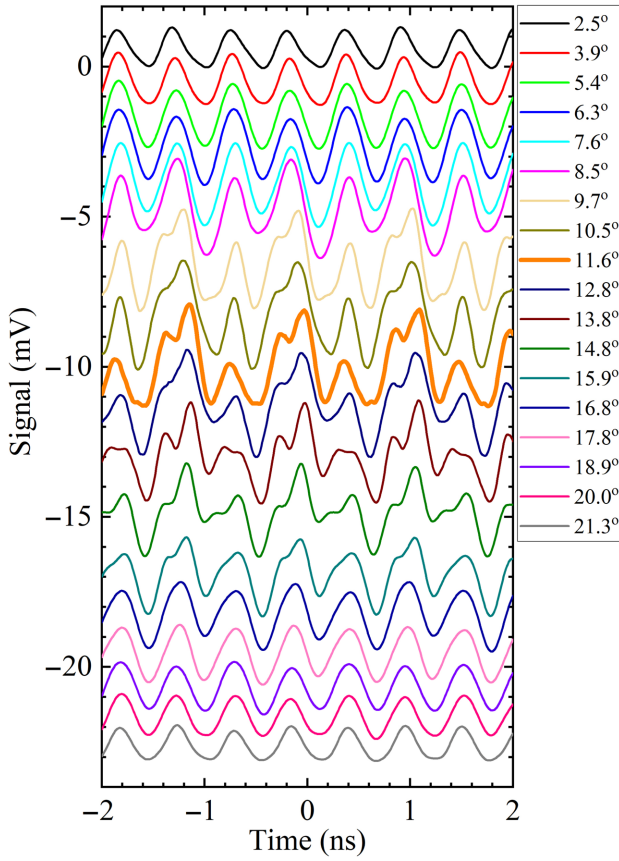


FIG. 7. Time dependence of the signal received by the detector dipole for an antenna-to-detector distance of 3.0 m and for the azimuthal angles shown in the key. The shape of the transmitted waveform [Fig. 6(a)] is only reproduced close to the “target” angle of  $11.6^\circ$  (orange trace). Experimental traces are offset vertically for clarity.

trace), the expected “triangular” Fourier spectrum [cf. Fig. 6(b)] is produced. On moving approximately  $\pm 2^\circ$  away, the relative amplitudes of the harmonics of 0.9 GHz change quite dramatically, showing that the frequency content present in the broadcast signal is being scrambled.

Measurements are then repeated at fixed transmitter-to-receiver distances either side of the target distance of  $R_0 = 3.0$  m [Figs. 8(b)–8(d)]. Even azimuthal angles close to the target value (red traces) fail to yield the broadcast “triangular” Fourier spectrum [compare with Figs. 8(a), 6(b)], showing that the frequency content of the original broadcast signal is only reproduced when the distance *and* the azimuthal angle are close to the target values. Fourier transforms taken over wider angular ranges are given in the contour plots of Fig. 9, showing that the “triangular” Fourier spectrum is not recovered as one moves farther from the target angle. Figure 10 shows the effect on the time dependence of the received signal caused by keeping the azimuthal angle close to  $\Phi_0 = 11.6^\circ$  and varying the

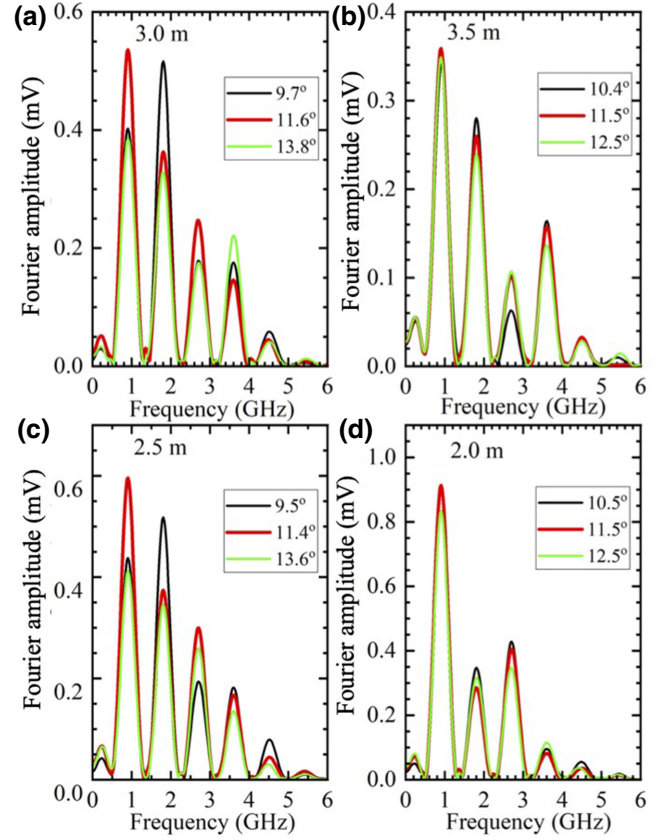


FIG. 8. Fourier transforms of the detector signal for azimuthal angles (shown in key) on either side of (green and black) and close to or at the target angle of  $11.6^\circ$  (red) and at different antenna-to-detector distances: (a) 3.0 m, (b) 3.5 m, (c) 2.5 m, and (d) 2.0 m.

transmitter-to-receiver distance. Comparing Fig. 10 with Fig. 6(a), it is clear that the broadcast signal’s time dependence (double peak, narrower and then wider minimum) is only reproduced faithfully at distances close to the target value of 3.0 m (orange, thicker curve).

## VI. DISCUSSION

The data displayed in Figs. 6 to 10 show that a continuous, linear, dielectric antenna in which a superluminal polarization-current distribution accelerates can be used to transmit a broadband signal that is reproduced in a comprehensible form at a chosen target distance and angle; as noted in the final paragraph of Sec. III, effectively this signal is distributed onto a half circle [24] in the current implementation of the experiment [26]. The requirement for this exact correspondence between broadcast and received signals is that each point in the polarization-current distribution approaches the observer-detector at the speed of light at all times during its transit along the antenna. This results in all of the radiation emitted



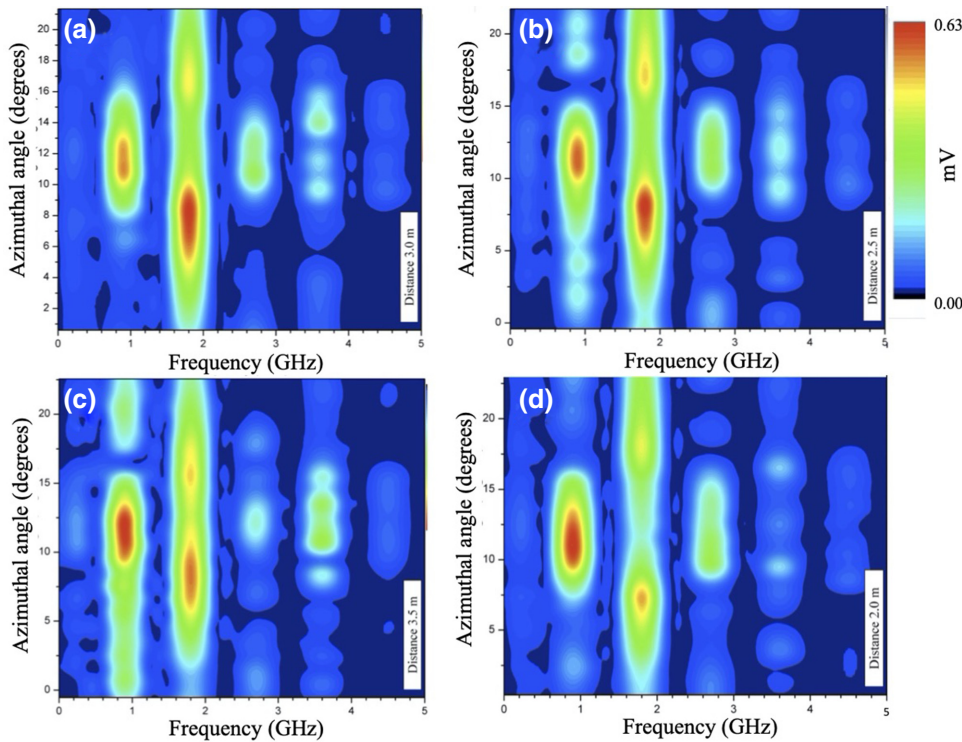


FIG. 9. Fourier transforms of the detector signal plotted as contour plots versus frequency and azimuthal angle for different antenna-to-detector distances: (a) 3.0 m, (b) 2.5 m, (c) 3.5 m, and (d) 2.0 m.

from this point as it traverses the antenna reaching the observer-detector at the same time [Fig. 4(a)]. For other observer-detector positions, the time dependence of the signal is scrambled, due to the nontrivial relationship between emission time and reception time [Figs. 4(b) and 4(c)].

The primary role of the current paper is to introduce the above effect and to demonstrate it experimentally. However, it is interesting to suggest how a PCA might be employed to transmit signals that contain information. Figure 11 depicts a simulation of a simple version of such a concept. The inset shows the time dependence of a wavepacket of launched  $E$  field that could function as a single “bit.” Like the waveforms employed in Figs. 3 and 4, it consists of the convolution of a Gaussian and a cosine. The main part of the figure shows a calculation (using the techniques detailed in the Supplemental Material [21]) of the received signal due to the broadcast of two of these “bits,” spaced in time by three periods of the cosine function. For ease of comparison, the antenna acceleration scheme [i.e., target angle ( $15^\circ$ ) and distance (5.0 m)] is the same as that employed in Fig. 4. At the target angle of  $15^\circ$ , the two “bits” can be distinguished clearly (labeled 1 and 2 in Fig. 11); as one moves the receiver away from the target angle by as little as  $5^\circ$ , the received signal falls off in amplitude and the individual “bits” become almost impossible to distinguish. This example shows only two “bits”; however, a longer string of similar “ones” and “zeros” would also suffer an analogous smearing as one moved away from the target position.

In this context, note that the *depth* of focus (i.e., the range of distance and angle over which the signal is comprehensible) depends strongly on the form and frequency content of the broadcast signal. For example, the waveform used in the experiment, which encompasses frequencies from 0.9 to 4.5 GHz (see Fig. 6), results in a received signal that distorts relatively quickly as the detector moves out beyond the target distance of  $R_0 = 3.0$  m at the target angle (Fig. 10). By contrast, a relatively narrow-band broadcast signal (e.g., Fig. 3) will be recognizable at the target angle over a wider range of detector distances [24]. A full discussion of the criteria for the tightness of “information focusing” demands detailed analysis of many different broadband signal types and goes beyond the scope of the current work; instead, it forms the basis of a subsequent paper [27].

This technique represents a contrast to conventional radio transmission methods. In many instances of the latter, signals are broadcast with little or no directivity, selectivity of reception being achieved through the use of one or more narrow frequency bands [17,28–30]. In place of this, the current paper uses a spread of frequencies to transmit information to a particular location; the signal is weaker and has a scrambled time dependence elsewhere (Fig. 4). A possible application may be in proposed 5G neighborhood networks, where a single active antenna will sequentially spray bursts of information into a selection of target buildings around it [31,32]; ensuring that neighbors cannot easily understand what you are transmitting and receiving will be a useful component.

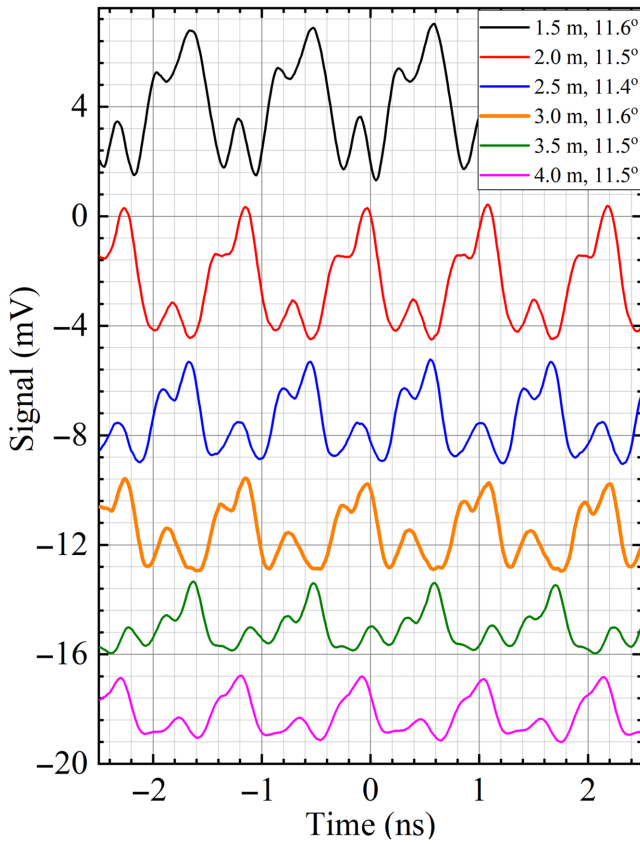


FIG. 10. Time dependence of the signal received by the detector dipole for azimuthal angle close to  $\Phi_0 = 11.6^\circ$  and for different antenna-to-detector distances shown in the key. The shape of the transmitted waveform [Fig. 6(a)] is only reproduced close to the “target”  $R_0 = 3.0$  m (orange trace).

The work in this paper may also be relevant to pulsars, rotating neutron stars that possess very large, off-axis magnetic fields and plasma atmospheres [33,34]. Pulsar periods of rotation  $2\pi/\eta$  range from 1.5 ms to 8.5 s; a back-of-the-envelope calculation shows that at surprisingly small distances (85 km for the 1.5 ms pulsar; 40 000 km for the 8.5 s one) from the rotation axis, the pulsar’s magnetic field will be traveling through its plasma atmosphere faster than the speed of light. Hydrodynamical models of pulsars [35–37] show the following: (i) electromagnetic disturbances (identifiable as polarization currents) exist outside the light cylinder, the orthogonal distance from the rotation axis  $r_L$  at which  $\eta r_L = c$ ; (ii) these disturbances rotate at the same angular velocity as the neutron star’s magnetic field (a requirement of Maxwell’s equations), and so travel superluminally at radii outside the light cylinder; and (iii) the most intense disturbances are compact, in that they occupy a small fraction of the pulsar’s atmosphere.

For such a compact source, traveling on a circular path at faster-than-light speeds, a derivation given in the Supplemental Material [21] shows that a plot of observation-detection time  $t_P$  versus emission time  $t$

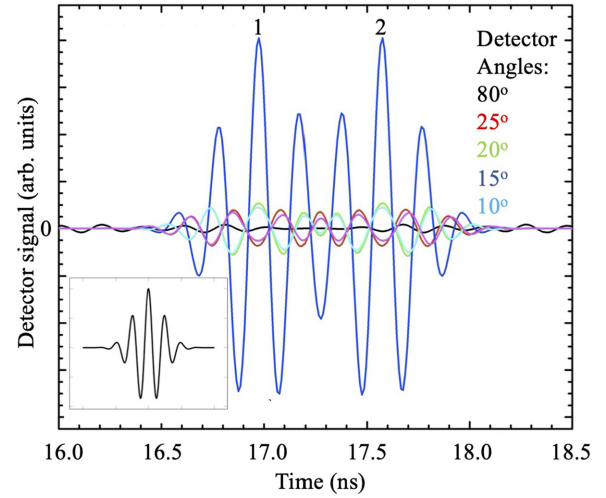


FIG. 11. Simulation of a notional method for transmitting information only to a target point. The inset shows a “bit” (consisting of a Gaussian convoluted with a cosine) as it would appear in the time dependence of the broadcast  $E$  field [compare with Fig. 3(c)]. The main figure shows a calculation of the detected signal at a range of 5 m. This results from time spacing two of these “bits” by three periods of the cosine function and then subjecting them to the same acceleration scheme that is used to produce Fig. 4. At the target angle of  $15^\circ$  (dark blue), the “bits” (labeled 1 and 2) may be easily resolved. However, as soon as the detector is moved to other angles (labeled by the colors in the key), the received signal is much weaker and the “bits” become virtually impossible to distinguish.

exhibits “plateaux” (see Fig. 7 of the Supplemental Material) at, and only at, a special polar angle determined by the source’s tangential speed. Apart from a single point at their center where  $dt_P/dt = 0$ , these “plateaux” are not, in fact, flat [24]. However, there is a reasonable region of  $t$  over which  $dt_P/dt \ll 1$ , so that a situation similar to that in Fig. 4(a) may be possible.

Pulsars can potentially emit electromagnetic radiation via many mechanisms [33,34], including thermal emission and other processes in their hot, plasma atmospheres, and dipole radiation from the rotating magnetic field of the neutron-star core; why then, might the pulsed radiation detected on Earth be dominated by the small volume of superluminal polarization current? The similarity of the “plateaux” in Fig. 7 of the Supplemental Material to Fig. 4(a) provides a useful clue. At the focus polar angle and over a short window of  $t_P$ , the frequency content of all of the emission processes occurring within the rotating polarization-current element will reproduce exactly, and result in a detected signal with greatly enhanced amplitude; the result is similar to coherent emission [38], but via a completely different mechanism. At all other observation angles and observation times, radiation from the emission processes will superpose incoherently [cf. Figs. 4(b) and 4(c)], leading to a greatly reduced amplitude, and

scrambled frequency content. The sharp focusing in the time domain at the focus polar angle is likely to allow the radiation produced by the superluminal (outside the light cylinder) mechanisms to dominate the pulses. Note that this explanation of the brightness of pulsar pulses does not depend on the incorrect proposal [39] of nonspherical decay advocated by Ardavan [40–42].

## VII. SUMMARY

The experiments in this paper show that a continuous, linear, dielectric antenna in which a superluminal polarization-current distribution accelerates can be used to transmit a broadband signal that is reproduced in a comprehensible form at a chosen target distance and angle. This is due to all of the radiation emitted from this point as it traverses the antenna reaching the observer-detector at the same time. For other observer-detector positions, the time dependence of the signal is scrambled, due to the nontrivial relationship between emission (retarded) time and reception time. The results may be relevant to 5G neighborhood networks and pulsar astronomy.

The data that support the findings of this study are available from the corresponding author upon reasonable request.

## ACKNOWLEDGMENTS

The experiments and calculations in this paper are supported by Los Alamos National Laboratory LDRD Projects 20200285ER and 20180352ER. We are grateful for additional support from *LANL FY17 Pathfinder Fund Call for Technology Demonstration, PADGS:16-036*. Much of this work is performed at the National High Magnetic Field Laboratory, USA, which is supported by NSF Cooperative Agreements DMR-1157490 and DMR-1644779, the State of Florida and U.S. DoE. J.S. acknowledges a Visiting Professorship from the University of Oxford that enabled some of the calculations reported in this paper to be initiated. We thank Ward Patitz for his hospitality, assistance and very helpful suggestions during antenna prototyping experiments carried out at the FARM Range of Sandia National Laboratory. We are grateful for a former collaboration with H and A Ardavan [9,10] that gave the first hints of the potential of polarization-current antennas.

- 
- [1] A. Sommerfeld, *Zur Elektronentheorie* (3 Teile), Nach. Kgl. Ges. Wiss. Göttingen, Math. Naturwiss. Klasse, 99–130, 363–439 (1904), 201–35 (1905).
  - [2] G. A. Schott, *Electromagnetic Radiation and the Mechanical Reactions Arising from it* (Cambridge University Press, Cambridge, UK, 1912).
  - [3] V. L. Ginzburg, Vavilov-Čerenkov effect and anomalous Doppler effect in a medium in which wave phase velocity

- exceeds velocity of light in vacuum, *Sov. Phys. JETP* **35**, 1:92 (1972).
- [4] B. M. Bolotovskii and A. V. Serov, Radiation of superluminal sources in vacuum, *Radiat. Phys. Chem.* **75**, 813 (2006).
- [5] B. M. Bolotovskii and A. V. Serov, Radiation of superluminal sources in empty space, *Phys. Usp.* **48**, 903 (2005).
- [6] A. V. Bessarab, A. A. Gorbunov, S. P. Martynenko, and N. A. Prudkoi, Faster-than-light EMP source initiated by short x-ray pulse of laser plasma, *IEEE Trans. Plasma Sci.* **32**, 1400 (2004).
- [7] A. V. Bessarab, S. P. Martynenko, N. A. Prudkoi, A. V. Soldatov, and V. A. Terenkhin, Experimental study of electromagnetic radiation from a faster-than-light vacuum macroscopic source, *Radiat. Phys. Chem.* **75**, 825 (2006).
- [8] Yu. N. Lazarev and P. V. Petrov, A high-gradient accelerator based on a faster-than-light radiation source, *Tech. Phys.* **45**, 971 (2000).
- [9] A. Ardavan, W. Hayes, J. Singleton, H. Ardavan, J. Fopma, and D. Halliday, Corrected article: “Experimental observation of nonspherically-decaying radiation from a rotating superluminal source”, *J. Appl. Phys.* **96**, 7760 (2004).
- [10] J. Singleton, A. Ardavan, H. Ardavan, J. Fopma, D. Halliday, and W. Hayes, in *Conference Digest of the 2004 Joint 29th International Conference on Infrared and Millimeter Waves and 12th International Conference on Terahertz Electronics* (IEEE, Piscataway, NJ, USA, 2004), Cat. No. 04EX857.
- [11] A. C. Schmidt-Zweifel, Master thesis, 2013, [digitalrepository.unm.edu/math\\_etds/45/](http://digitalrepository.unm.edu/math_etds/45/). Accessed January 2020.
- [12] John Singleton, Houshang Ardavan, and Arzhang Ardavan, Apparatus and method for phase fronts based on superluminal polarization current, U.S. Patent No. 8,125,385 (February 2012).
- [13] John Singleton, Lawrence M. Earley, Frank L. Krawczyk, James M. Potter, William P. Romero, and Zhi-Fu Wang, Superluminal antenna, U.S. Patent No. 9,948,011 (February 2012, reissued April 2018).
- [14] Frank Krawczyk, John Singleton, and Andrea Caroline Schmidt, Continuous antenna arrays, U.S. Patent, filed August 2018 [USN 62/721,031].
- [15] John Singleton and Andrea Caroline Schmidt, Antenna and transceiver for transmitting a secure signal, U.S. Patent No. 9,722,724 (August 2017).
- [16] J. D. Jackson, *Classical Electrodynamics* (John Wiley & Sons, Inc., New York, 1999), 3rd ed.
- [17] C. A. Balanis, *Advanced Engineering Electromagnetics* (John Wiley & Sons, Inc., Hoboken, NY, 2012), 2nd ed.
- [18] B. I. Bleaney and B. Bleaney, *Electricity and Magnetism*, The Oxford Classic Text Edition (Oxford University Press, Oxford, UK, 2013).
- [19] O. D. Jefimenko, *Electricity and Magnetism: An Introduction to the Theory of Electric and Magnetic Fields* (Electret Scientific, Waynesburg, PA, 1989), 2nd ed.
- [20] Philip Willmott, *An Introduction to Synchrotron Radiation: Techniques and Applications* (John Wiley and Sons, Chichester, 2019), 2nd ed.
- [21] See Supplemental Material at <http://link.aps.org/supplemental/10.1103/PhysRevApplied.14.064046> for additional experimental and theoretical details.

- [22] Aldo Petosa, *Dielectric Resonator Antenna Handbook* (Artech House, Boston, 2007).
- [23] Frank Krawczyk (to be published).
- [24] A. C. Schmidt-Zweifel, Ph.D. thesis, University of New Mexico, 2020, available from [digitalrepository.unm.edu](https://digitalrepository.unm.edu).
- [25] As mentioned above, the  $x$  and  $z$  extent of the antenna are small compared to its length. Therefore we ignore the slight variations in distance caused by the nonzero  $x$  depth and  $z$  height of the antenna and represent the motion of the volume-distributed polarization current by a function depending only on  $y$  and  $t$ .
- [26] K. Nichols, J. Singleton, and A. C. Schmidt-Zweifel (to be published).
- [27] A. C. Schmidt and J. Singleton (to be published).
- [28] L. C. Godara (ed.), *Handbook of Antennas in Wireless Communications* (CRC Press, Boca Raton, 2002).
- [29] David L. Adamy, *EW 103, Tactical Battlefield Communications – Electronic Warfare* (Artech House, Norwood, MA, 2009), 1st ed.
- [30] Kenneth D. Johnston, *Analysis of Radio Frequency Interference Effects on a Modern Coarse Acquisition Code Global Positioning System Receiver* (Biblioscholar, New York, 2012).
- [31] A. Nordrum and K. Clark, Everything You Need to Know About 5G, IEEE Spectrum (27 January, 2017) (<https://spectrum.ieee.org> – retrieved December 31, 2019).
- [32] 5G Technology Introduction, <https://telcomaglobal.com/blog/17780/5g-technology-introduction> (retrieved February 01, 2020).
- [33] D. R. Lorimer and M. Kramer, *Handbook of Pulsar Astronomy* (Cambridge University Press, Cambridge, UK, 2005).
- [34] A. G. Lyne and F. Graham-Smith, *Pulsar Astronomy* (Cambridge University Press, Cambridge, UK, 2006).
- [35] C. Kalapotharakos, I. Contopoulos, and D. Kazanas, The extended pulsar magnetosphere, *Mon. Not. R. Astron. Soc.* **420**, 2793 (2012).
- [36] I. Contopoulos and C. Kalapotharakos, The pulsar synchrotron in 3D: Curvature radiation, *Mon. Not. R. Astron. Soc.* **404**, 767 (2010).
- [37] A. Spitkovsky, Time-dependent force-free pulsar magnetospheres: Axisymmetric and oblique rotators, *Astrophys. J. Lett.* **648**, L51 (2006).
- [38] G. A. Brooker, *Modern Classical Optics* (Oxford University Press, Oxford, 2003).
- [39] A. Schmidt and J. Singleton, Flaws in the theory of electromagnetic radiation “whose decay violates the inverse-square law”: Mathematical and physical considerations, *Plasma Phys.* (to be published).
- [40] H. Ardavan, The mechanism of radiation in pulsars, *Mon. Not. R. Astron. Soc.* **268**, 361 (1994).
- [41] H. Ardavan and J. E. Ffowcs Williams, Violation of the inverse square law by the emissions of supersonically or superluminally moving volume sources, arXiv:astro-ph/9506023v1 (1995).
- [42] H. Ardavan, Generation of focused, nonspherically decaying pulses of electromagnetic radiation, *Phys. Rev. E* **58**, 6659 (1998).



# Supplementary material for the paper “Information carried by electromagnetic radiation launched from accelerated polarization currents”

John Singleton, Andrea C. Schmidt, Connor Bailey, and James Wigger  
National High Magnetic Field Laboratory, MPA-MAGLAB, MS-E536,  
Los Alamos National Laboratory, Los Alamos, NM 87545, U.S.A.\*

Frank Krawczyk  
Accelerators and Electrodynamics, AOT-AE, MS-H851,  
Los Alamos National Laboratory, Los Alamos, NM 87545, U.S.A.

## I. DEMONSTRATION OF SPEED CONTROL OF POLARIZATION CURRENTS

### A. Superluminal speeds

As an illustration, Sec. 2 of the main paper describes the simplest method to produce a polarization current moving at a constant speed<sup>1–5</sup>; the  $j$ th ( $j = 1, 2, 3, \dots$ ) element of the antenna is supplied with time-dependent voltage differences

$$V_j = [V_U - V_L]_j = V_0 \cos[\omega(t - j\Delta t)], \quad (1)$$

where the symbols are defined in the main paper. The voltages  $V_j$  are usually  $\leq 1$  V; under these, and much higher voltages, alumina behaves as a linear dielectric, so that the polarization  $\mathbf{P}$  in the  $j$ th element will be proportional to the electric field<sup>6–8</sup> generated by  $V_j$ . The polarization current that emits the radiation from the antenna is thus “dragged along” by the time-dependent voltages applied to the elements at a speed  $v = a/\Delta t$ , where  $a$  is the separation of the centers of adjacent elements.

In the early years of the 20<sup>th</sup> Century, both Sommerfeldt<sup>9</sup> and Schott<sup>10</sup> showed that emission of electromagnetic radiation from such a moving source can only occur when  $v > c$ , the speed of light *in vacuo*. Schott demonstrated<sup>10</sup> that the Huygens wavelets from each point in the moving polarization current form a conical envelope with aperture  $\sin^{-1}(c/v)$  [Fig. 1(a)]. Translating this to an extended, moving polarization current that fills the entire antenna, this results in emitted power that should peak at an azimuthal angle

$$\phi = \sin^{-1}(c/v). \quad (2)$$

To demonstrate this effect, we use data from the antenna<sup>3</sup> shown in Fig. 2(a). Like the antenna in the main paper, it comprises 32 elements and employs alumina ( $\epsilon_r \approx 10$ ) as a dielectric, but it has a smaller element spacing of  $a = 10.87$  mm. The detected power is monitored using a Schwarzbeck Mess calibrated dipole whilst the antenna is rotated on a turntable to vary the azimuthal angle  $\phi$ .

Fig. 2(b) shows detected power (in  $\mu\text{W}$ ) versus  $\phi$  for the antenna running at a series of constant speeds  $v$ , set by varying  $\Delta t$  in Eq. 1. When plotted in these linear power units, the azimuthal dependence is clearly dominated by a single, large peak, the angle of which depends on  $v$ . Fig. 2(c) shows that the azimuthal angle  $\phi$  at which peak power occurs varies with  $v$  as expected for the vacuum Čerenkov effect<sup>10</sup> [Eq. 2].

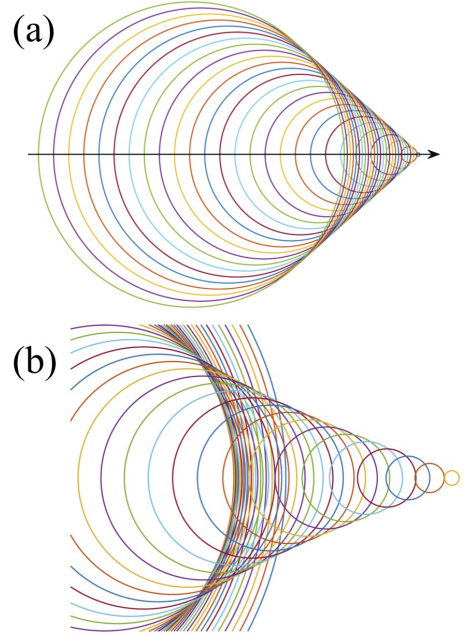


FIG. 1. (a) Huygens wavelets emitted by a small source of electromagnetic radiation traveling along a rectilinear path with constant *superluminal* speed,  $v/c = 1.5$ . Since the source travels faster than the waves it emits, it leads the advancing wave-front; the envelope of the Huygens wavelets is a vacuum Čerenkov cone with half-angle  $\sin^{-1}(c/v)$ . (b) Huygens wavelets emitted by a small source moving along a straight line with constant acceleration. Having broken the “light barrier”, the source leaves a Čerenkov envelope in its wake that has a slightly concave lateral surface. Note the clustering of many Huygens wavelets to either side (*i.e.*, in a ring around the source’s path); this represents the arrival, in a relatively short period of observation time, of radiation emitted over an extended length of the source’s path. In the main paper, we optimize the acceleration so that the Huygens wavelets emitted over the *entire* path of a point source arrive simultaneously at a chosen “target”. [After Ref. 14, adapted from Schott<sup>10</sup>.]

### B. Subluminal speeds

When polarization-current antennas are run at constant speeds  $v/c < 1$ , the power detected oscillates as a function of azimuthal angle. Fig. 3(a) gives an example of this behavior; to obtain these data, the antenna shown in Fig. 2(a) was run at  $v/c = 0.5$ . In addition to the oscillations, the peak power is

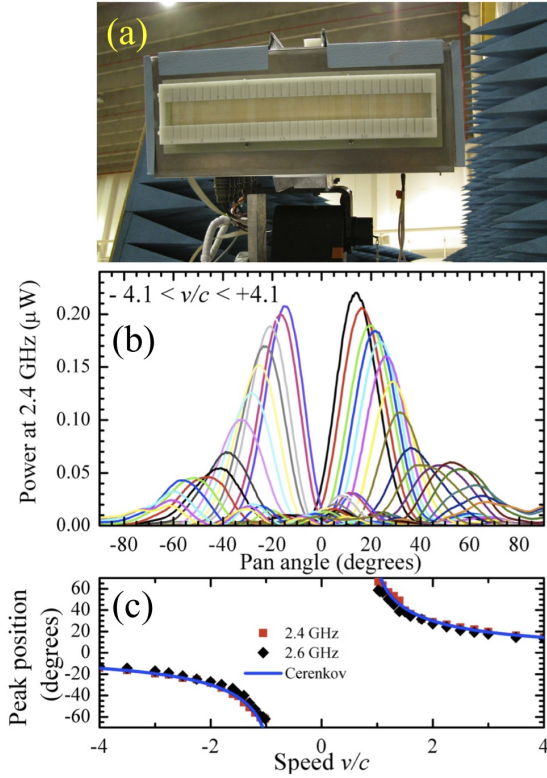


FIG. 2. (a) The antenna used in the vacuum Čerenkov demonstration placed on a stepper-motor-driven pan/tilt mount. (b) Power received from the antenna run at several different constant speeds  $v$ , ranging from  $-4.1c$  to  $-1.1c$  and  $+1.1c$  to  $+4.1c$ , versus azimuthal (pan) angle. The emitted frequency is  $\frac{\omega}{2\pi} = 2.4$  GHz and the detector is 5.36 m from the antenna in an anechoic chamber. (c) Peak power angle versus polarization-current speed  $v$  with  $\frac{\omega}{2\pi} = 2.4$  GHz and  $\frac{\omega}{2\pi} = 2.6$  GHz (points); the curve is the prediction for the vacuum Čerenkov effect [Eq. 2].

some 15 – 20 dB lower than for speeds  $v/c \approx 2 - 4$ .

The power oscillations in Fig. 3(a) are similar to those from a two-slit diffraction experiment in which the light from one slit is  $(2\aleph + 1)\pi$  out of phase with that from the other, where  $\aleph$  is an integer. In the far field, such a two-slit experiment would give minima that occur when<sup>11</sup>

$$b \sin \phi = l\lambda, \quad (3)$$

where  $b$  is the spacing of the slits,  $l$  is an integer and  $\lambda$  is the wavelength. Hence, a plot of  $\sin \phi$  versus  $l$  should be a straight line, with gradient  $\lambda/b$ . Fig. 3 shows that the minima indeed obey this relationship. The reasons for this will be discussed in more detail below.

## II. FEEDS TO ANTENNA ELEMENTS

An important ingredient of the design of polarization-current antennas is the way in which radiofrequency (RF) signals are transformed from cylindrical propagating modes in 50  $\Omega$  coaxial cable to a linear electric field applied by the

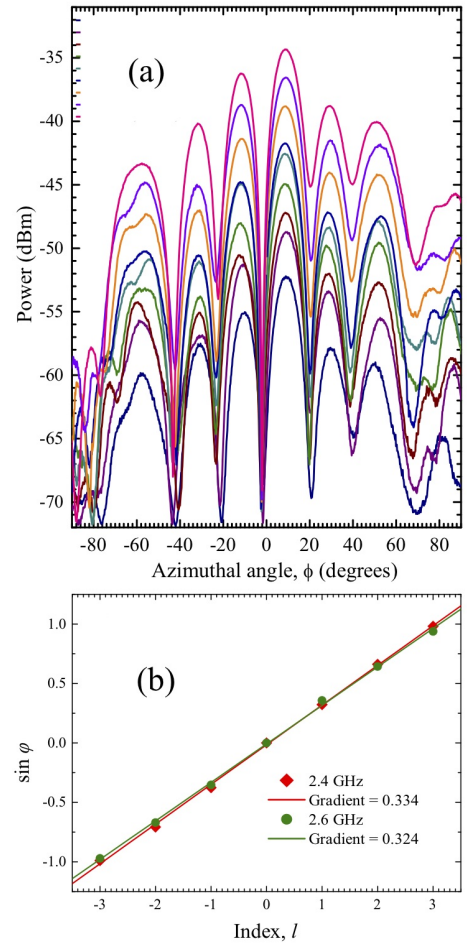


FIG. 3. (a) Received power versus azimuthal angle  $\phi$  for antenna-to-detector distances 0.95, 1.4, 1.8, 2.3, 3.2, 4.1, 5.2, 5.4 and 8.6 m, and subluminal source speed  $v/c = 0.5$ ; the antenna used is that in Fig. 2(a) and data are shown for  $\omega/2\pi = 2.6$  GHz. (b) A plot of  $\sin \phi$  versus index  $l$ , where  $\phi$  denotes the angle at which a minimum in power occurs, for a distance of 8.6 m [see (a)]. Data are points, and the lines are straight-line fits, giving gradients of 0.33 and 0.32 for  $\omega/2\pi = 2.4$  GHz and 2.6 GHz points respectively.

electrodes to the dielectric<sup>3,4,14</sup>. Figs. 4(a,b) show how this is achieved in the antenna depicted in Fig. 2 of the main paper. Most of the antenna element is made from G10 composite, with the upper surface plated with copper. The radiofrequency signal is fed from an SMA connector (50  $\Omega$ ) and coupled to an impedance-matched micro-stripline built on standard circuit board. The final transformation into the desired, linear field pattern to be applied to the dielectric is achieved by a rectangular patch underneath the cut-out opening and the shape of the stepped opening above.

Note that the individual elements cannot be designed, modelled or tested on their own; isolated, they do not have the desired characteristics for the function of the antenna. Instead, their performance depends on the presence of neighboring elements. Fig. 4(c) shows how the fields from the polarization current in the element radiate out of the top surface only; the transverse components of the fields are suppressed

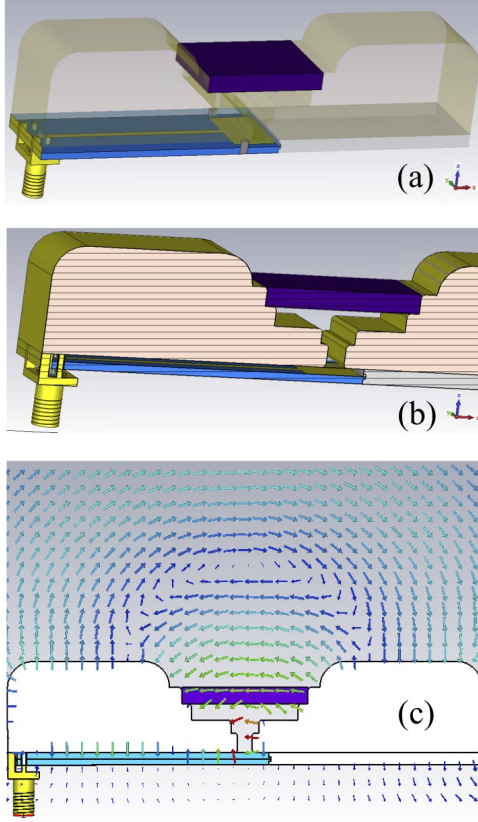


FIG. 4. (a, b) Two views of an individual element of the antenna shown in Fig. 2 of the main paper. The RF signal is fed from an SMA connector and coupled to a micro-stripline (gold on blue). The final rectangular patch underneath the cut-out opening and the shape of the stepped opening above transform the field pattern into a linearly polarized electric field across the alumina dielectric (purple) between the electrodes. The whole upper part of the element is made up from two pieces of copper-plated G10. (c) The fields (arrows) from the polarization current in the element radiate out of the top surface only. Transverse components of the fields are suppressed by the proximity of the neighboring antenna elements.

by the proximity of the adjacent antenna elements. The design of the elements also suppresses radiation out of the back of the antenna, increasing the directivity.

In practice, the antenna elements can be built individually and then combined into different configurations optimized for particular applications<sup>14</sup>. Alternatively, all of the elements for an antenna can be fashioned on a single monolithic substrate (machined from a G10 block by a CNC mill) for strength and rigidity.

### III. CALCULATION OF EMITTED RADIATION

#### A. Basic principles

Simulated antenna emissions are used to illustrate the principles of the experiment in the main body of the paper. Therefore, a brief explanation of the simulations and a validation via

comparison with experimental data taken using the antenna shown in Fig. 2(a) are now given.

Despite the discrete nature of the electrodes, simulations of our antennas performed with off-the-shelf electromagnetic software packages show that fringing fields of adjacent electrode pairs lead to a voltage phase that varies under the electrode<sup>12</sup>; *i.e.*, the phase varies much more smoothly than the discrete electrodes suggest. Therefore we represent the position dependence of the voltage applied across the dielectric as a continuous function, giving two examples below.

(i) **For a constant speed** (*c.f.* Eq. 1) we consider a traveling, oscillatory voltage applied symmetrically across the dielectric in the vertical  $z$  direction,  $V = V_0 e^{i(\omega t - ky)}$ . Here  $y$  is the distance along the antenna's long axis and  $V_0$  and  $k$  are constants. Let the dielectric extend from  $z = -z_0$  to  $z = +z_0$  in the vertical direction; assuming that it is uniform, the potential at a general position  $(y, z)$  in the dielectric is

$$V(y, z, t) = V_0 \frac{z}{2z_0} e^{i(\omega t - ky)}. \quad (4)$$

(ii) **For the wavepacket** shown in Fig. 2, main paper, the voltage is given by  $V_0 e^{i\omega[t-p(y)]} e^{-\alpha^2[t-p(y)]^2}$ , where  $\alpha$  is a constant. This consists of a Gaussian convoluted with a travelling wave; both have the  $(y, t)$  dependence [given by  $p(y)$ ] required for the motion described in the main paper. Under the same assumptions as (i), the potential at  $(y, z)$  in the dielectric is

$$V(y, z, t) = V_0 \frac{z}{2z_0} e^{i\omega[t-p(y)]} e^{-\alpha^2[t-p(y)]^2}. \quad (5)$$

For either equation, the polarization  $\mathbf{P}$  is obtained<sup>8</sup> by

$$\mathbf{P} = \epsilon_0(\epsilon_r - 1)\mathbf{E} = \epsilon_0(\epsilon_r - 1)[- \nabla V(y, z, t)]. \quad (6)$$

Differentiating with respect to time, we obtain a polarization-current density<sup>8</sup>

$$\mathbf{J}(y, z, t) = \frac{\partial \mathbf{P}}{\partial t} \quad (7)$$

In evaluating the emitted radiation, we consider only the contribution of  $\mathbf{J}$  in the dielectric; there is a negligible conduction current, and we neglect the free charges that exist only at the interface between the dielectric and the electrodes. In this situation, the following equation<sup>7,8,13</sup> can be used to evaluate the magnetic vector potential  $\mathbf{A}$  at the observer/detector's remote location  $\mathbf{r}_P = (X, Y, Z)$  and at the observation time  $t_P$ :

$$\mathbf{A}(\mathbf{r}_P, t_P) = \frac{\mu_0}{4\pi} \int_{-z_0}^{z_0} \int_{-y_0}^{y_0} \int_{-x_0}^{x_0} \frac{\mathbf{J}(\mathbf{r}, t)}{|\mathbf{r}_P - \mathbf{r}|} dx dy dz \quad (8)$$

Here,  $\mathbf{r} = (x, y, z)$  is a coordinate within the dielectric. The integration is carried out over the volume of the dielectric; as in the main paper, its length is  $2y_0$  and its thickness in the  $x$  direction is  $2x_0$ . The retarded time  $t$  varies for different locations  $\mathbf{r}$  within the dielectric:

$$t = t_P - \frac{|\mathbf{r}_P - \mathbf{r}|}{c}. \quad (9)$$



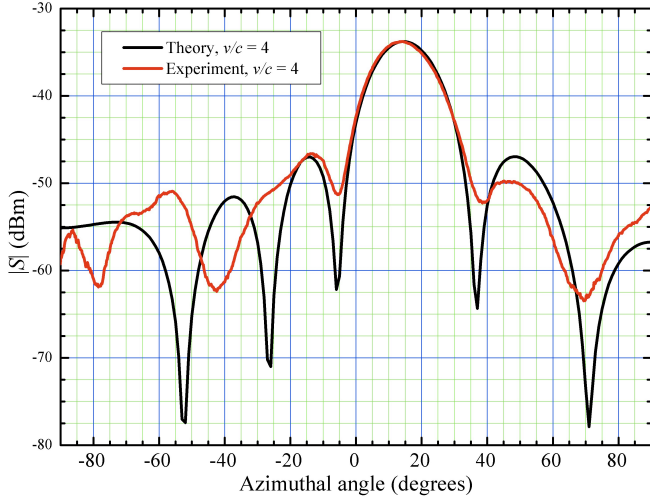


FIG. 5. Modulus of Poynting vector  $|S|$  [Eq. 12] versus azimuthal angle  $\phi$  (black) predicted by the calculations. The antenna dimensions are based on the example shown in Fig. 2(a). The frequency is  $\omega/2\pi = 2.4$  GHz,  $v/c = 4$  and the antenna to detector distance is 5 m. Experimental data for the same antenna, measured at the same distance (5 m) in an anechoic chamber, are shown in red. After correction for the gain of the detector dipole and losses in its cables, there is a reasonable quantitative match between experiment and calculation.

Here  $c$  again denotes the speed of electromagnetic waves in the medium (assumed to be uniform) between the source and the observer.

The corresponding radiation fields are derived from differentiating  $\mathbf{A}$  with respect to the *observer's* coordinates  $(X, Y, Z, t_P)$ . The electric field is given by<sup>6,8</sup>

$$\mathbf{E}(X, Y, Z, t_P) = \frac{\partial \mathbf{A}(X, Y, Z, t_P)}{\partial t_P}, \quad (10)$$

and since the magnetic flux is always solenoidal (*i.e.*,  $\nabla \cdot \mathbf{B} = 0$ ), the magnetic flux density  $\mathbf{B}$  is given by<sup>6,8</sup>

$$\mathbf{B}(X, Y, Z, t_P) \equiv \nabla \times \mathbf{A}(X, Y, Z, t_P). \quad (11)$$

We again emphasize that the curl operator ( $\nabla \times$ ) employs *observer* coordinates  $(X, Y, Z)$ . In free space, the magnetic field is simply  $\mathbf{H} = \frac{1}{\mu_0} \mathbf{B}$ . The received power is computed by evaluating the Poynting vector<sup>7,8</sup>

$$\mathbf{S}(X, Y, Z, t_P) = \mathbf{E}(X, Y, Z, t_P) \times \mathbf{H}(X, Y, Z, t_P). \quad (12)$$

The steps up to and including Eq. 7 are carried out analytically; the integral [Eq. 8], the two derivatives [Eqs. 10 and 11] and their cross-product [Eq. 12] are evaluated numerically<sup>14</sup>.

## B. Numerical results

An example of the numerical calculations for constant  $v/c$  is compared with experimental data in Fig. 5. The experimental conditions [voltage applied to the electrodes, polarization-current speed ( $v/c = 4$ ), dielectric dimensions- the antenna

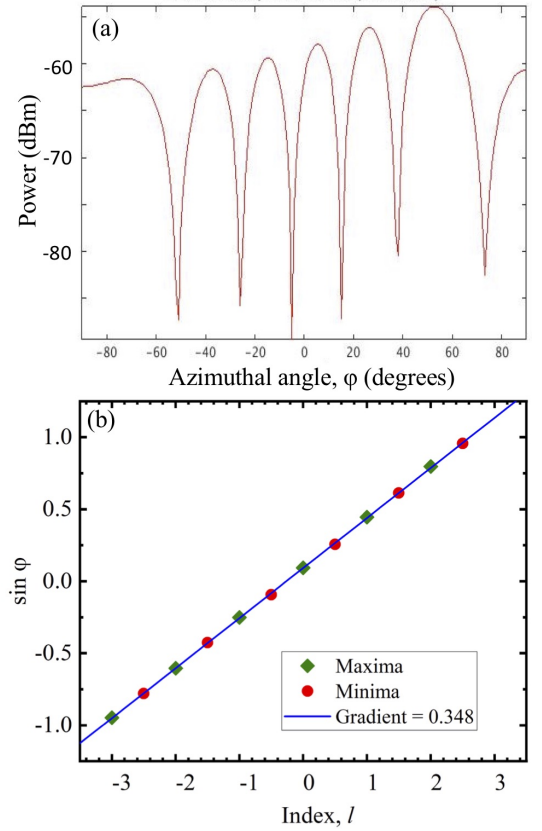


FIG. 6. a) Simulated received power versus azimuthal angle  $\phi$  for an antenna-to-detector distance of 10.0 m, and subluminal source speed  $v/c = 0.5$ ; the antenna simulated is that in Fig. 2(a) and data are shown for  $\omega/2\pi = 2.5$  GHz. As is the case for the experimental data shown in Fig. 3(a), the simulated power oscillates with azimuthal angle. (b) A plot of  $\sin \phi$  versus index  $l$ , where  $\phi$  denotes the angle at which a maximum (blue) or minimum (red) in power occurs, for the numerical data in (a). The gradient of the fitted line is 0.35, very close to the experimental values shown in Fig. 3(b).

is that shown in Fig. 2(a)] are used as model input parameters. After correction for the gain of the receiver dipole and cabling used in the experiment, there is a reasonable quantitative match between data and theory, especially close to the main lobe. At larger angles, the match is less good. This is understandable, because the subsidiary minima are very dependent on the precise phases of the signals applied to each antenna element, which are subject to errors of a few degrees in the experiment<sup>14</sup>. Similar quantitative agreement between model and anechoic chamber data was obtained for all speeds above  $v/c = 2$ .

Turning to subluminal speeds, Fig. 6(a) shows a simulation of the antenna shown in Fig 2(a) run at  $v/c = 0.5$ , frequency  $\omega/2\pi = 2.5$  GHz and for an antenna-to-detector distance of 10 m. The calculated power oscillates with azimuthal angle in a similar manner to the experimental data [see Fig. 3(a)]. Fig. 6(b) plots the  $\sin \phi$  versus index  $l$  for the model calculation shown in Fig. 6(a); positions of both minima and maxima are shown. The gradient of the fitted line is 0.35, close to the experimental gradients shown in Fig. 3(b).



The results in Figs. 3 [experimental] and 6 [model] may be understood as follows<sup>14</sup>. Ideally, *no* vacuum Čerenkov radiation should be emitted for  $|v/c| < 1$ , as the emission angle  $\sin^{-1} c/v$  becomes imaginary<sup>10,15</sup>. In this context, “ideal” implies an infinitely-long source of identical elements, in which the radiation from all elements superposes to produce no net emission. However, the 32-element antenna shown in Fig. 2(a) is of finite length, so that the radiation measured in the  $v/c = 0.5$  experiments is likely to come mostly from the *ends* of the array; the elements at the ends have adjacent elements on only one side. Hence, one might expect that about half of their emitted power would be cancelled out, so that the two end elements behave like a double-slit experiment emitting a total power  $\sim (1/2) \times 2 \times (1/32) = 1/32$  of the total power of the array. Converting into dB,  $10\log_{10}(1/32) = -15$  dB, explaining why the peak subluminal emission in both experiment and simulations is 15 – 20 dB lower than the peak vacuum Čerenkov power produced at speeds  $v/c > 2$ , where all 32 elements contribute.

Using Eq. 3 with the relevant wavelengths  $\lambda = 2\pi c/\omega$ , the gradients of the experimental data for  $\omega/2\pi = 2.4$  GHz and 2.6 GHz [Fig. 3(b)] yield  $b = 370$  mm and  $b = 360$  mm, and the simulation [ $\omega/2\pi = 2.5$  GHz; Fig. 6(b)]  $b = 347$  mm, values that are very close to the 348 mm overall length of the array of 32 elements [Fig. 2(a)]. Moreover, for  $v/c = 0.5$ , the phase difference of elements  $j = 1$  and  $j = 32$  is very close to  $11\pi$ , explaining why the experimental “interference pattern” has *minima* quite close to the values of  $\phi$  given by Eq. 3<sup>14</sup>.

Examples of simulated emission from propagating pulses produced by driving voltages analogous to that given in Eq 5 are displayed in the main body of the paper.

#### IV. SMALL REGION OF POLARIZATION CURRENT IN SUPERLUMINAL ROTATION

Consider a polarization-current element of small volume that rotates in the  $xy$ -plane at radius  $r$  with angular velocity  $\eta$  and emits radiation (hereafter referred to as *the source*). In terms of the cylindrical coordinates  $r$ ,  $\phi$  and  $z$ , the path  $\mathbf{r}(t) = (r, \phi, z)$  of the source is given by

$$r = \text{const}, \quad \phi = \phi_Z + \eta t, \quad z = 0, \quad (13)$$

where the coordinate  $\phi_Z$  denotes the initial azimuthal position of  $\phi$  and is, without loss of generality, assumed to be zero from now on. The wave fronts that are emitted by this point source in an empty and unbounded space can then be described by

$$|\mathbf{r}_P - \mathbf{r}| = c(t_P - t); \quad (14)$$

as before, the constant  $c$  denotes the wave speed and the observation/detection point is defined as  $(\mathbf{r}_P, t_P) = (r_P, \phi_P, z_P, t_P)$ . Inserting (13) into (14) and utilizing the theorem of Pythagoras we find that the distance  $R$  which separates the source from the observer/detector is given by

$$R(t) = [z_P^2 + r_P^2 + r^2 - 2rr_P \cos(\phi_P - \eta t)]^{1/2}. \quad (15)$$

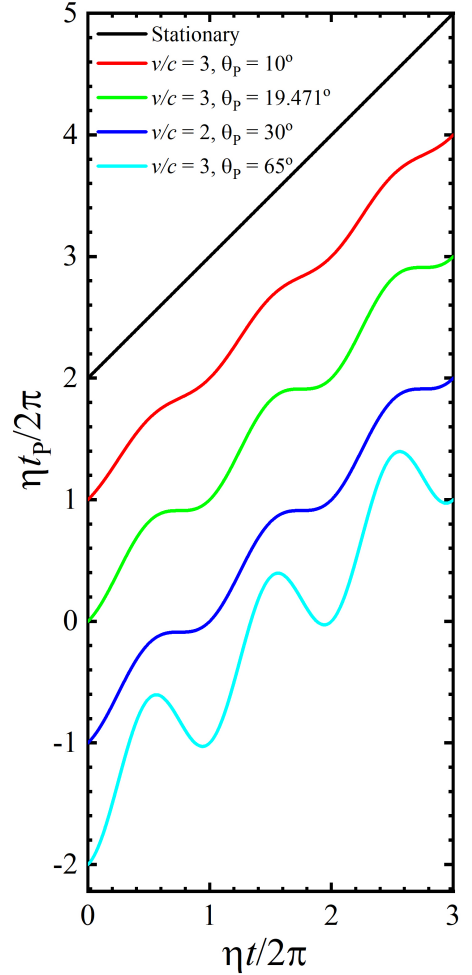


FIG. 7. Various forms that Eq. 16 can take depending on the position of the observer (refer to Fig. 8); the times on both axes are scaled by the source angular velocity,  $\eta$ . The curves are shown for  $r_P = 100r_L$ , where  $r_L = c/\eta$  is the light-cylinder radius, and  $\phi_P = 0$ ; finite  $\phi_P$  merely introduces a phase shift. The observation polar angles  $\theta_P$  and the source tangential speed  $v$  are shown in the inset key. Note that  $\theta_P = \sin^{-1}(c/v)$  for the green and dark blue curves. Curves are offset by vertical increments of  $\eta t_P/2\pi = 1$  for clarity, and, for reference, the black line shows the 1 : 1 correspondence between emission and observation time that would occur for a stationary source. (Curves similar to those shown in light blue and red were first derived in Ref. 10; curves analogous to those shown in green and dark blue are presented in Ref. 16.)

In consequence, the relationship between the emission time  $t$  and the reception (detection) time  $t_P$  must satisfy

$$t_P = t + \frac{R(t)}{c} \quad (16)$$

$$= t + \frac{1}{c} [z_P^2 + r_P^2 + r^2 - 2rr_P \cos(\phi_P - \eta t)]^{1/2}.$$

Fig. 7 shows the three generic forms that Eq. 16 can take, whilst Fig. 8 identifies the observer positions corresponding to these forms. In the following discussion, it is helpful to

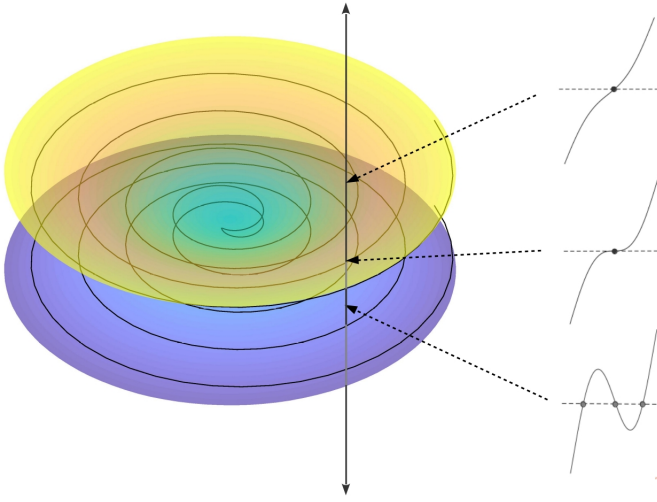


FIG. 8. Illustrations of the regions in which Eq. 16 takes the various forms shown in Fig. 7. The  $z$  axis is vertical, and the circular source orbit lies in the green ( $z = 0$ ) plane. The “double-funnel” structure (yellow and purple; symmetrical about the rotation plane  $z = 0$ ) represents observer positions at which the source momentarily approaches with an instantaneous speed of  $c$  and with zero acceleration. Instantaneous positions of points of this nature are shown as the “spiralling” fine line superimposed on the surface. The shape of Eq. 16 for each region is shown by the curves plotted around the figure, with arrows linking each curve to the place in which it would be observed. The central arrow point lies exactly on the double-funnel structure; the black vertical line traverses the surfaces and is included to clarify the positions of the arrow points. [After Ref. 14.]

define the observer’s polar angle as

$$\theta_P = \tan^{-1} \left( \frac{r_P}{z_P} \right). \quad (17)$$

First, the green and dark-blue curves in Fig. 7 correspond to an observer positioned on (or very close indeed to) the yellow/purple surface shown in Fig. 8; this surface represents observer positions at which the source momentarily approaches with an instantaneous speed of  $c$  and with zero acceleration. The surface can be found (with some effort) by differentiating Eq. 15 and setting  $(dR/dt) = -c$  and  $(d^2R/dt^2) = 0$ . With increasingly large distances  $[(r_P^2 + z_P^2)^{1/2} \gg r]$ , the surfaces asymptotically tend to cones with half angles  $\theta_P = \sin^{-1}(c/v)$ , where  $v = r\eta$  is the instantaneous (tangential) speed of the source. The green and dark blue curves in Fig. 7 correspond to such an observation angle.

Inside the surface (Fig. 8), plots of Eq. 16 will be similar to the red curve in Fig. 7, whilst outside it, an oscillatory form exemplified by the light blue curve occurs.

The discussion in the final section of the main paper focuses on  $t_P$  versus  $t$  curves such as the green and dark blue examples shown in Fig. 7. Apart from a single point at their center where  $dt_P/dt = 0$ , the “steps” are not flat<sup>14</sup>. However, there is a reasonable region of  $t$  over which  $dt_P/dt \ll 1$ .

\* jsingle@lanl.gov

<sup>1</sup> A. Ardavan, W. Hayes, J. Singleton, H. Ardavan, J. Fopma, and D. Halliday, *Corrected Article: “Experimental observation of nonspherically-decaying radiation from a rotating superluminal source”* J. Appl. Phys. **96**, 7760, (2004).

<sup>2</sup> J. Singleton, A. Ardavan, H. Ardavan, J. Fopma, D. Halliday, and W. Hayes, *Experimental demonstration of emission from a superluminal polarization current – A new class of solid-state source for MHz – THz and beyond*, Conference Digest of the 2004 Joint 29th International Conference on Infrared and Millimeter Waves and 12th International Conference on Terahertz Electronics, IEEE Cat. No. 04EX857, (2004).

<sup>3</sup> John Singleton, Lawrence M. Earley, Frank L. Krawczyk, James M. Potter, William P. Romero, Zhi-Fu Wang, *Superluminal Antenna*, US Patent number 9948011 (February 2012, reissued April 2018).

<sup>4</sup> Frank Krawczyk, John Singleton, Andrea Caroline Schmidt, *Continuous antenna arrays*, US Patent, filed August 2018 [USSN 62/721,031]

<sup>5</sup> John Singleton, Andrea Caroline Schmidt *Antenna and transceiver for transmitting a secure signal* US Patent number 9722724 (August 2017).

<sup>6</sup> J. D. Jackson, *Classical Electrodynamics*, Third Edition, John Wiley & Sons, Inc., New York, 1999.

<sup>7</sup> C. A. Balanis, *Advanced Engineering Electromagnetics*, Second Edition, John Wiley & Sons, Inc., Hoboken, NY, 2012.

<sup>8</sup> B. I. Bleaney and B. Bleaney, *Electricity and Magnetism*. The Oxford Classic Text Edition, Oxford University Press, Oxford, UK, 2013.

<sup>9</sup> A. Sommerfeld, *Zur Elektronentheorie* (3 Teile), Nach. Kgl. Ges. Wiss. Göttingen, Math. Naturwiss. Klasse, 99–130, 363–439 (1904), 201–35 (1905).

<sup>10</sup> G. A. Schott, *Electromagnetic radiation and the mechanical reactions arising from it*, (Cambridge University Press, 1912).

<sup>11</sup> G.A. Brooker, *Modern Classical Optics* (Oxford University Press, Oxford, 2003).

<sup>12</sup> Frank Krawczyk, to be published.

<sup>13</sup> O. D. Jefimenko, *Electricity and Magnetism: An Introduction to the Theory of Electric and Magnetic Fields*, Second Edition, Electret Scientific, Waynesburg, PA, 1989.

<sup>14</sup> A. C. Schmidt-Zweifel, *Theoretical and Experimental Studies of the Emission of Electromagnetic Radiation by Superluminal Polarization Currents*. PhD thesis, University of New Mexico, (2020).

<sup>15</sup> V. L. Ginzburg, *Vavilov-Čerenkov effect and anomalous Doppler effect in a medium in which wave phase velocity exceeds velocity of light in vacuum*, Sov. Phys. JETP, **35** 1:92 (1972).

<sup>16</sup> H. Ardavan, *Generation of focused, nonspherically decaying pulses of electromagnetic radiation*, Phys. Rev. E, **58**, 6659 (1998).

[DISCOVER](#) / [NEWS](#) / [0323 LIGHTSLINGER](#)

# **Smaller, more versatile antenna could be a communications game-changer**

**‘Lightslinger’ antenna has potential applications for 5G and defense communications**

MARCH 23, 2022

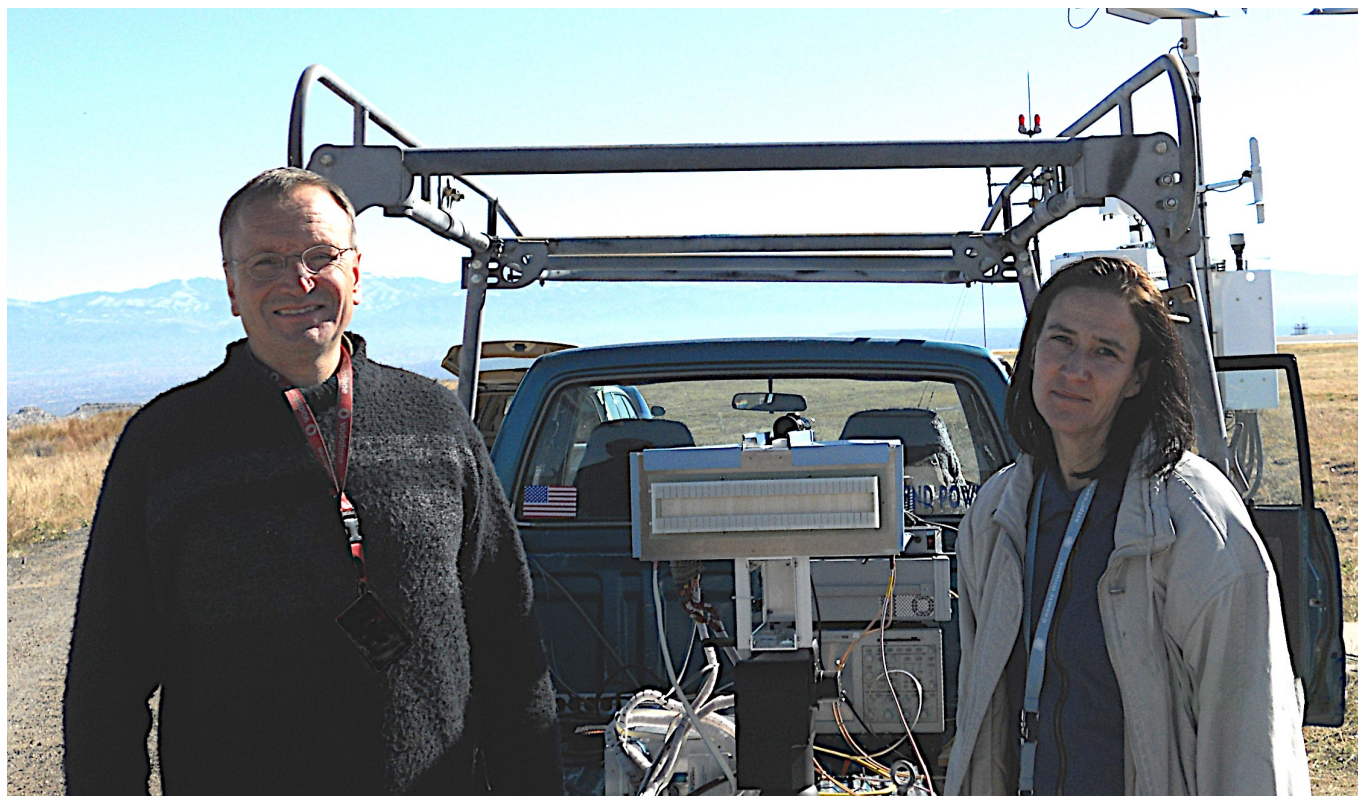


As wireless communications technology continues to advance, the need for smaller, more versatile and energy- and cost-efficient antennas is becoming increasingly important. Now, scientists and engineers at Los Alamos National Laboratory have developed a new type of antenna, called LightSlinger, to meet this need.

“We have been developing LightSlingers at Los Alamos for more than 15 years,” said John Singleton, condensed matter physicist and one of the two principal investigators on the project. “They were initially developed as fundamental science models for violent astronomical phenomena, but we soon realized that they were more efficient and considerably more flexible than conventional antennas of a similar size.”



Added his colleague and co-investigator Andrea Schmidt, “Our hope is that LightSlingers will, in the near future, replace outdated base-station antenna technology around the globe and expedite the rollout of 4G.”



A prototype LightSlinger flanked by the co-Pis John Singleton and Andrea Schmidt at Los Alamos airport. The prototype machine successfully performed a high-fidelity transmission of music.

Their small size, relatively light weight, power efficiency and resiliency against abusive treatment make them more versatile than equivalent conventional antennas. In addition, LightSlingers can be built in unusual shapes such as flat panels, cylinders or disks that are uniquely optimized to particular situations and applications. For example, they could form part of ceramic armor applied to a tank or unmanned ground vehicle.

LightSlingers use volume-distributed polarization currents, animated within a dielectric to faster-than-light speeds, to emit electromagnetic waves. (By contrast, traditional antennas employ surface currents of subluminally moving massive particles on localized metallic elements such as dipoles.) Owing to the superluminal motion of the radiation source, LightSlingers are capable of “slinging” tightly focused wave packets with high precision toward a location of choice. This gives them potential advantages over phased arrays in



secure communications such as 4G and 5G local networks as well as warfighter communications and radar applications.

Several prototypes of Lightslinger have been tested in lab environments and in the field over distances of up to 76 km. Also, three of them were independently validated by a U.S. telecommunications company. Los Alamos is now looking to transition the antennas to commercial prototypes that can be field tested and mass-produced by additive manufacturing and robotic processing.

LA-UR-22-22473

---

## CONTACT

[Laura Mullane](#) | (505) 412-7733 | [mullane@lanl.gov](mailto:mullane@lanl.gov)

---

## TOPICS

[Science](#) | [Technology](#)

---

## MORE STORIES

[All News >](#)

**'Frustrated'  
nanomagnets order**

**Perseverance analyzes  
first sounds from Mars**



## SUBSCRIBE TO OUR NEWSLETTER

Sign up to receive the latest news and feature stories from Los Alamos National Laboratory

**SIGN UP**

## Los Alamos National Laboratory

P.O. Box 1663

Los Alamos, NM 87545

(505) 667-5061



## INFORMATION

[Emergency, Fire](#)

[Events, Lectures](#)

[Ombuds](#)

[Resources](#)

[Reading Room](#)

[Science Museum](#)

## AT THE LAB

[Business Opportunities](#)

[Jobs](#)

[Organizations](#)

[Research Library](#)

[User Facilities](#)

## FOR EMPLOYEES

[AskIT](#)

[LANLInside](#)

[MyMail](#)

[New Hire Process](#)

[SSL Portal](#)

[Training](#)

[Contact Us](#) | [Terms of Use/Privacy](#) | [Site Feedback](#)

Managed by Triad National Security, LLC for the U.S. Dept. of Energy's NNSA

Copyright 2022 Triad National Security, LLC. All Rights Reserved.

[Learn about the Department of Energy's Vulnerability Disclosure Program](#)

# Emitting Radio Waves with Polarization Currents

An unconventional antenna technology can focus the radio waves emitted from the acceleration of polarization currents, aiding use of the waves in communication applications.

By Erika K. Carlson

In conventional radio technology, radio waves are generated by accelerating charged particles, such as electrons. Now, John Singleton of Los Alamos National Laboratory, New Mexico, and colleagues have demonstrated a way to focus information carried by radio waves that are instead emitted by accelerated polarization currents—the propagation of fluctuations in the dipole moments of molecules [1]. Unlike electrons or ions, polarization currents can propagate faster than the speed of light. This factor, and the ability of these currents to radiate from a large volume, gives the technology capabilities inaccessible to conventional antennas, the researchers say.

The antenna consists of a dielectric layer sandwiched by two rows of electrodes. The researchers increase and decrease the voltage differences across pairs of opposing electrodes to manipulate dipole moments in the dielectric. Making those dipole moments larger and smaller creates a polarization

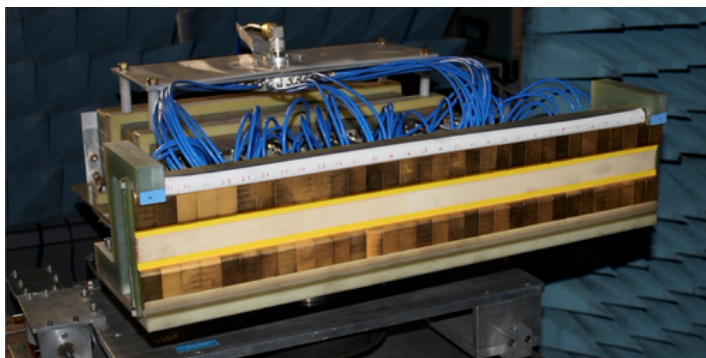
current that runs through the whole dielectric in the same way that sports fans standing and waving their arms in succession create a stadium wave. By carefully timing the voltage changes, the researchers generate a polarization current that accelerates to a speed much faster than that of light.

The current's properties grant the antenna special features. The antenna can create intense concentrations of emitted radiation that amplify a signal, similar to the way a jet accelerating through the speed of sound can create a sonic boom. That means that operators could broadcast signals in such a way that only a detector at a specific point in space can receive the signal in the same form that it was emitted, enabling a polarization-current antenna to send private wireless signals.

Erika K. Carlson is a Corresponding Editor for *Physics* based in New York City.

## REFERENCES

1. J. Singleton *et al.*, “Information carried by electromagnetic radiation launched from accelerated polarization currents,” *Phys. Rev. Applied* **14**, 064046 (2020).



Credit: J. Singleton *et al.* [1]



# Meet the Lightslingers

Andrea Schmidt<sup>1</sup>, John Singleton<sup>2</sup>,  
<sup>1</sup>ISR-2

<sup>2</sup>National High Magnetic Field Laboratory, MPA-MAGLAB  
Los Alamos National Laboratory, NM 87545, USA

Electromagnetic applications such as Radar or telecommunications use decades-old technology: dipoles, dish/horn antennas, phased arrays.

- High transmit powers
- Environmental/health concerns.
- Overload of available frequency spectrum.

**Need new approach!**





Hostile plane  
picks up stray  
signals



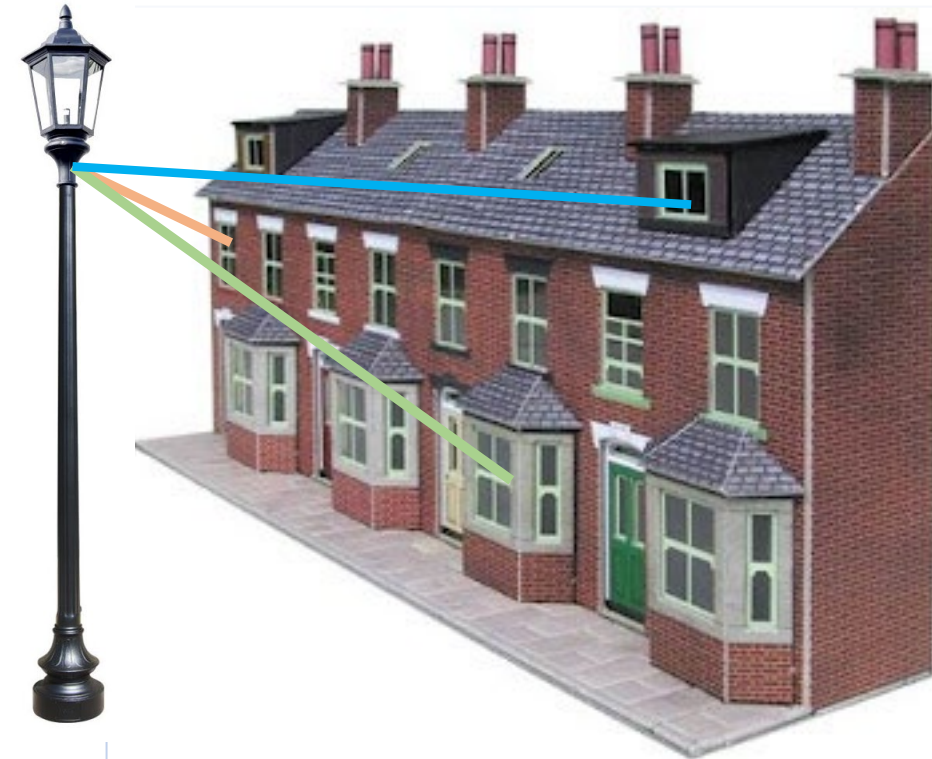
Friendly  
drone



Conflict zone: several (semi-) autonomous vehicles exchange data about threats, targets; don't want hostiles to know what they know.

**The problem:** conventional radio is not very directional unless antenna is enormous; selectivity is via narrow frequency bands. Situation has not changed much since Battle of Jutland (1916). Security compromised.

Coming soon: 5G local network concept: small array (~35 GHz) mounted on existing infrastructure; sends signals successively into individual apartments or rooms.



Can your neighbor see what you ordered on Amazon? Will it be possible to work on sensitive projects at home?

## **Lightslingers:** Polarization-current antennas

Maxwell's 3<sup>rd</sup> and 4<sup>th</sup> equations:

$$\nabla \times \mathbf{E} + \frac{\partial \mathbf{B}}{\partial t} = 0$$

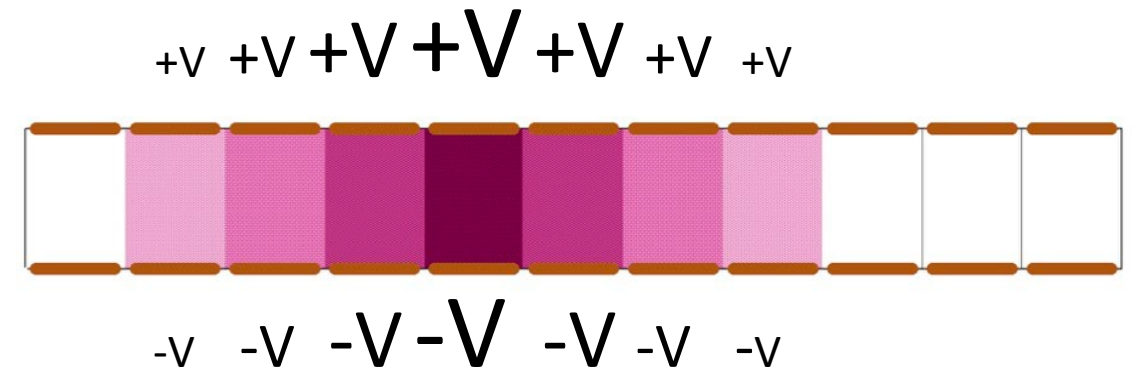
$$\nabla \times \mathbf{H} - \epsilon_0 \frac{\partial \mathbf{E}}{\partial t} = \mathbf{J}_{\text{free}} + \frac{\partial \mathbf{P}}{\partial t}$$

- Left-hand side: propagation of electromagnetic radiation.
- Right-hand side: source terms.

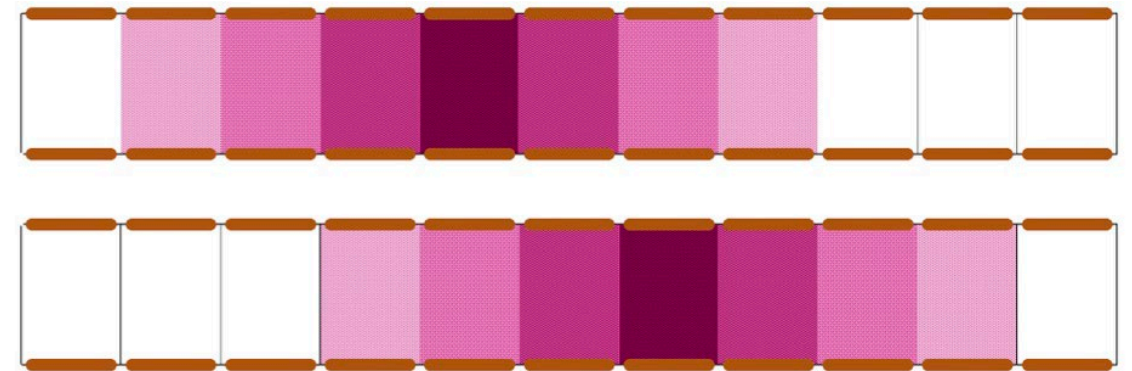
$\mathbf{J}_{\text{free}}$  = current of free electrons (ordinary antennas, light bulbs, synchrotrons).

Our antennas use a moving **polarization current**  $\partial \mathbf{P} / \partial t$  as the source.

**Making polarization  $\mathbf{P}$ :** apply voltages to Cu electrodes either side of a strip of alumina:



**Making it move:** shift voltages to neighbouring electrodes: polarization moves as well.



It moves, so we have  $\partial \mathbf{P} / \partial t$ .



## **Lightslingers:** Polarization-current antennas

Maxwell's 3<sup>rd</sup> and 4<sup>th</sup> equations:

$$\nabla \times \mathbf{E} + \frac{\partial \mathbf{B}}{\partial t} = 0$$

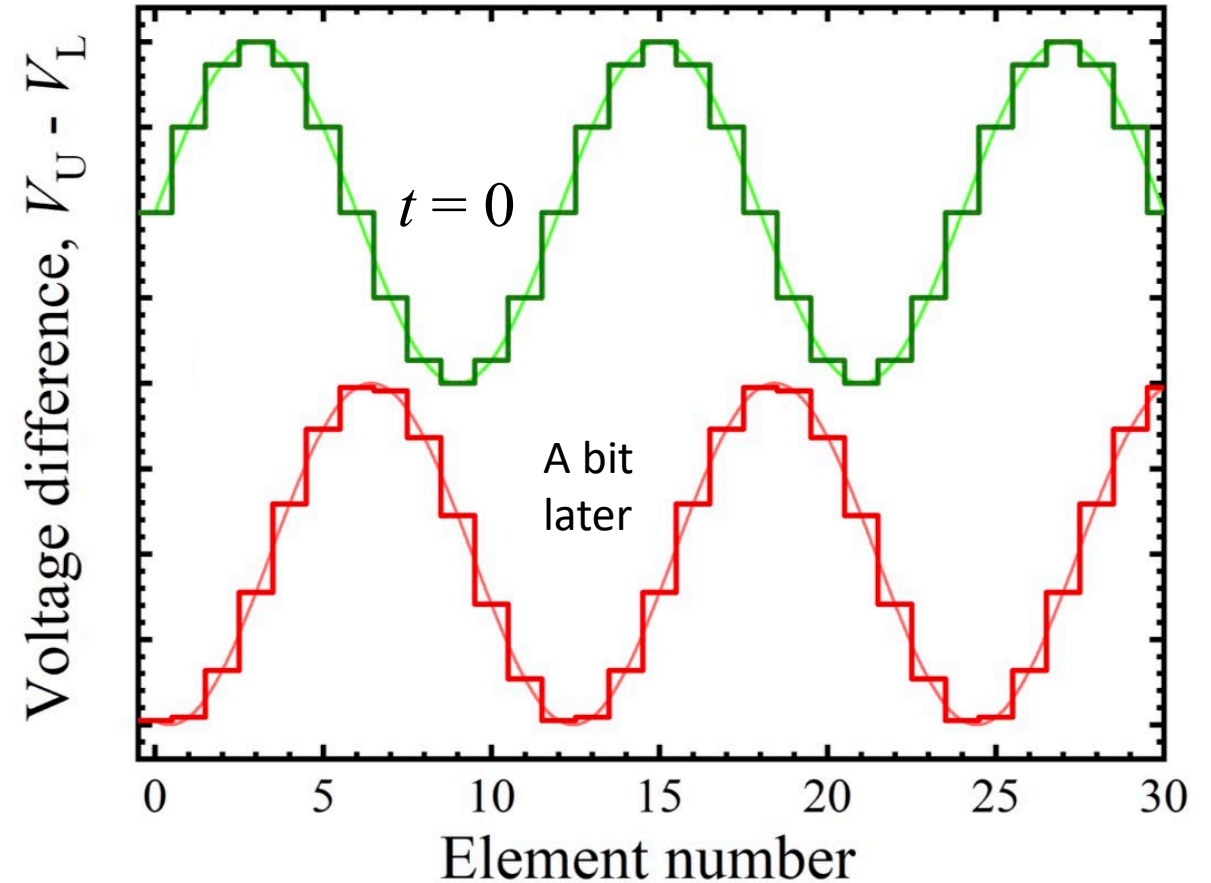
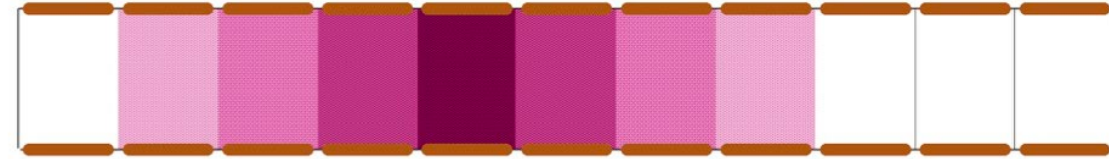
$$\nabla \times \mathbf{H} - \epsilon_0 \frac{\partial \mathbf{E}}{\partial t} = \mathbf{J}_{\text{free}} + \frac{\partial \mathbf{P}}{\partial t}$$

- Left-hand side: propagation of electromagnetic radiation.
- Right-hand side: source terms.

$\mathbf{J}_{\text{free}}$  = current of free electrons (ordinary antennas, light bulbs, synchrotrons).

Our antennas use a moving **polarization current**  $\partial \mathbf{P} / \partial t$  as the source.

In practice, we feed signals with suitable phase differences to each electrode pair.

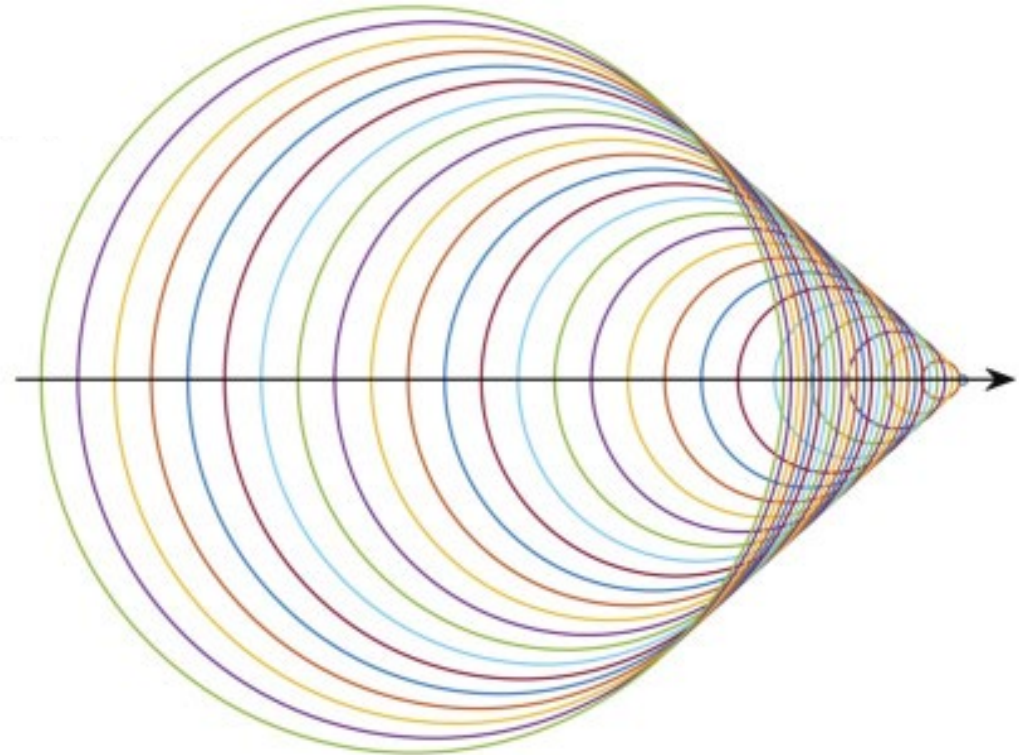


**Speeds** can be set by varying the phase differences between adjacent electrode pairs.



# Conventional Čerenkov Radiation

Usually, this is due to charged particles that travel faster than the speed of light  $c'$  in a medium such as water.



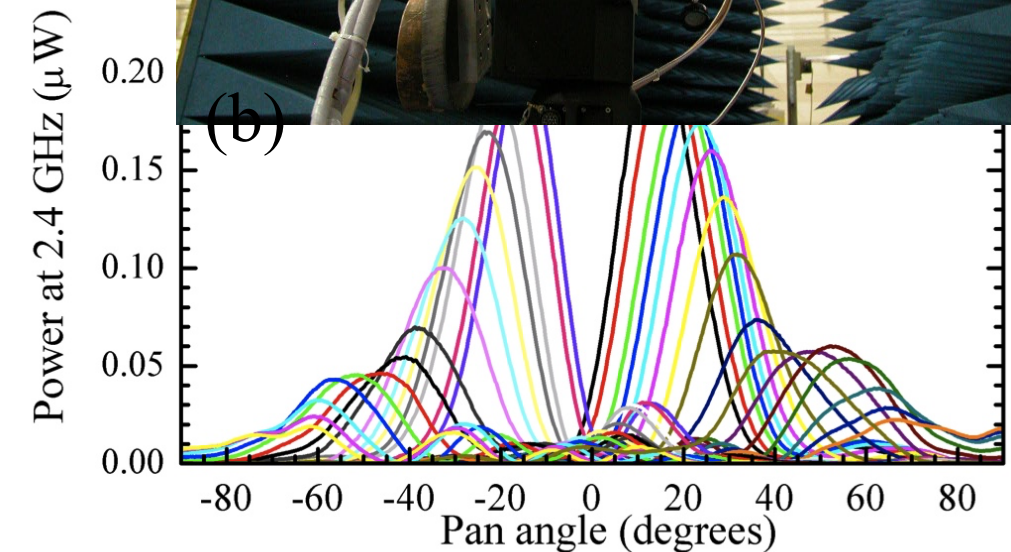
Analogous to Mach cone in acoustics: angle  $\sin \theta = c'/v$ .

(a)

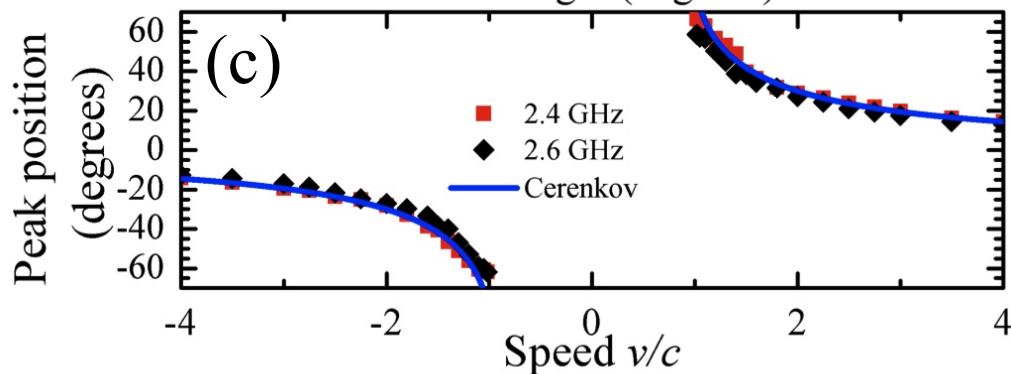


Lightslinger TD2

(b)

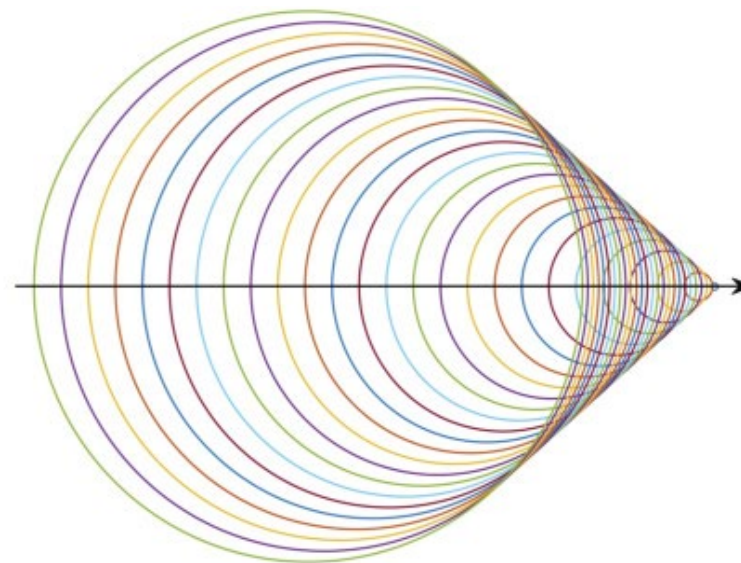


(c)



## Test: *Vacuum Vavilov-Čerenkov effect*

- Remember that polarization current is like a current of charged particles.
- Now, however, the “charge” travels faster than light in a vacuum.
- Run polarization current through antenna at many different speeds.
- Emitted radiation comes off at the correct angle: it is *vacuum Vavilov-Čerenkov radiation*.



# Why bother? Isn't this just a phased array? NO!

## Phased array

- The signal in a phased array is emitted from a series of discrete elements - point-like (electrically small antennas- ESAs) or line-like (dipoles).
- Skin depth effects in the metal elements mean that the emission is from surface currents.

## *Lightslinger:*

- The signal is emitted from the *entire volume of the dielectric by a volume-distributed current*.
- This eliminates fringing effects- antenna is more efficient.
- Other novel things we can do with a volume-distributed source: accelerate it smoothly, for example.
- Antenna can be any shape, optimized to a particular application.

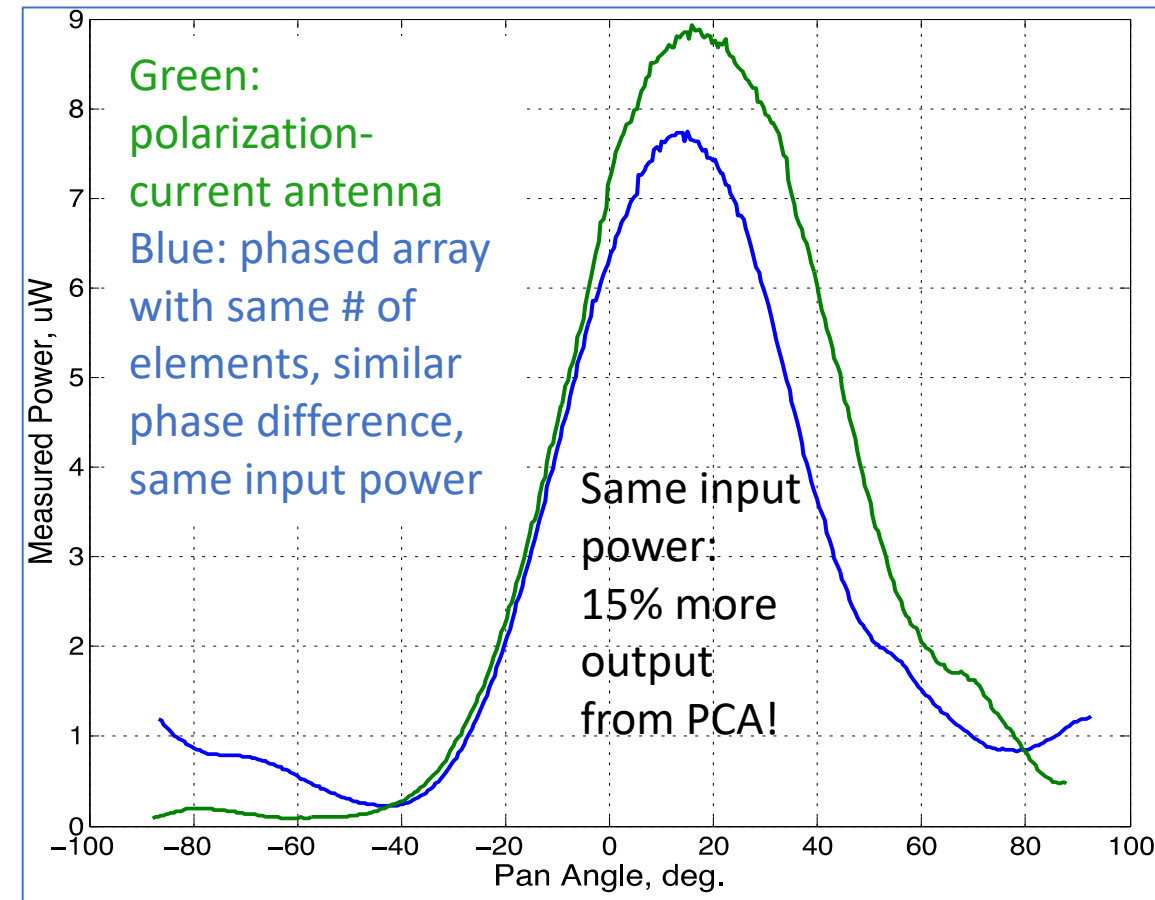
# Why bother? Isn't this just a phased array? NO!

## Phased array

- The signal in a phased array is emitted from a series of discrete elements - point-like (electrically small antennas- ESAs) or line-like (dipoles).
- Skin depth effects in the metal elements mean that the emission is from surface currents.

## *Lightslinger:*

- The signal is emitted from the ***entire volume of the dielectric by a volume-distributed current.***
- **This eliminates fringing effects- antenna is more efficient. (No radiation from back.)**
- Other novel things we can do with a volume-distributed source: accelerate it smoothly, for example.
- Antenna can be any shape, optimized to a particular application.





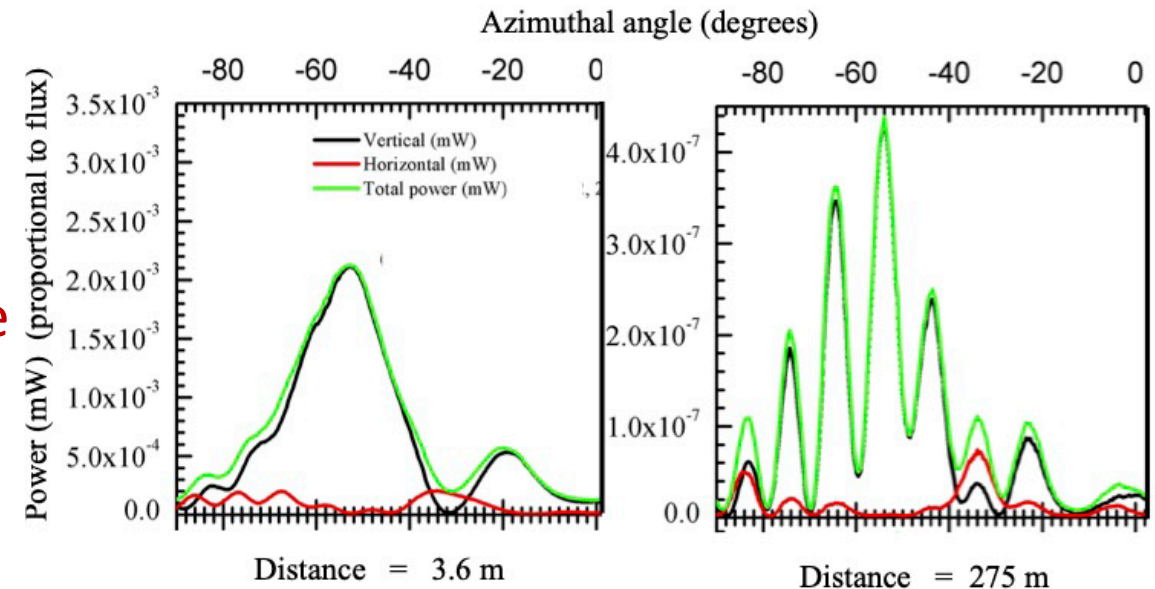
# Why bother? Isn't this just a phased array? NO!

## Phased array

- The signal in a phased array is emitted from a series of discrete elements - point-like (electrically small antennas- ESAs) or line-like (dipoles).
- Skin depth effects in the metal elements mean that the emission is from surface currents.

## *Lightslinger:*

- The signal is emitted from the *entire volume of the dielectric by a volume-distributed current*.
- This eliminates fringing effects- antenna is more efficient.
- Other novel things we can do with a volume-distributed source: accelerate it smoothly, for example.
- Antenna can be any shape, optimized to a particular application.



Data from tests at Sandia National Laboratory. At large distances, antenna acts like a coherent source. Peaks are a radio analogue of *laser speckle*. Ward Patitz (Range Superintendent) "I have never seen a phased array behave like this". **DIRECTED ENERGY APPs**. (More on similar things later.)

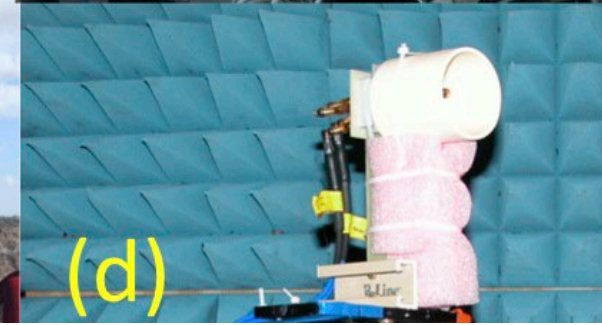
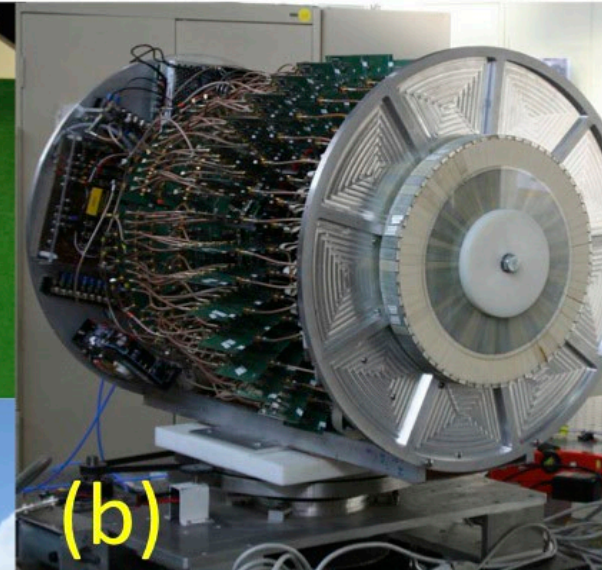
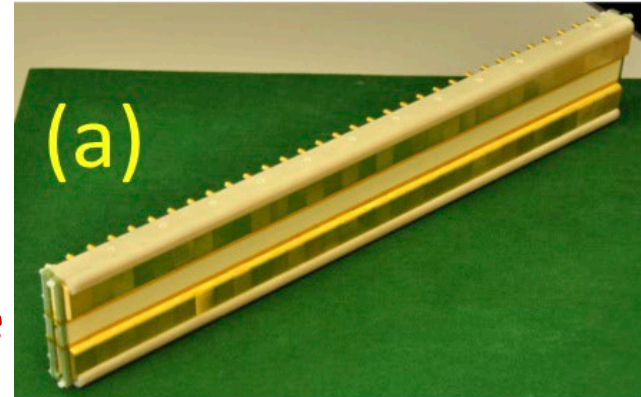
# Why bother? Isn't this just a phased array? NO!

## Phased array

- The signal in a phased array is emitted from a series of discrete elements - point-like (electrically small antennas- ESAs) or line-like (dipoles).
- Skin depth effects in the metal elements mean that the emission is from surface currents.

## *Lightslinger:*

- The signal is emitted from the *entire volume of the dielectric by a volume-distributed current*.
- This eliminates fringing effects- antenna is more efficient.
- Other novel things we can do with a volume-distributed source: accelerate it smoothly, for example.
- **Antenna can be any shape, optimized to a particular application.**



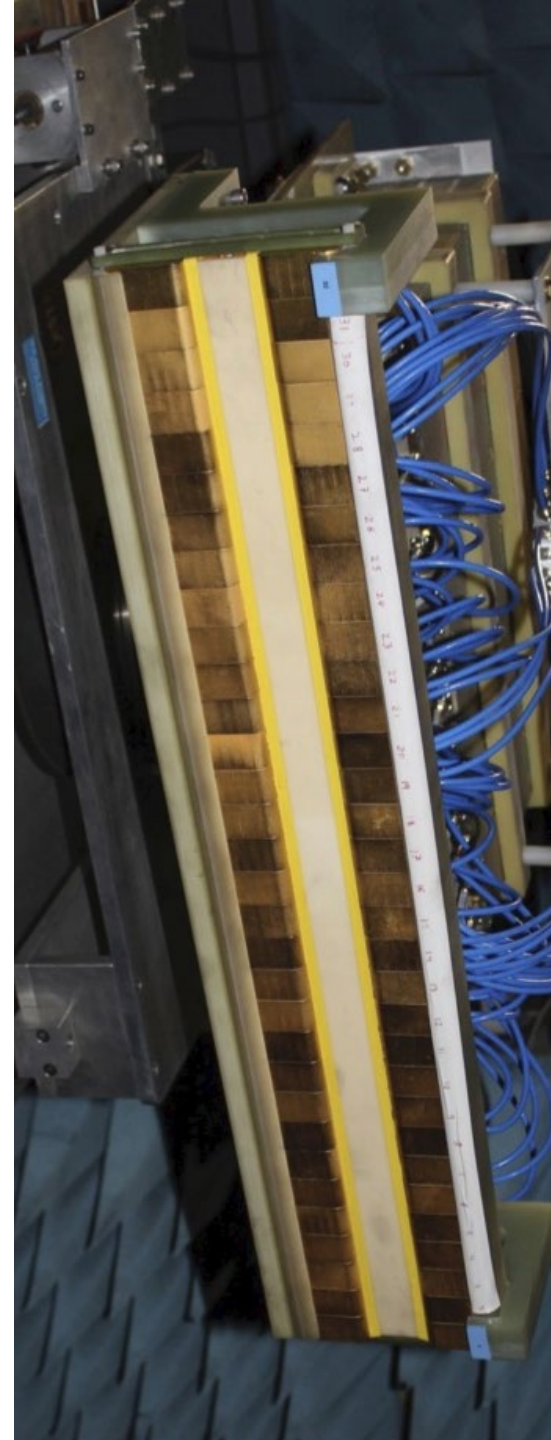
# Conventional roles: why *Lightslingers* are better

## (a) SWAP

- **Size:** *Lightslinger* is c. 25 % smaller than equivalent phased array.
- **Weight:** *Lightslingers* can be made very thin, with almost no metal components.
- **Assembly:** current base-station antennas have hundreds of small parts, assembled by hand in China; *Lightslingers* are monolithic structures amenable to 3D printing or CNC milling plus robot assembly. Let's bring antenna manufacture home to the US!
- **Power:** *Lightslinger* elements are designed only to emit forward- no fringing effects- c. 15 % more efficient than phased array.

## (b) Design

- *Lightslinger* shape can be tailored to particular role- use topology optimization/machine learning to design most efficient antenna possible.
- *Lightslinger* could take any shape- e.g., conforming to the bodywork of a vehicle or robot.
- *Lightslinger* can be made from ceramics- can be embedded seamlessly in ceramic armor of UAVs.

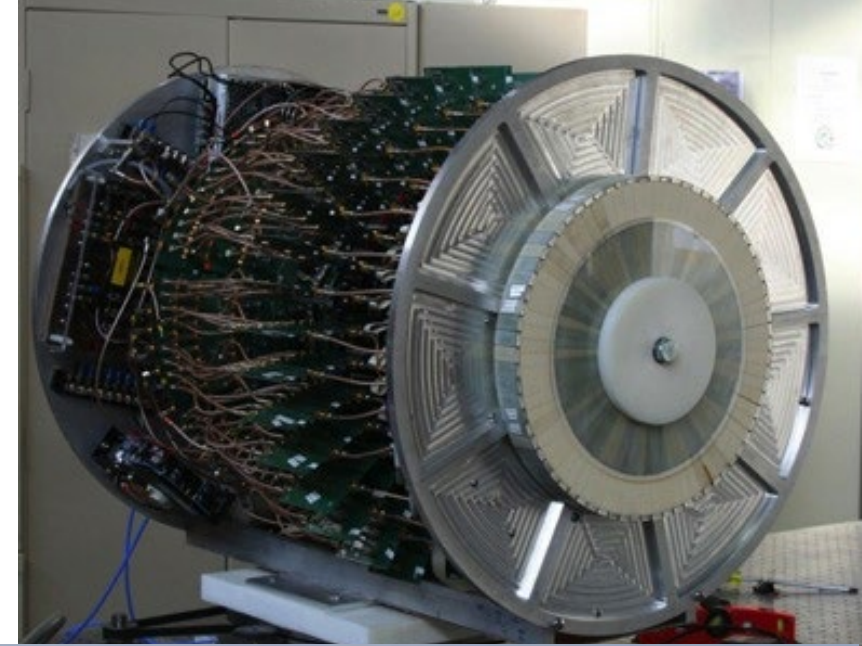




# New roles unique to *Lightslingers*

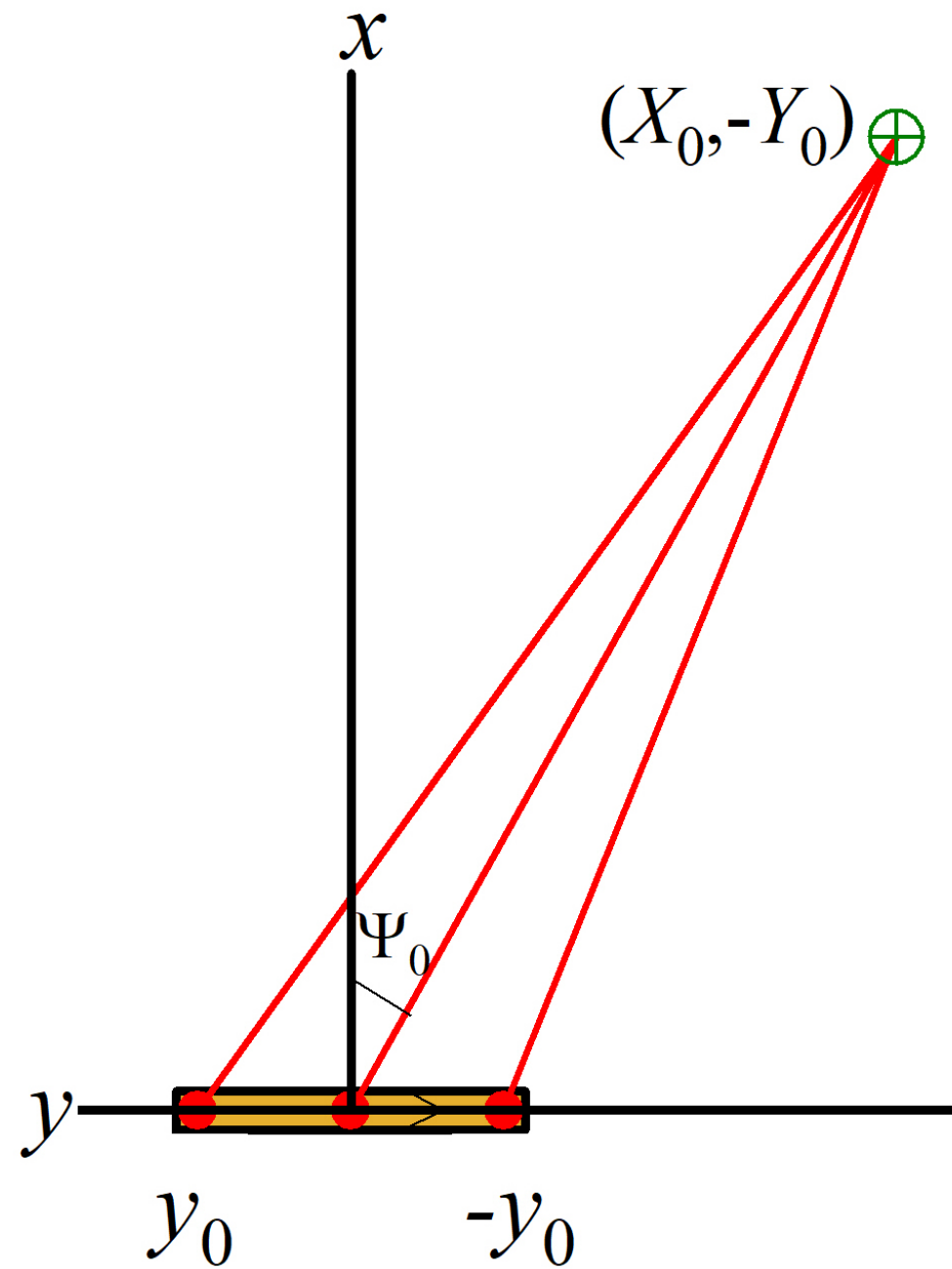
1. Directed energy/coherent sources.
2. Optical angular momentum.
3. Confusing phase fronts to make RADAR less vulnerable to countermeasures (patent issued).
4. Information focus by broadband transmission from an accelerated polarization current (patent).

As an example, focus on no. 4.





## Experimental concept



Run the antenna so that a small blob of polarization current travels such that the component of its velocity towards a target  $\oplus$  is always  $c$ . Source to target distance is  $r$ :

$$r^2 = X_0^2 + (Y_0 + y)^2$$

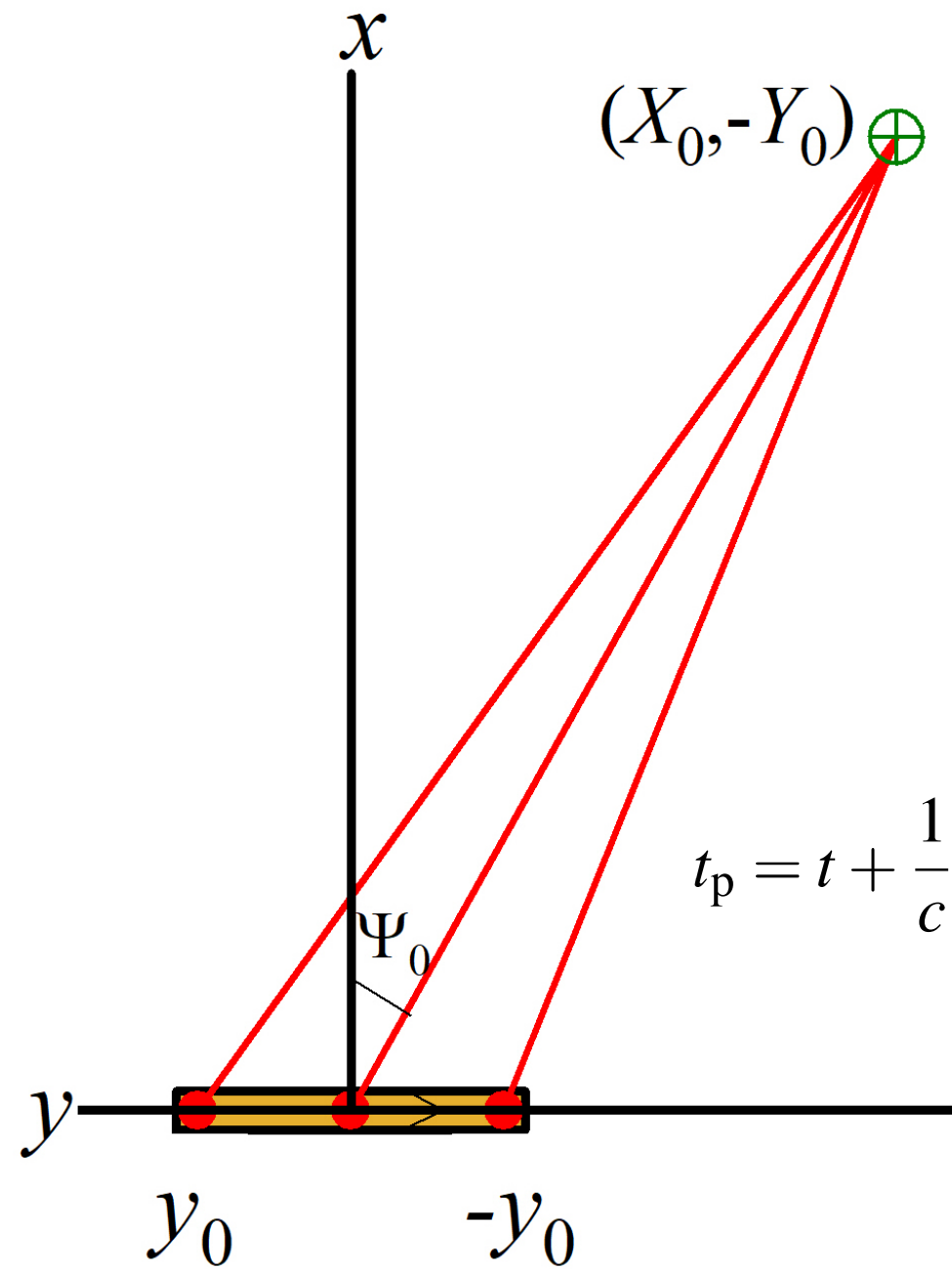
Now  $dr/dt = -c$  so that blob speed along antenna is:

$$\frac{dy}{dt} = -c \frac{[X_0^2 + (Y_0 + y)^2]^{\frac{1}{2}}}{Y_0 + y}$$

Integrating, the time that the blob is at position  $y$  is

$$t = \frac{1}{c} \left[ (X_0^2 + (Y_0 + y_0)^2)^{\frac{1}{2}} - (X_0^2 + (Y_0 + y)^2)^{\frac{1}{2}} \right]$$

## Experimental concept



Run the antenna so that a small blob of polarization current travels such that the component of its velocity towards a target  $\oplus$  is always  $c$ .

The time that the blob is at position  $y$  is

$$t = \frac{1}{c} \left[ (X_0^2 + (Y_0 + y_0)^2)^{\frac{1}{2}} - (X_0^2 + (Y_0 + y)^2)^{\frac{1}{2}} \right]$$

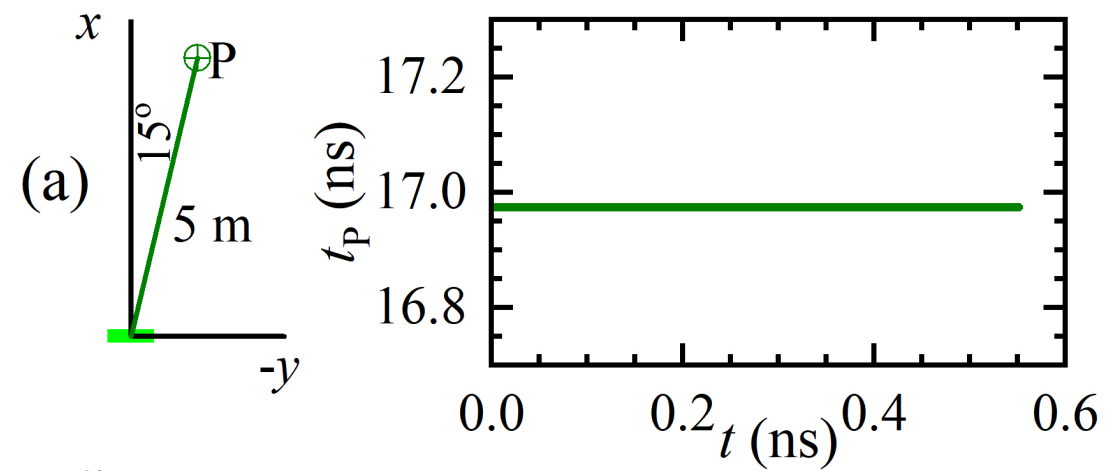
The blob emits light as it goes along. Consider a general receiver position  $(X, -Y)$ . The radiation arrives here at

$$t_p = t + \frac{1}{c} (X^2 + (Y + y)^2)^{\frac{1}{2}} = \frac{1}{c} \left[ (X_0^2 + (Y_0 + y_0)^2)^{\frac{1}{2}} - (X_0^2 + (Y_0 + y)^2)^{\frac{1}{2}} + (X^2 + (Y + y)^2)^{\frac{1}{2}} \right]$$

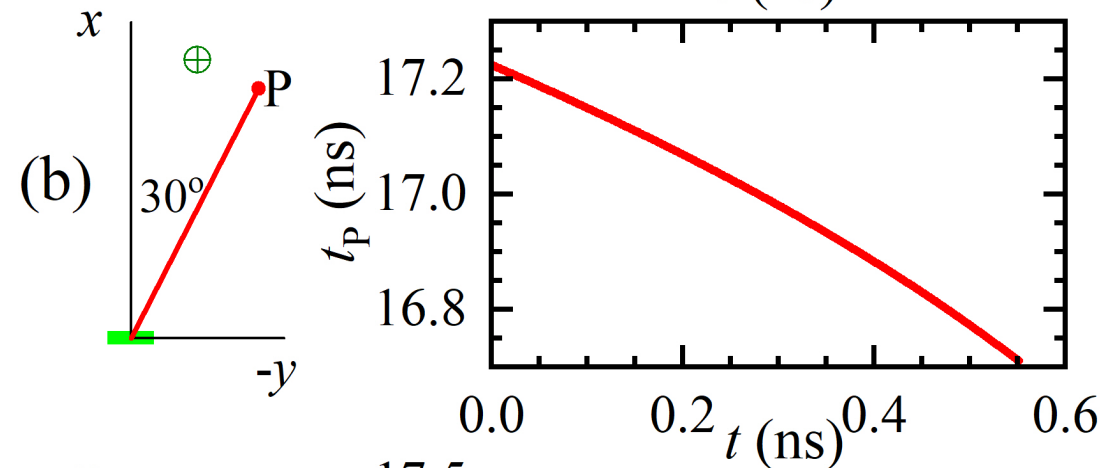
*Nota bene:* if, and only if,  $(X, -Y) = (X_0, -Y_0)$  this expression yields a constant.

Set the target position 5 m away from the centre of the antenna,  $15^\circ$  “off boresight”.

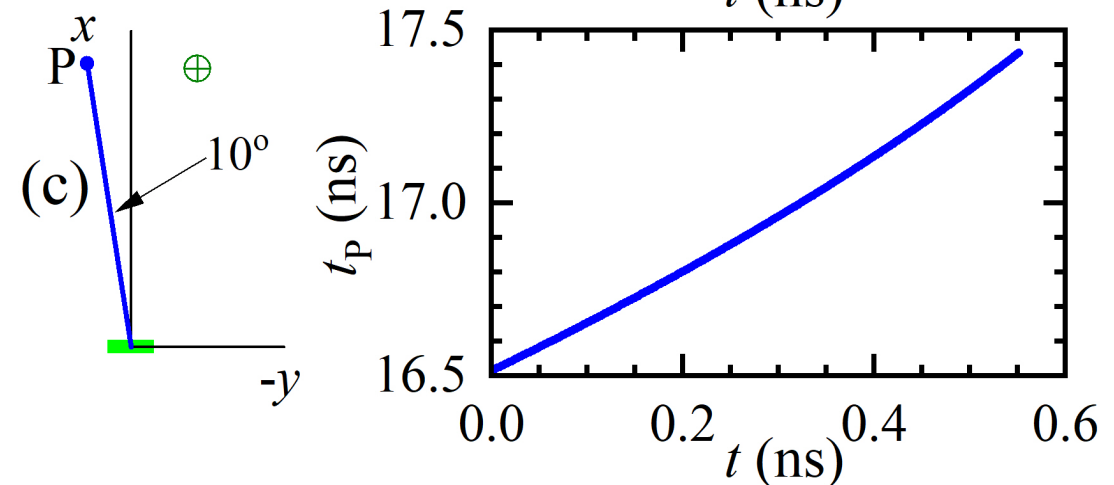
Plot arrival time of radiation from blob at target versus emission time. It’s a constant (see previous equation).

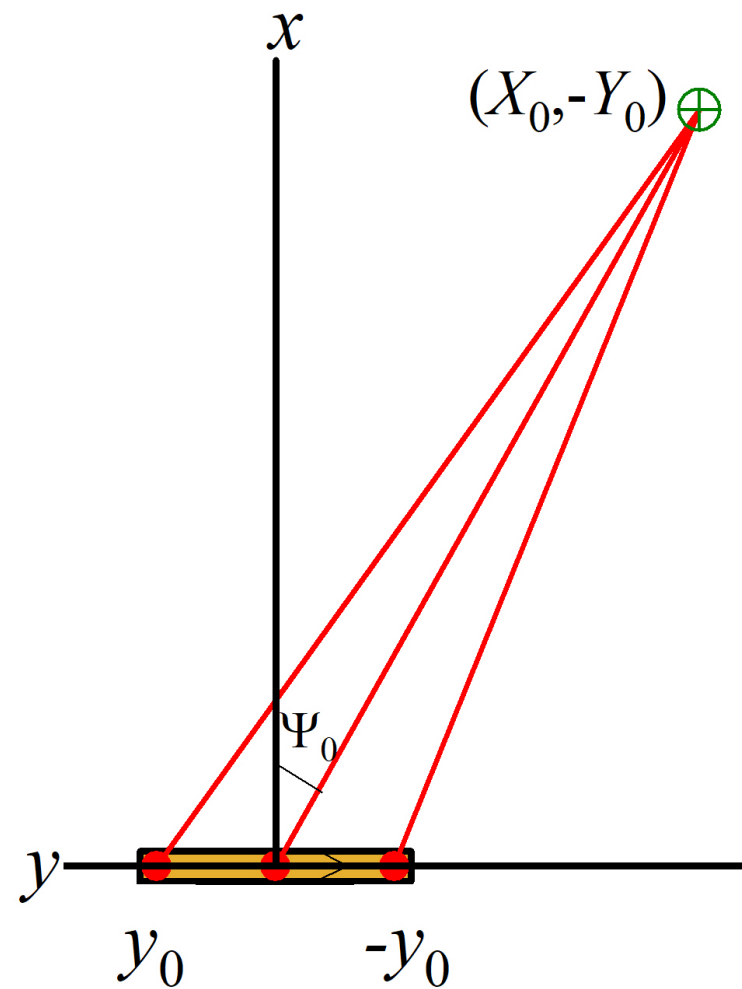


Now put receiver P at  $30^\circ$  off boresight. The arrival time of the radiation is a function of the emission time.



Place receiver P at  $-10^\circ$  off boresight. The arrival time of the radiation is a *different* function of the emission time.

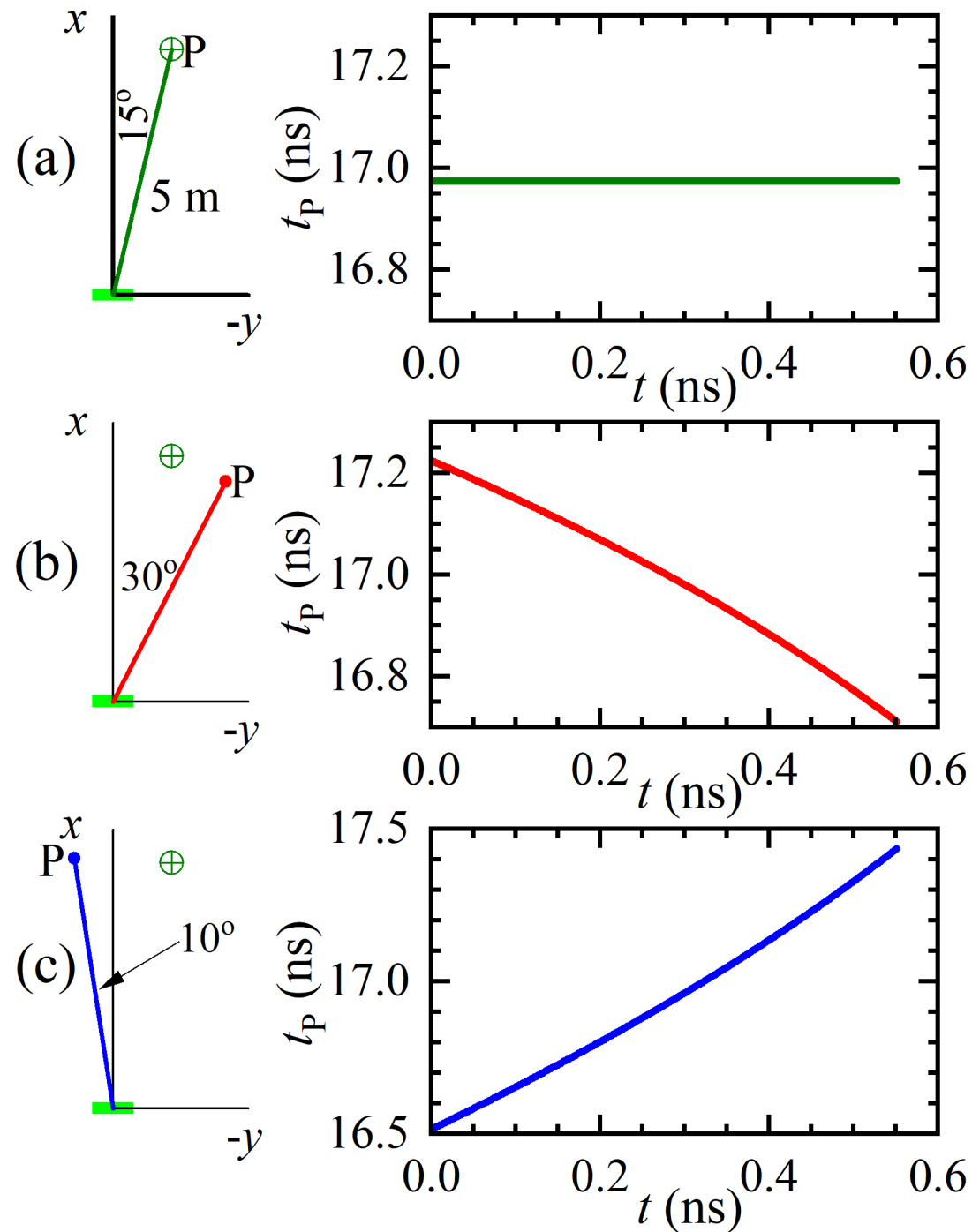




## What's happening?

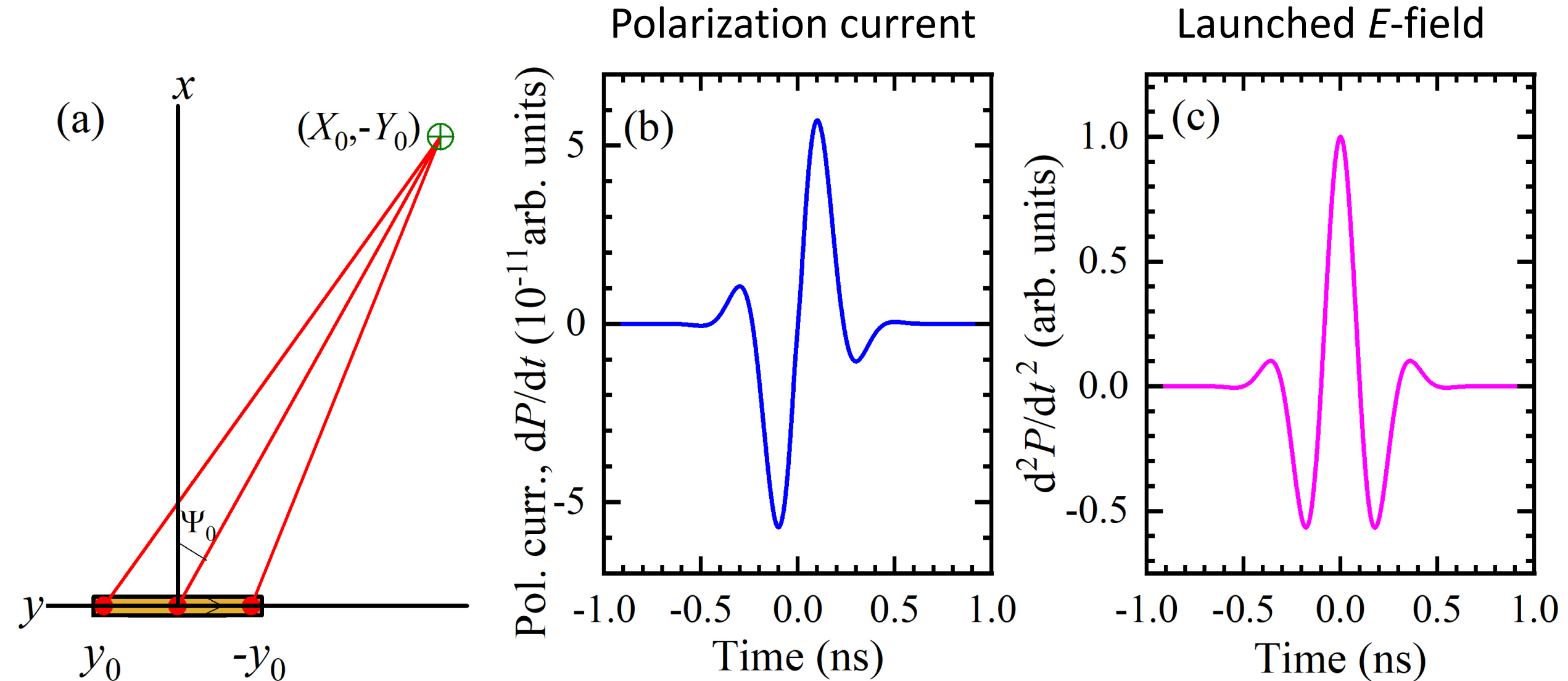
Concept: run the antenna so that a small blob of polarization current travels such that the component of its velocity towards a target  $\oplus$  is always  $c$ .

The motion of the blob/source exactly compensates for the difference in path lengths between the emission and reception points *only in case (a)*.



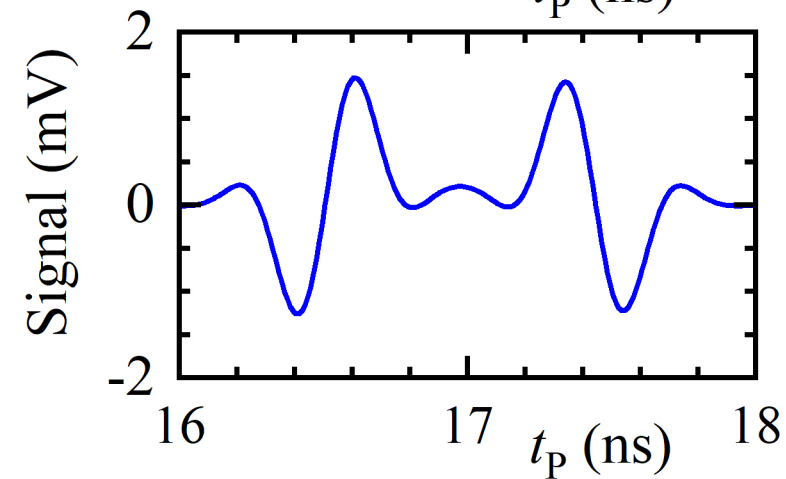
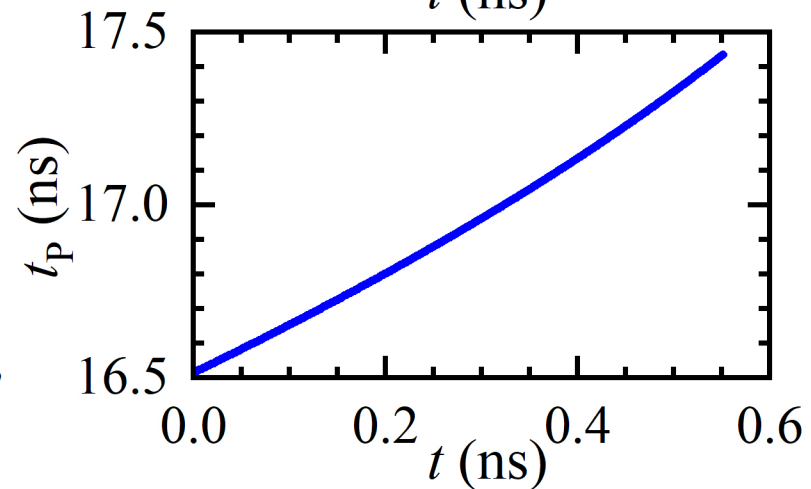
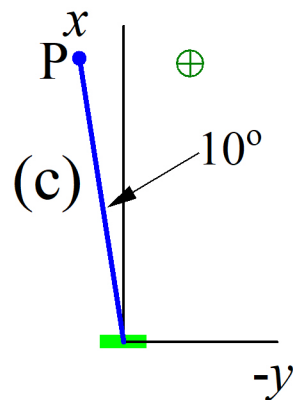
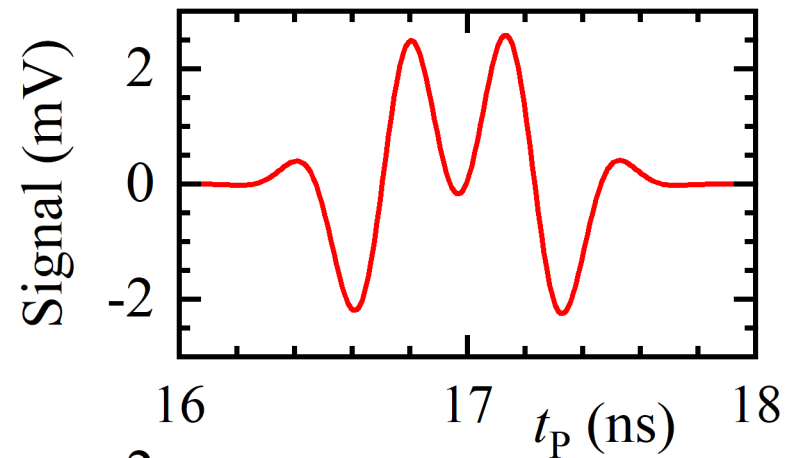
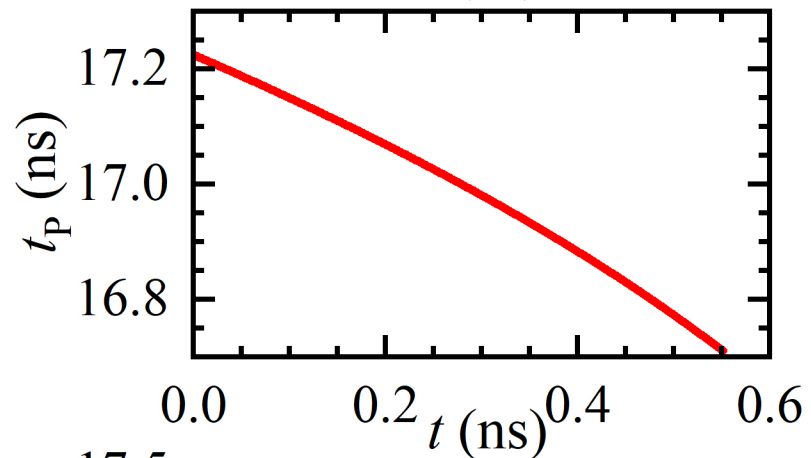
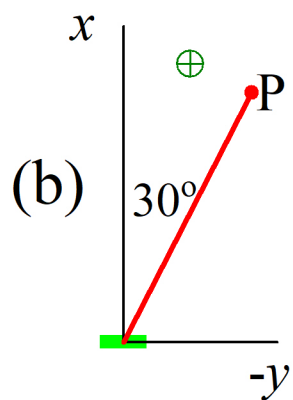
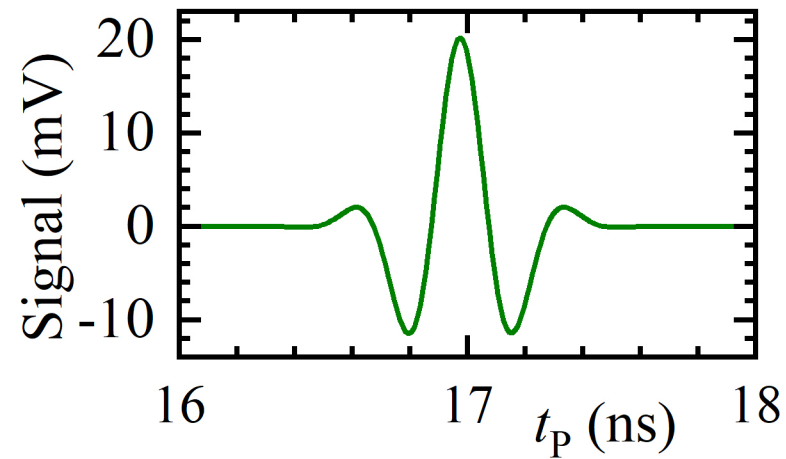
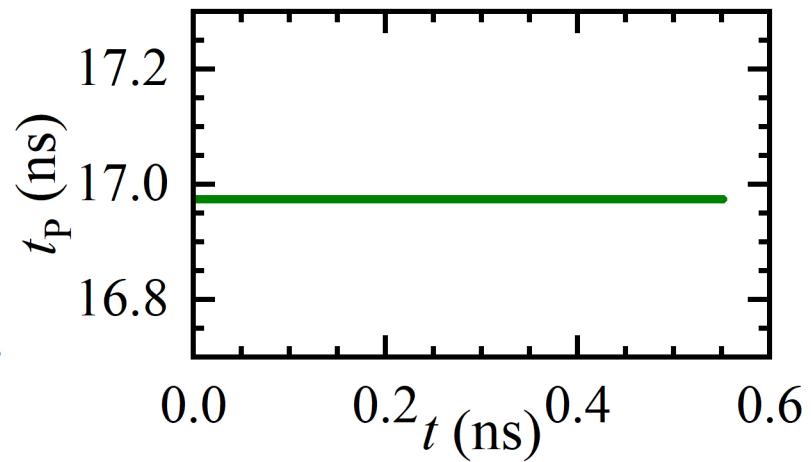
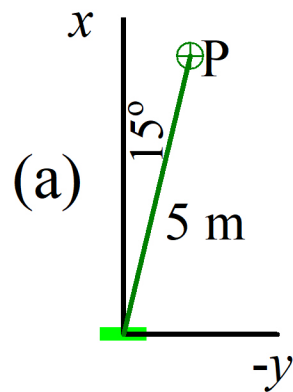


We now send a polarization current wavepacket along the antenna. Each point on the wave packet follows the same acceleration scheme as the blob discussed before.



## Information focus:

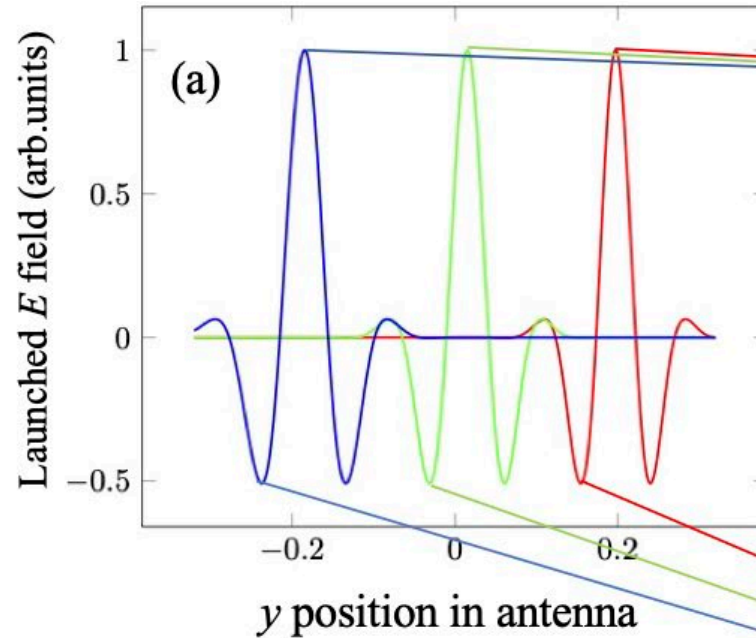
At the target angle and distance, detected signal reproduces the shape of the launched  $E$ -field exactly. Away from the target position, detected signal is much smaller and has altered frequency content and shape.



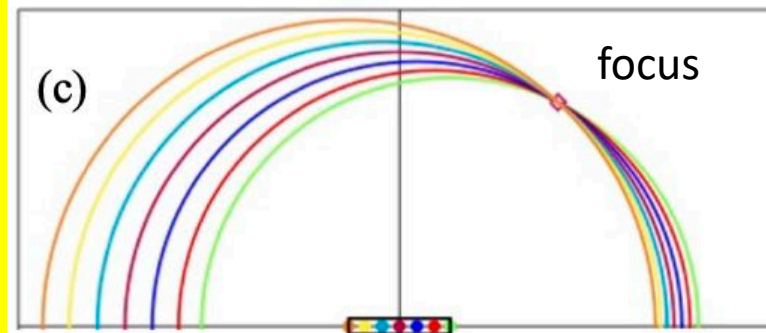
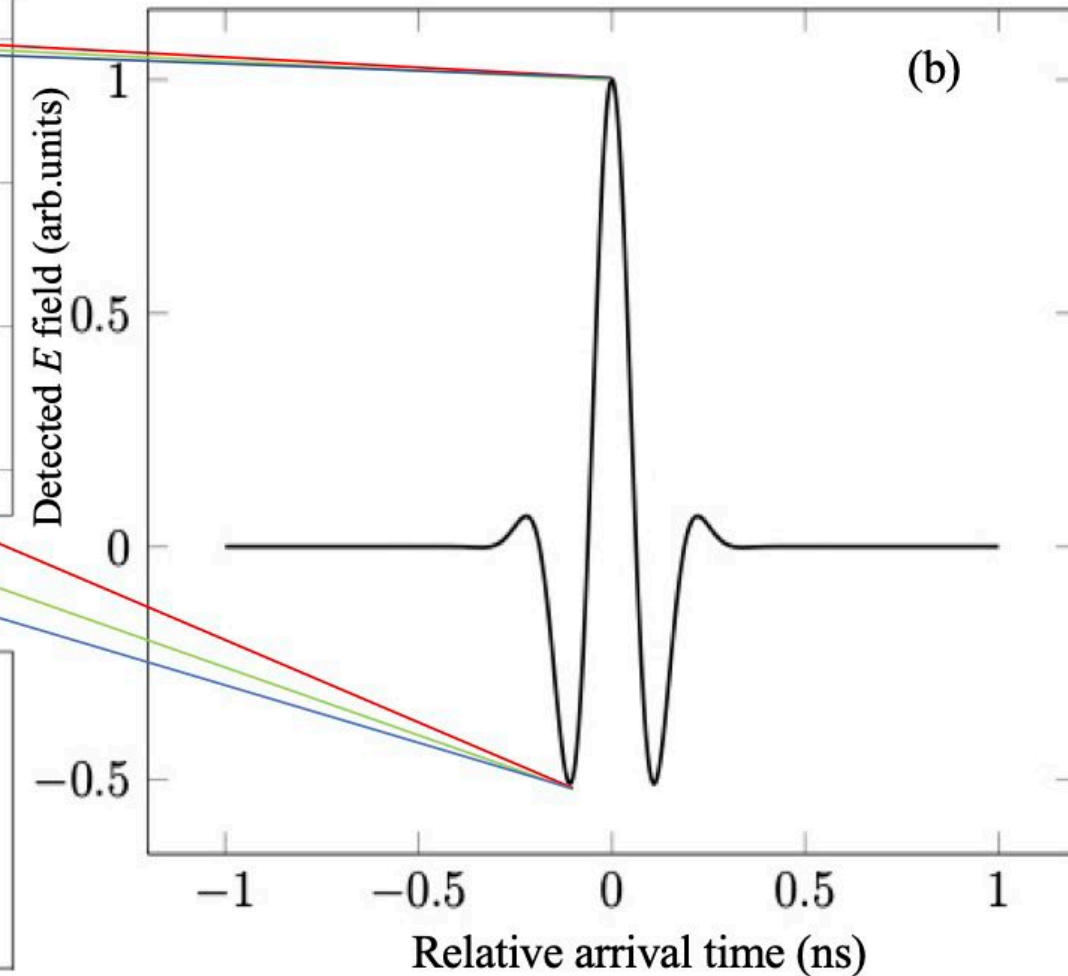
## Explanation:

The acceleration scheme ensures that all emission from a particular point on the wavepacket as it traverses the antenna will arrive at the focus simultaneously. Indeed, emission from any point on the wavepacket will behave similarly, the arrival time being the time at which that point entered the antenna at  $y = y_0$  plus the time taken for light to travel from  $(0, y_0)$  to the target.

Wave packet as it traverses antenna

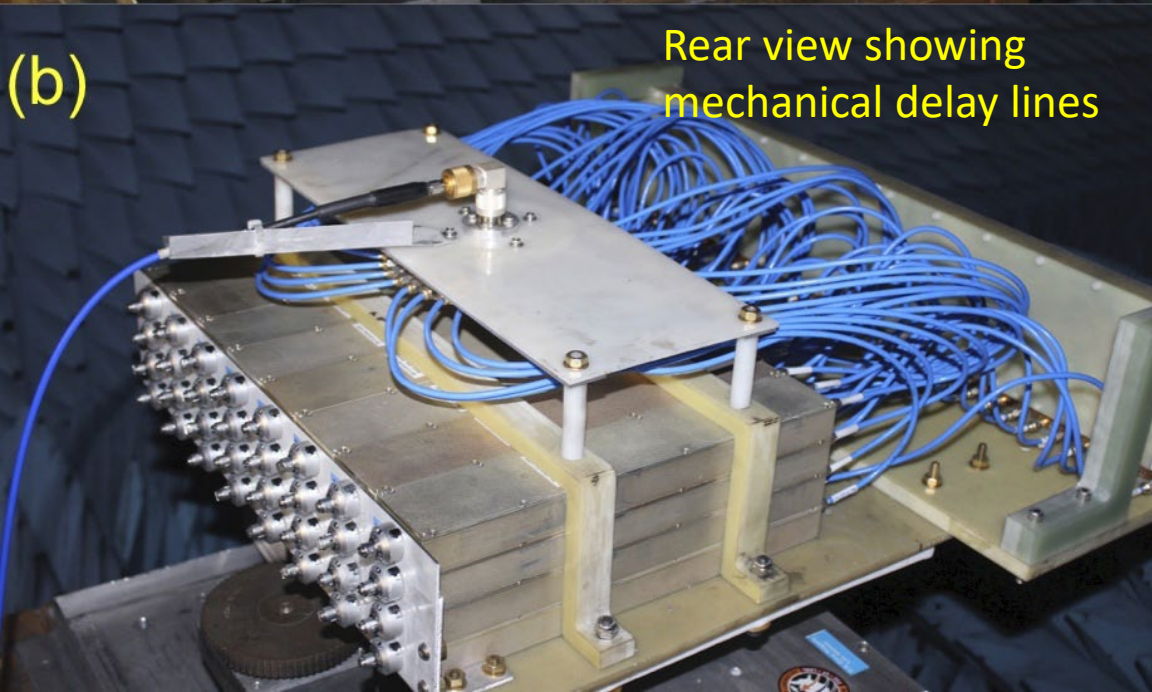
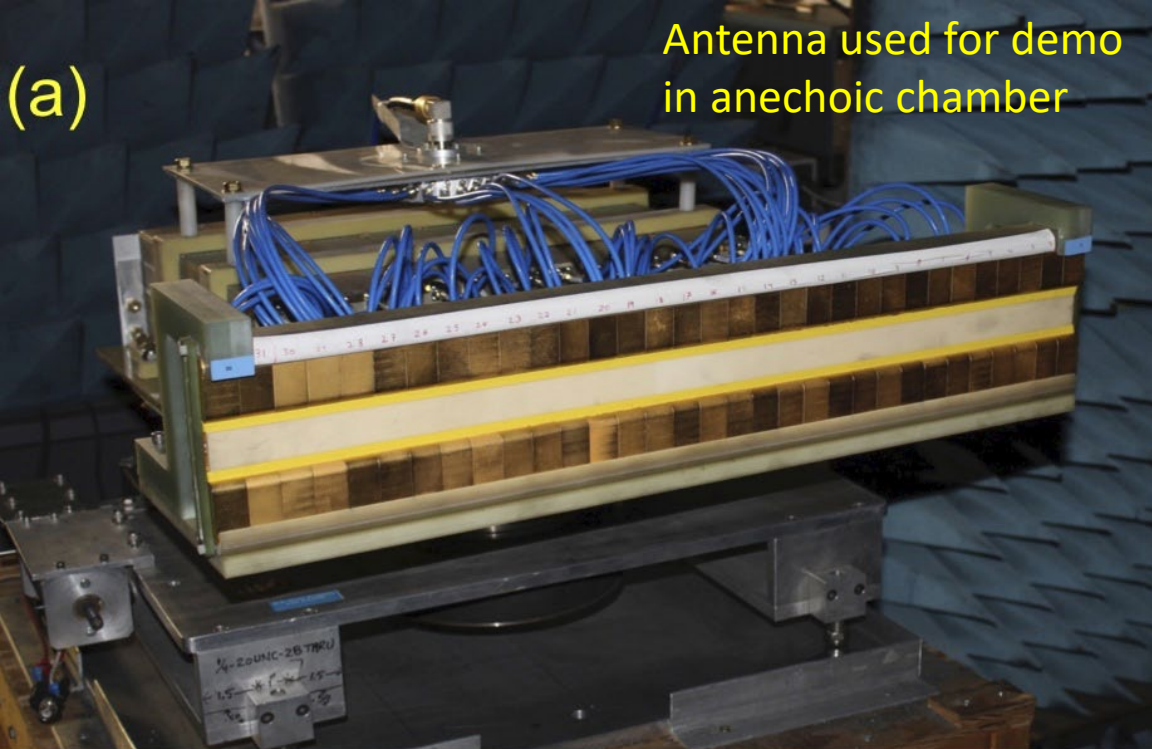


Signal detected at focus point



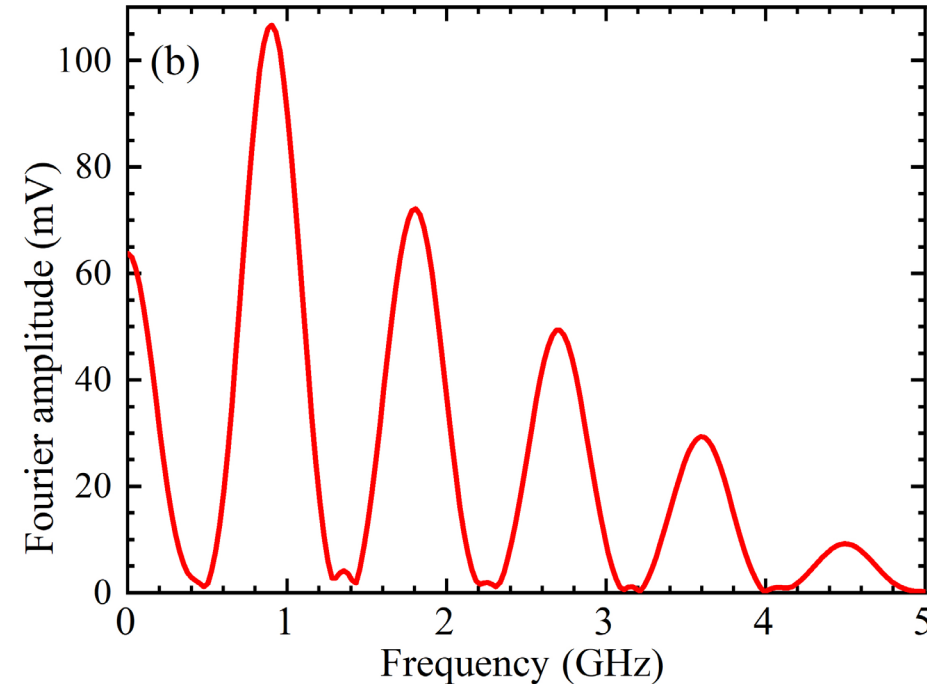
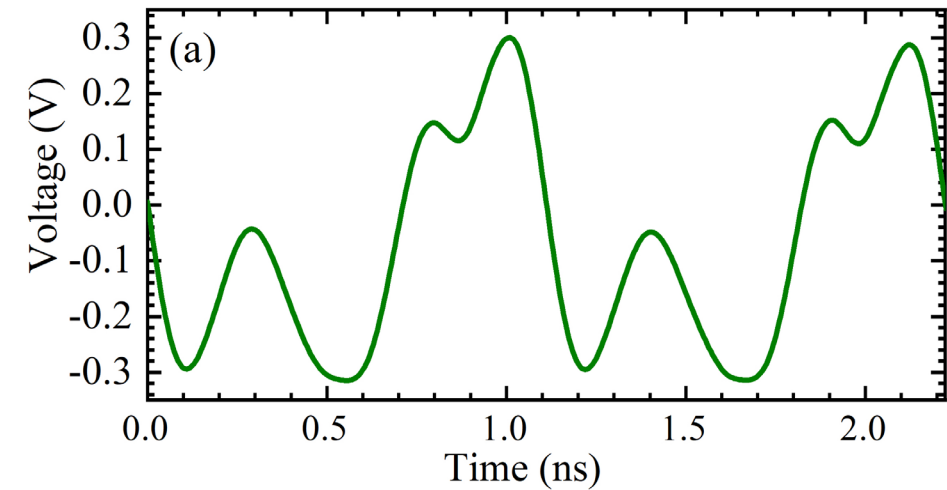
Huyghens wavelet explanation



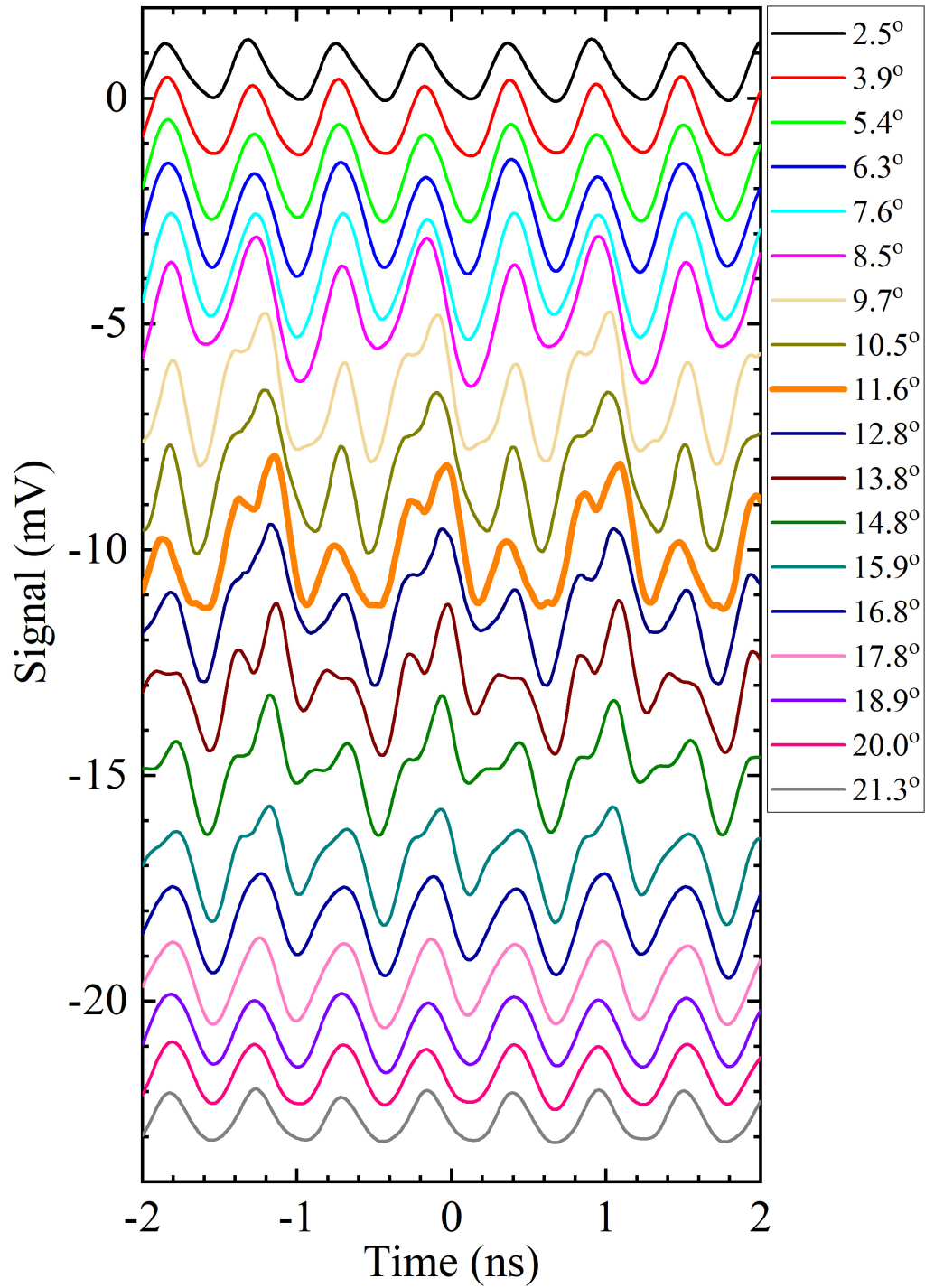


Right:  
broadcast  $E$ -  
field (a) and its  
Fourier  
transform (b).  
Note the  
simple form of  
the FT- a  
triangular  
envelope-  
makes the  
correct signal  
easy to find.  
Set  
acceleration  
for target  
coordinates:  
3m @  $11.6^\circ$ .

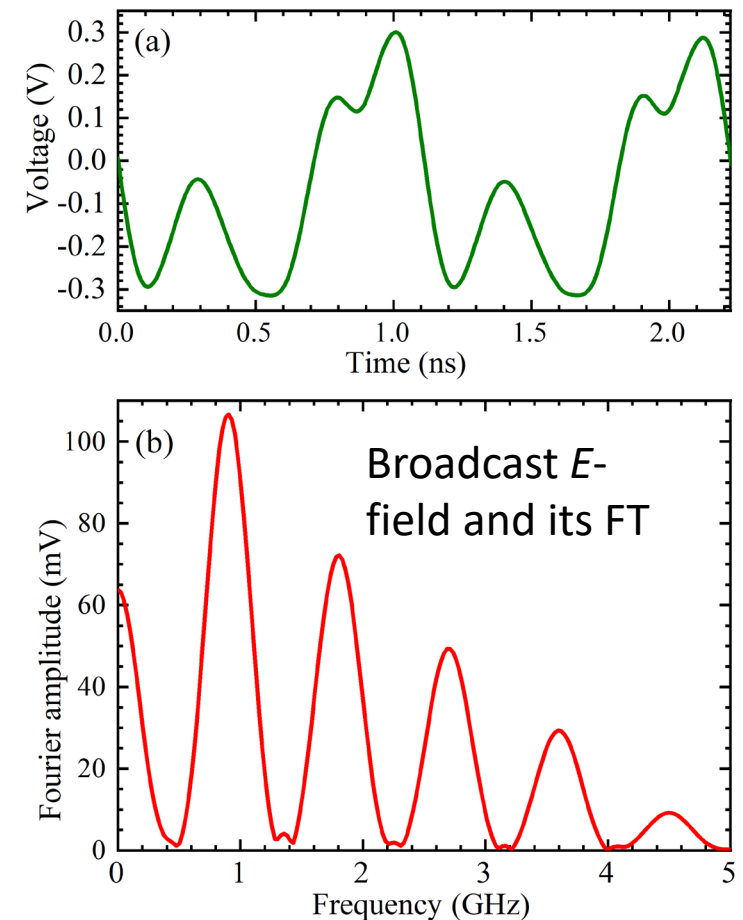
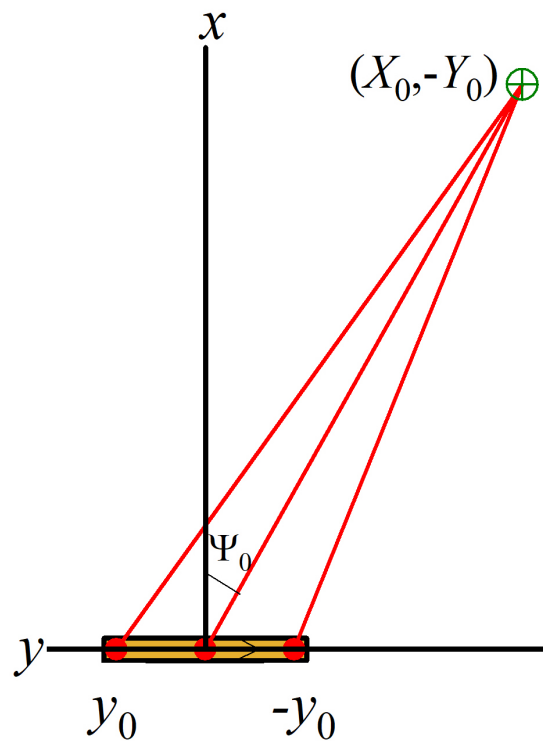
## Experimental demo

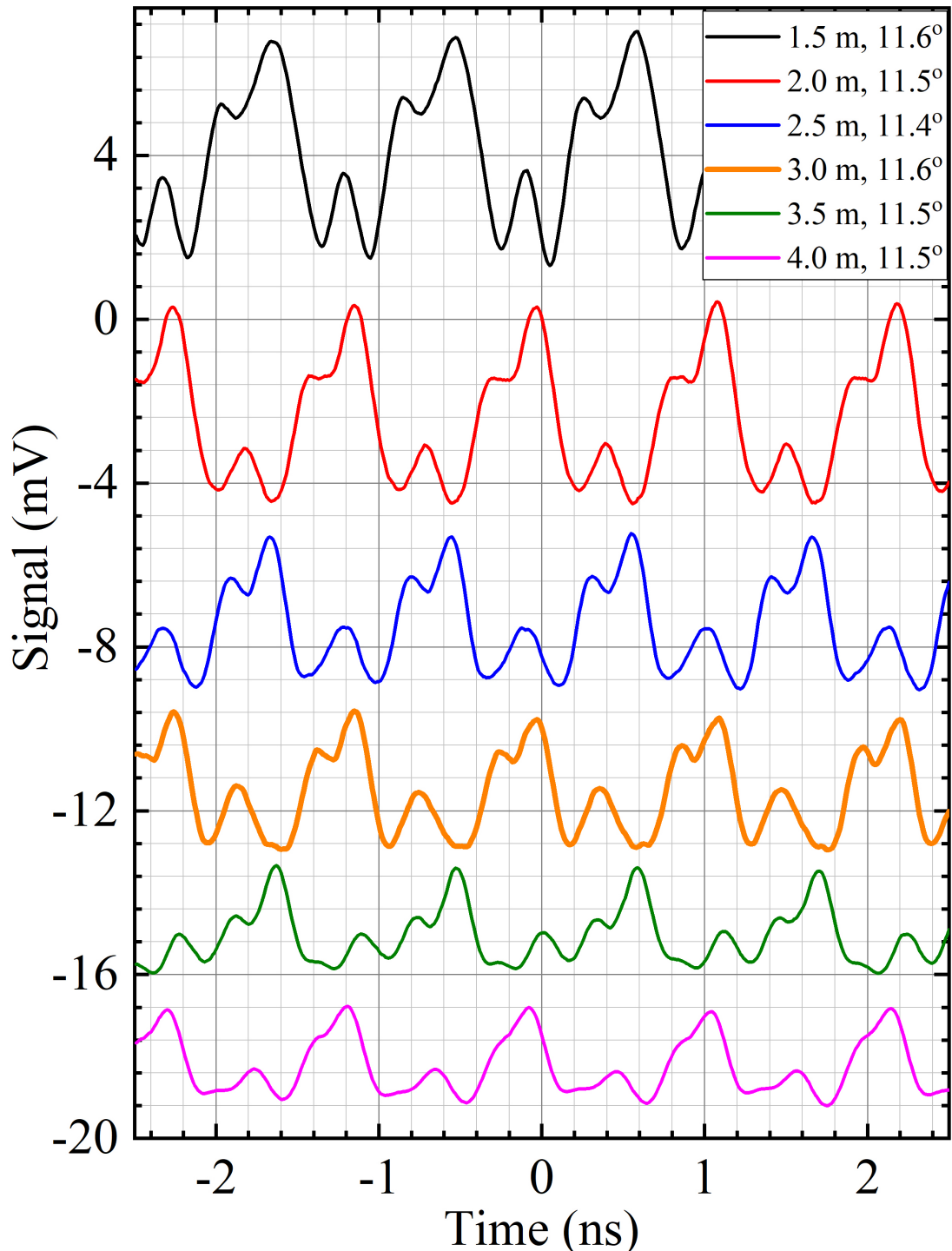






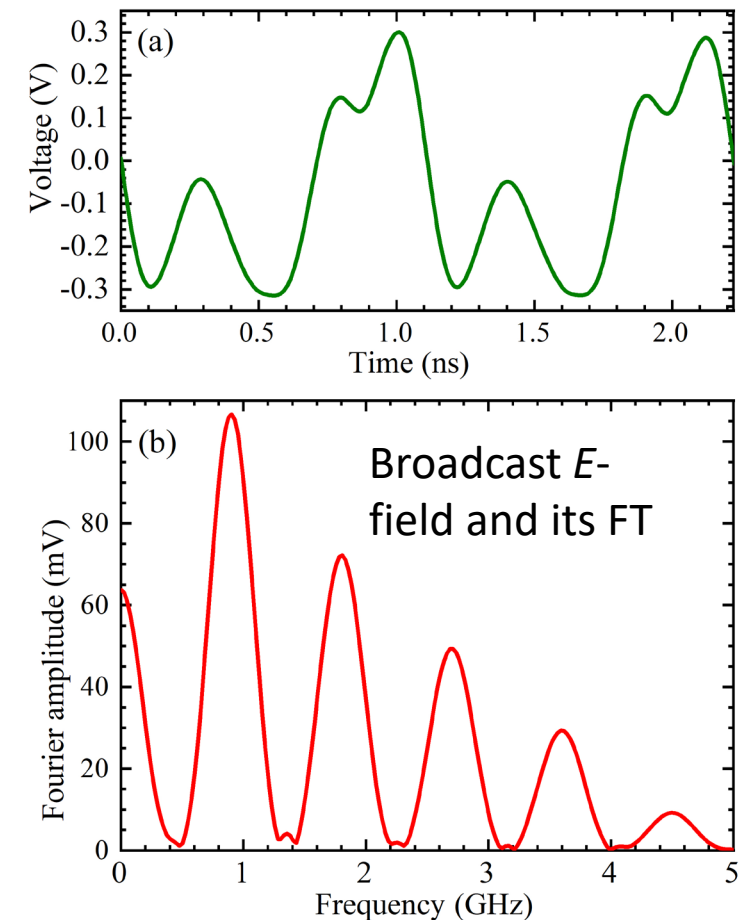
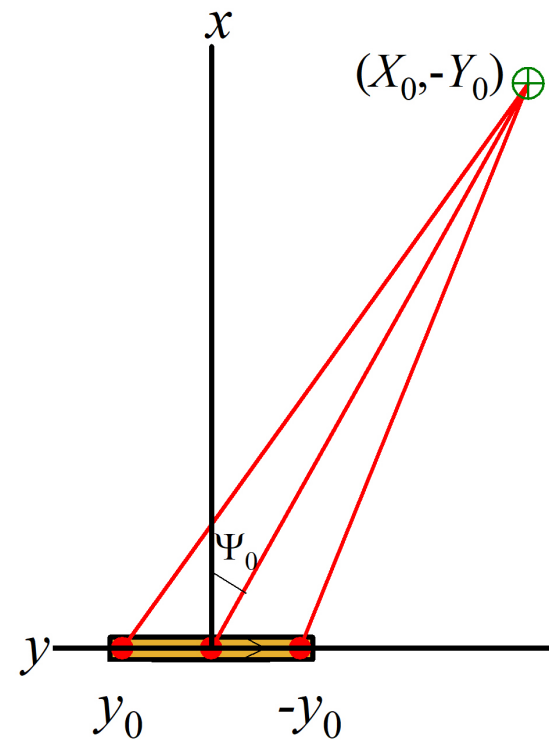
Place detector dipole at target distance of 3.0 m away from antenna and record detected  $E$ -field at several closely spaced angles. The shape of the broadcast  $E$ -field is only reproduced at the target angle of  $11.6^\circ$  (orange trace).



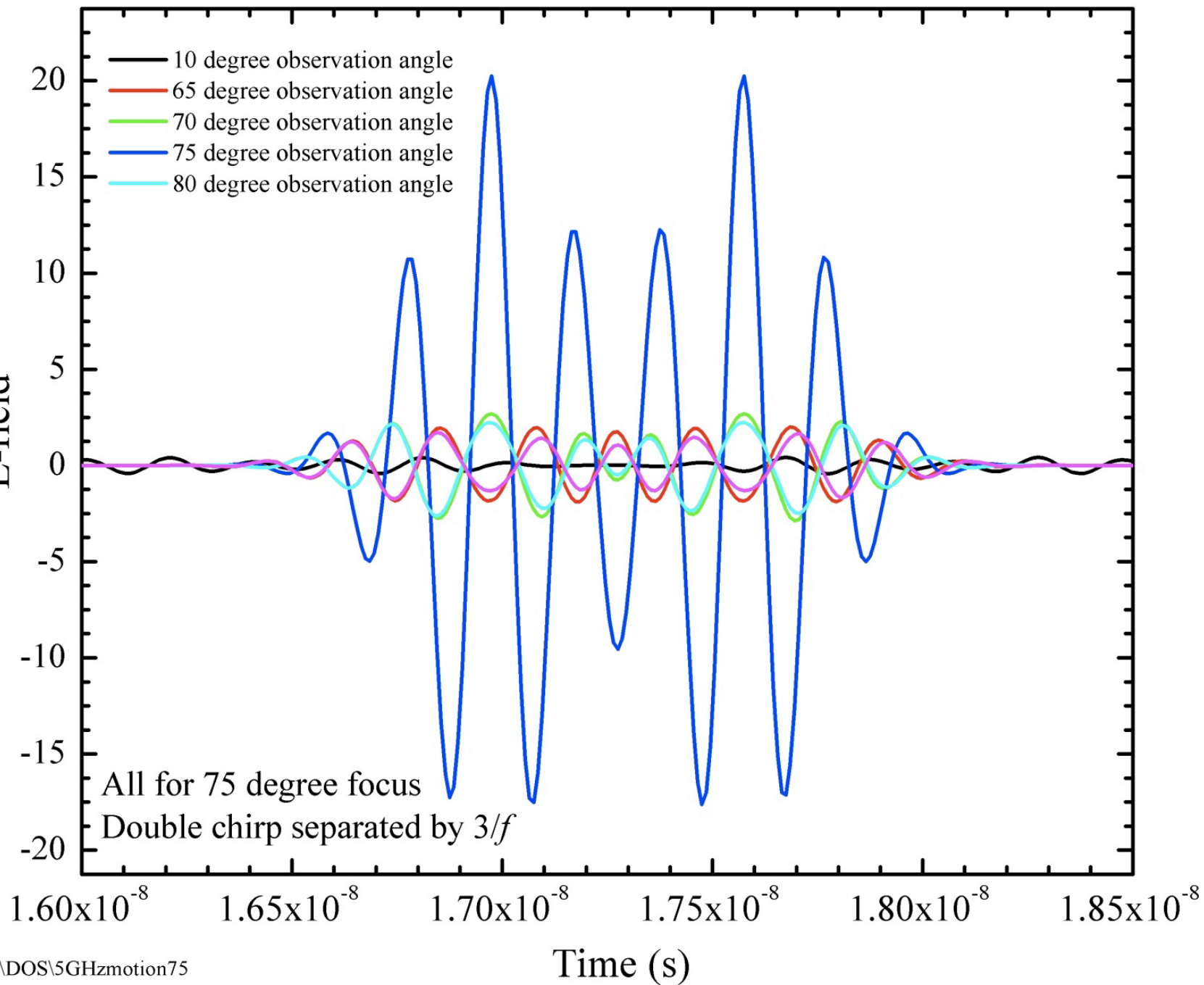


Place detector dipole close to target angle ( $11.6^\circ$ ) and record detected  $E$ -field at several distances.

The shape of the broadcast  $E$ -field is only reproduced at the target distance (3.0 m - orange trace).



"E-field"



Modulated signal  
(double  
wavepacket)

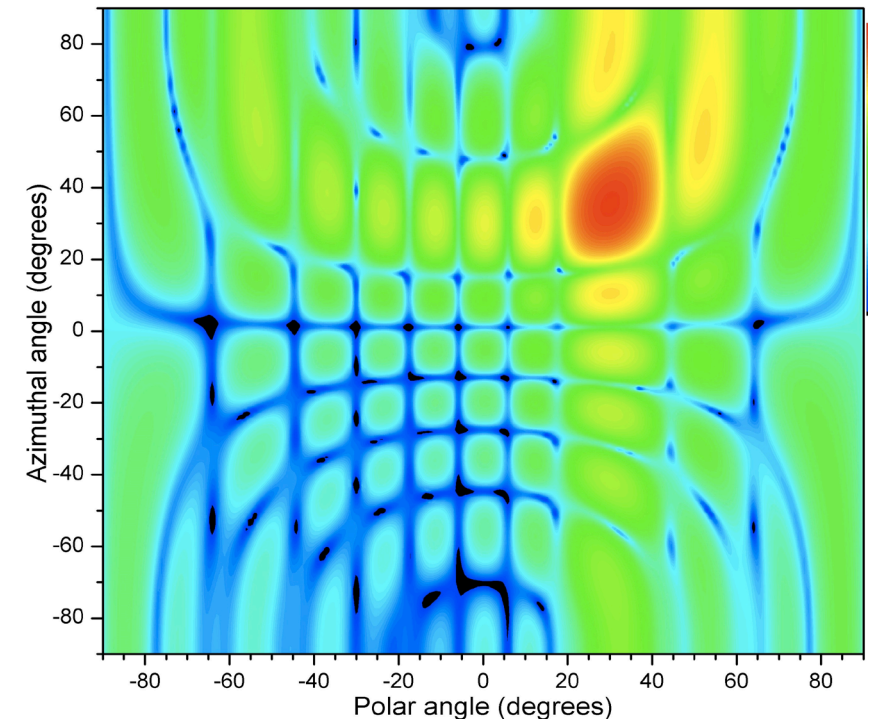
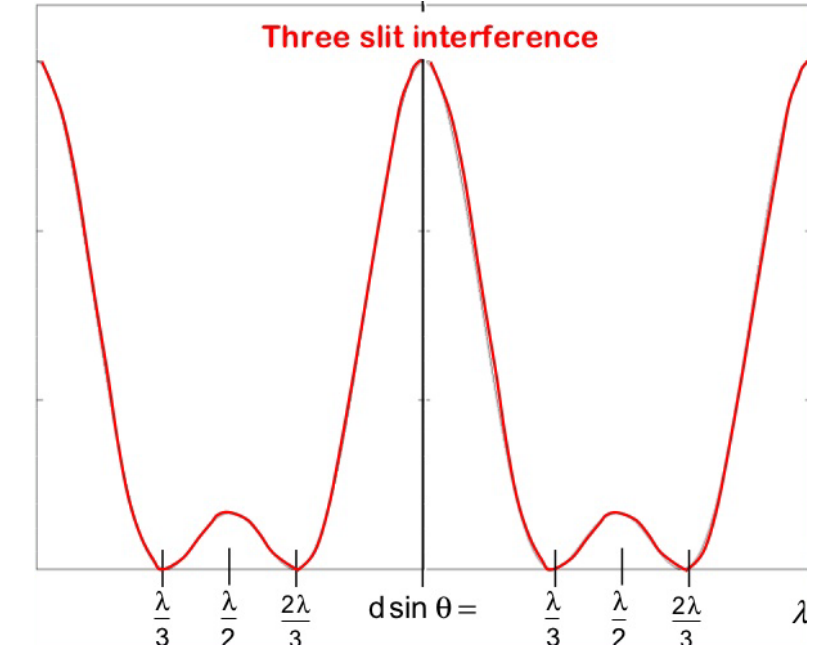
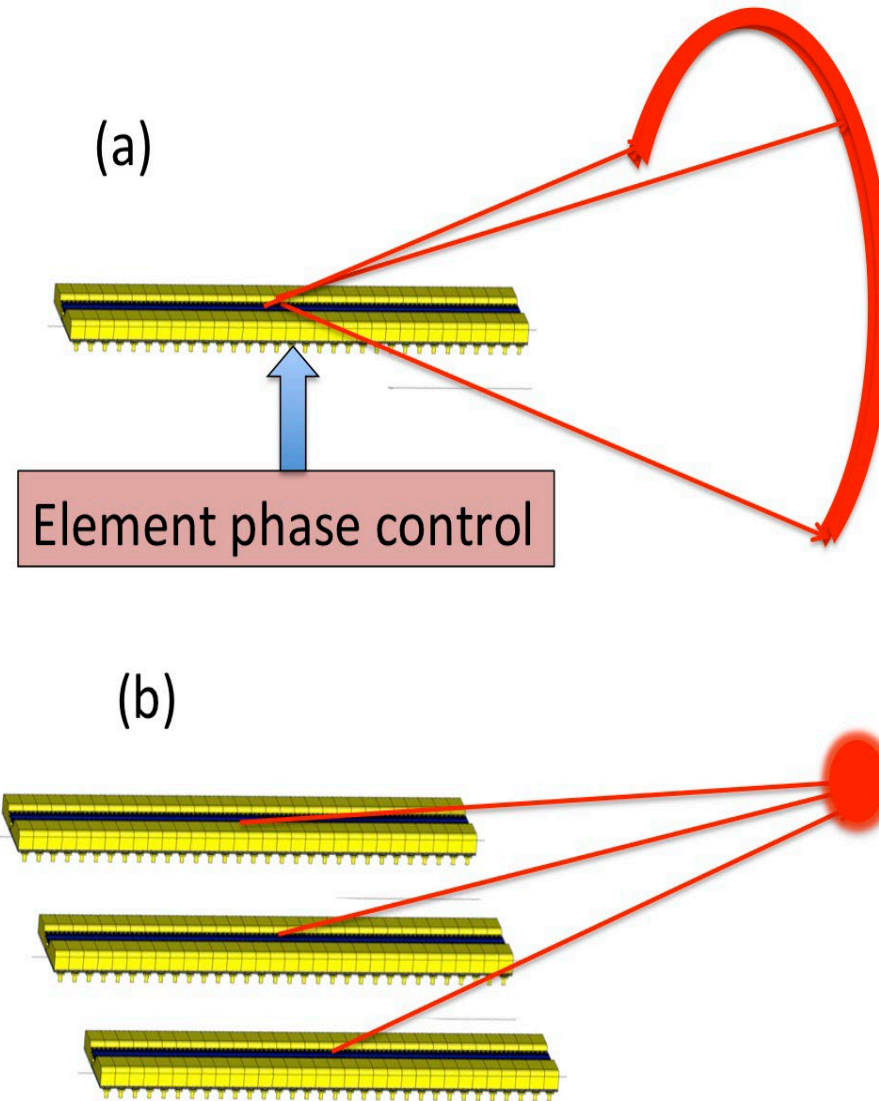
“Bits”- two wavepackets  
separated by the time  
equivalent of the  
“Rayleigh criterion”.

The proper shape of the  
double wavepacket signal  
is reproduced at the  
target angle, but nowhere  
else: information is only  
easily understood at  
desired location.



# Three-dimensional information focus using array of three antennas:

- Convolute polar focus due to acceleration within each antenna with a three-slit diffraction pattern.
- Steer in azimuthal direction using a phase offset between each antenna in array.
- Single area of information focus (red) is possible.





# Summary- a new way of communicating by wireless

- The experiments show that a continuous, linear, dielectric antenna in which a superluminal polarization-current distribution accelerates can transmit a broadband signal that is reproduced comprehensibly only at a chosen target.
- Requirement: each point in the polarization-current distribution approaches the observer/detector at the speed of light at all times during its transit along the antenna.

**Conventional radio transmission methods:** signals broadcast with little or no directivity; selectivity is from the use of one or more narrow frequency bands.

**New technique:** a spread of frequencies transmits information to a particular location; the signal is weaker and has a scrambled time dependence elsewhere. To receive, you have to be at the right place. **Possible applications- 5G neighbourhood networks.**

A completely new problem in mathematical physics requires an **ab-initio mathematical treatment**. This work was originally motivated by the fact that the radiation data collected from our practical machines did not match predictions made by others. It all begins with Maxwell's equations and ends with a fundamental causal solution that can be used to model the emission from polarization currents **with regular domains of integration**.

## Maxwell's Equations

$\mathbf{E}$ ,  $\mathbf{H}$  = Electric and magnetic field intensity

$\mathbf{D}$ ,  $\mathbf{B}$  = Electric and magnetic flux density

$\rho$  = Electric charge density

$\mathbf{J}$  = Current density of free charges

$$\begin{aligned}\nabla \cdot \mathbf{D} &= \rho, \\ \nabla \cdot \mathbf{B} &= 0, \\ \nabla \times \mathbf{E} &= -\frac{\partial}{\partial t} \mathbf{B}, \\ \nabla \times \mathbf{H} &= \mathbf{J} + \frac{\partial}{\partial t} \mathbf{D},\end{aligned}$$

## Constituent Relations

$\mu$  = magnetic permeability

$\epsilon$  = electric permittivity

$$\mathbf{B} = \mu \mathbf{H},$$

$$\mathbf{D} = \epsilon \mathbf{E}.$$



$$\nabla^2 \mathbf{E} - \epsilon \mu \frac{\partial^2}{\partial t^2} \mathbf{E} = \frac{1}{\epsilon} \nabla \rho + \mu \frac{\partial}{\partial t} \mathbf{J}$$

$$\nabla^2 \mathbf{H} - \epsilon \mu \frac{\partial^2}{\partial t^2} \mathbf{H} = -\nabla \times \mathbf{J}.$$

Inhomogeneous wave equations that govern the fields

## Inhomogeneous wave equations that govern the fields

$$\nabla^2 \mathbf{E} - \varepsilon \mu \frac{\partial^2}{\partial t^2} \mathbf{E} = \frac{1}{\varepsilon} \nabla \rho + \mu \frac{\partial}{\partial t} \mathbf{J}$$

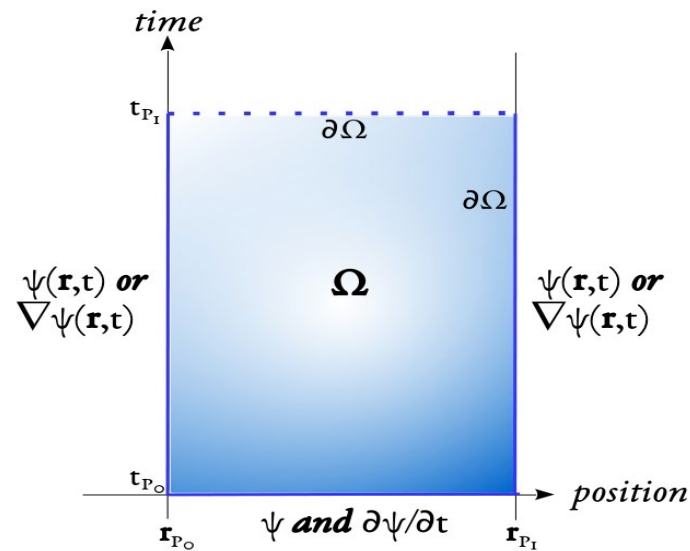
$$\nabla^2 \mathbf{H} - \varepsilon \mu \frac{\partial^2}{\partial t^2} \mathbf{H} = -\nabla \times \mathbf{J}.$$

In general form:

$c$  = wave speed

$\mathbf{r}$  = a point  $(x, y, z)$  in a Cartesian coordinate system

$q$  = source of electromagnetic radiation



$$\left( \frac{1}{c^2} \frac{\partial^2}{\partial t^2} - \nabla^2 \right) \psi(\mathbf{r}, t) = 4\pi q(\mathbf{r}, t) \quad \text{in } \mathbb{R}^3 \times (0, \infty)$$



By itself, this equation is meaningless as a problem of mathematical physics. To find physically relevant solutions we need to define the state of the system at some initial time  $t$  (initial conditions) and the conditions at the boundary of the problem domain (boundary conditions).

We choose Cauchy initial conditions (i.e., both,  $\psi(\mathbf{r}, t_0)$  and  $\partial \psi(\mathbf{r}, t_0) / \partial t$  and Dirichlet or Neumann boundary conditions (i.e.,  $\psi(\mathbf{r}, t)$  or  $\nabla \psi(\mathbf{r}, t)$  but not both!) on an open surface. The problem domain is  $\Omega$  with boundary  $\partial \Omega$ .

Many calculations later we arrive at the full Green's function solution with satisfaction of all initial and boundary conditions

$$\psi(\mathbf{r}_P, t_P) = u(\mathbf{r}_P, t_P) + v(\mathbf{r}_P, t_P) + w(\mathbf{r}_P, t_P)$$

where

$$u(\mathbf{r}_P, t_P) = \int_{t_{P_0}}^{t_P^+} dt \int_{\Omega} d^3\mathbf{r} G(\mathbf{r}_P, t_P | \mathbf{r}, t) q(\mathbf{r}, t),$$

Volume integral: source term

$$v(\mathbf{r}_P, t_P) = \frac{1}{4\pi} \int_{t_{P_0}}^{t_P^+} dt \int_{\partial\Omega} d^2\mathbf{r} \hat{n} \cdot \left[ G(\mathbf{r}_P, t_P | \mathbf{r}_{\partial\Omega}, t) \nabla \psi(\mathbf{r}_{\partial\Omega}, t) - [\nabla G(\mathbf{r}_P, t_P | \mathbf{r}_{\partial\Omega}, t)] \psi(\mathbf{r}_{\partial\Omega}, t) \right],$$

Surface integral: boundary term  $\rightarrow$  disappears in free space

and

$$w(\mathbf{r}_P, t_P) = -\frac{1}{4\pi c^2} \int_{\Omega} d^3\mathbf{r} \left[ \frac{\partial G(\mathbf{r}_P, t_P | \mathbf{r}, t_{P_0})}{\partial t} \psi(\mathbf{r}, t_{P_0}) - \frac{\partial \psi(\mathbf{r}, t_{P_0})}{\partial t} G(\mathbf{r}_P, t_P | \mathbf{r}, t_{P_0}) \right].$$

Initial state of the system  $\rightarrow$  can always be set equal to 0 for “null initial conditions”



# Green's functions in action: Comparison of the model to experimental data:

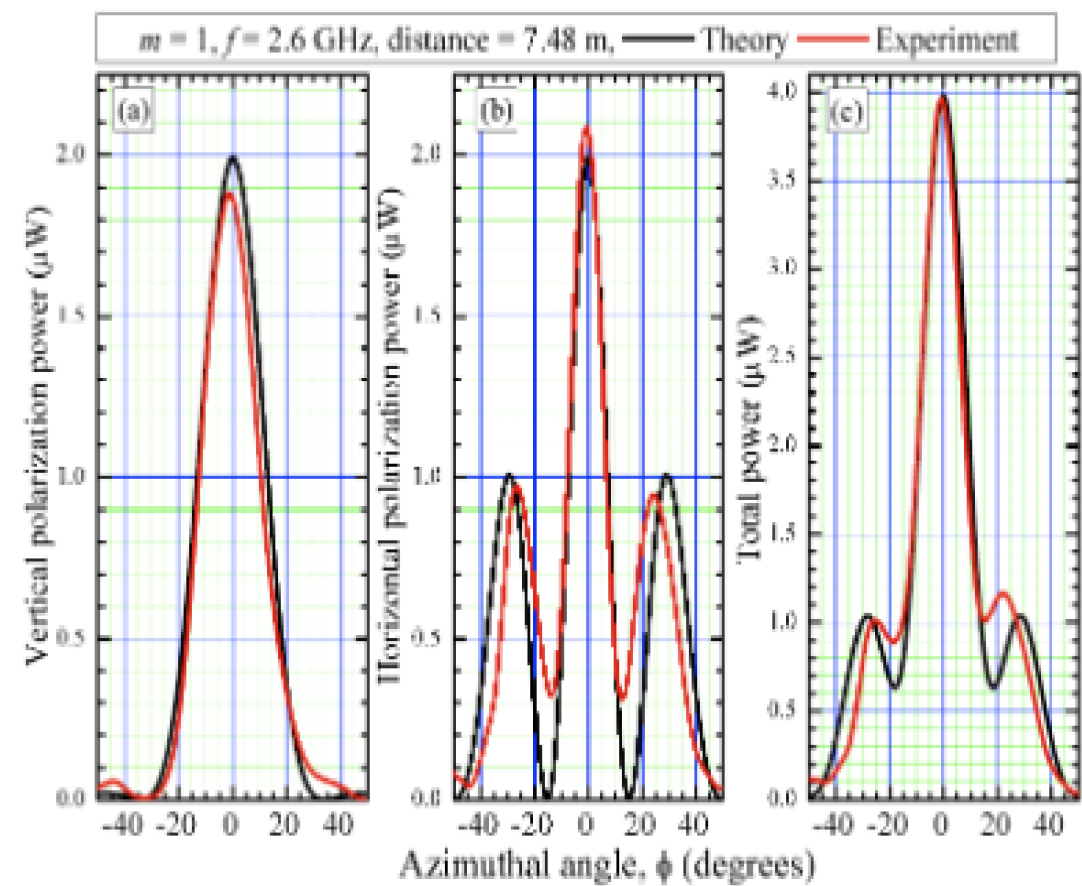


Figure 7.7: Model (black) of circular antenna TD 1 ( $m = 1$ ,  $f = 2.6$  GHz) compared with experimental data (red) measured in the FARM Anechoic Chamber: (a) vertical polarization power; (b) horizontal polarization power; (c) total power. Powers are in  $\mu W$  and other parameters are in the key.

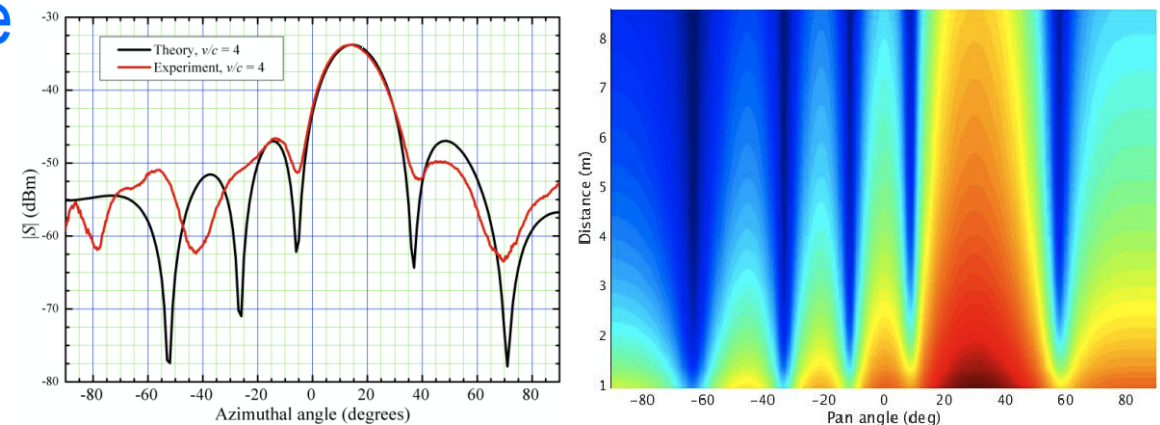
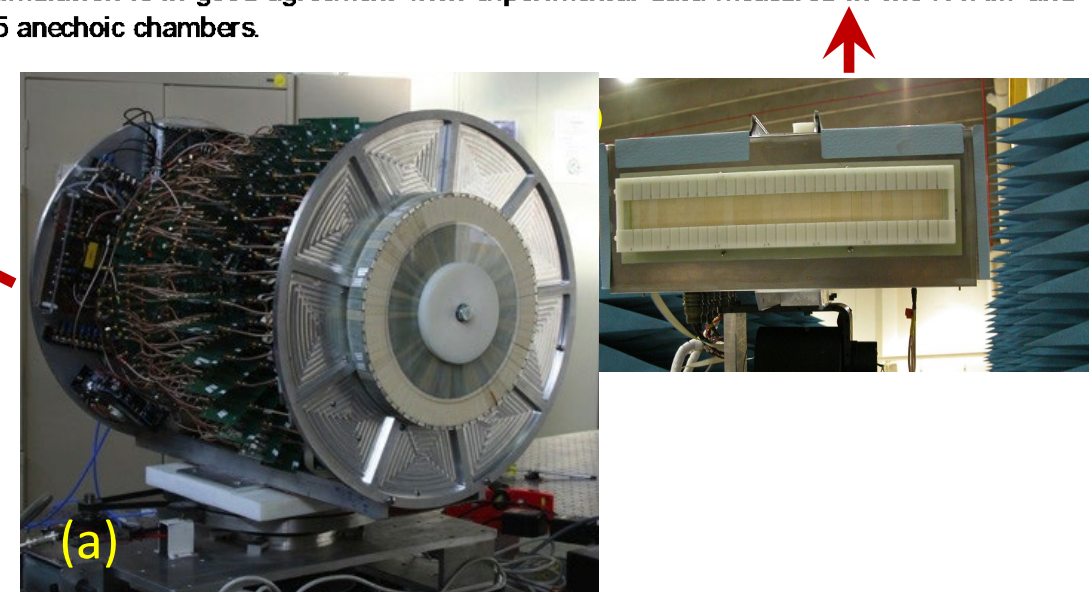


Figure 7.3: Left: modulus of Poynting vector  $|S|$  versus azimuthal (pan) angle  $\phi$  (black) predicted by the model of TD 2 (Fig. 3.1 center panel). The frequency is 2.4 GHz,  $v/c = 4$  and the antenna to detector distance is 5 m. Experimental data for the same antenna, measured at the same distance (5 m) in the Sandia FARM anechoic chamber are shown in red. After correction for the gain of the detector antenna, there is a very good quantitative match between experiment and theory. Right: modulus of Poynting vector  $|S|$  (colour contours) versus azimuthal (pan) angle  $\phi$  and distance predicted by the model of the linear superluminal antenna. The frequency used was 2.5 GHz and the source speed was  $v/c = 2$ . The simulation is in good agreement with experimental data measured in the FARM and TA-35 anechoic chambers.





Digi International  
October 23, 2020

## Solving 5G Antenna Design Challenges

As the cellular industry continues to move forward to fulfill the need of higher data rates, lower latency and greater reliability, RF system design has again become the bottleneck for any cellular devices or networks that aim to deliver more data to more users in more demanding use cases.

While 3rd Generation Partnership Project (3GPP) continues to release more specifications addressing the emerging demands and pushing the industry deeper into the era of 5G, confusion and misunderstanding also emerge, casting doubts among device OEMs on plans to launch their next-generation 5G products.

The antenna design is by far the most confusing part of this process as it is almost entirely depended on the end device form

factor and OEMs' preferences.

## New 5G Features and How They Differ from Current 4G LTE

To understand the reason for 5G being able to deliver a much higher data rates than the current 4G technology, it might be helpful to look at Shannon-Hartley theorem first:

$$C = M * B \log_2(1 + S/N)$$

- C is the channel capacity in bit/second
- M is the number of channels
- B is the bandwidth of each channel
- S/N is signal to noise ratio

It is actually intuitive based on the theorem that in order to have a higher channel capacity, improvements must be done to adjust the system M, B and S/N. 5G, which evolves from 4G, implements some well-known and long-existing techniques in its architecture to improve its channel capacity:

- Carrier Aggregation (CA) > Increased bandwidth (B)
- Multiple-in-multiple-out architecture (MIMO)>increase the number of channels (M)
- Allocating new frequency bands > Increased bandwidth (B)
- Adaptively adopt higher-order modulation schemes > S/N and B

Compared to 4G, 5G pushes the same set of techniques to the next level of capability and complexity. This inevitably pushes antenna design for 5G devices to the next level to fit the ever-increasing requirements for greater bandwidth, more frequency

bands and better interference immunity.

## How the New 5G Features Create New Antenna Design Challenges

To plan and design antennas for the functionality of 5G, it's important to understand the challenges and how to address them. Here we review those considerations.

### **Actively Tunable Antenna System**

Due to stringent size constraints, modern wireless devices typically use active antenna tuners as an effective mean to shrink antenna size. It can tune antenna smartly based on the changing operating environment, frequency band, and bandwidth coverage. With a potentially higher order of CA in 5G and additional cellular bands, the antenna tuning system must be able to support more tuner state as well as wider frequency bandwidth per tuner state.

### **New Frequency Bands**

Based on 3GPP Release 15, two basic frequency ranges (FR1 and FR2) are to be used for 5G:

**FR1:** 410 MHz to 7.125 GHz; **FR2:** 24.25 to 52.6 GHz

In FR1, 5G adopts 3.3 ~ 3.8, 3.8 ~ 4.2, and 4.4 ~ 4.9 GHz bands on top of the existing sub-3GHz bands in 4G LTE. This posts new requirements for cellular antennas to provide additional frequency coverages in the sub-6GHz frequency range.



**Table 1: 5G New Radio (NR) operating bands in FR1 1**

NR Operating Band	Uplink (UL) operating band		Downlink (DL) operating band		Duplex Mode
	BS receive		BS transmit		
	UE transmit		UE receive		
	F <sub>UL_low</sub> – F <sub>UL_high</sub>	total BW	F <sub>DL_low</sub> – F <sub>DL_high</sub>	total BW	
n1	1920 MHz-1980 MHz	60	2110 MHz-2170 MHz	60	FDD
n2	1850 MHz-1910 MHz	60	1930 MHz-1990 MHz	60	FDD
n3	1710 Mhz -1785 MHz	75	1805 MHz-1880 MHz	75	FDD
n5	824 -849 MHz	25	869 MHz-894MHz	25	FDD
n7	2500 MHz-2570 MHz	70	2620 MHz-2690 MHz	70	FDD
n8	880 MHz-915 MHz	35	925 MHz-960 MHz	35	FDD
n20	832 MHz-862 MHz	30	791 MHz-821 MHz	30	FDD
n28	703 MHz-748 MHz	45	758 MHz-803 MHz	45	FDD
n38	2570 MHz-2620 MHz	50	2570 MHz-2620 MHz	50	TDD
n41	2496 MHz-2690 MHz	194	2496 MHz-2690 MHz	194	TDD
n50	1432 MHz-1517 MHz	85	1432 MHz-1517 MHz	85	TDD
n51	1427 MHz-1432 MHz	5	1427 MHz-1432 MHz	5	TDD
n66	1710 MHz-1780 MHz	70	2110 MHz-2200 MHz	90	FDD
n70	1695 MHz-1710 MHz	15	1995 MHz-2020 MHz	25	FDD
n71	663 MHz-698 MHz	35	617 MHz-652 MHz	35	FDD
n74	1427 MHz-1470 MHz	43	1475 MHz-1518 MHz	43	FDD
n75	N/A		1432 Mhz -1517 MHz	85	SDL
n76	N/A		1427 Mhz -1432 MHz	5	SDL
n78	3300 MHz-3800 MHz	500	3300 MHz - 3800 MHz	500	TDD
n77	3300 MHz- 4200 MHz	900	3300 MHz - 4200 MHz	900	TDD
n79	4400 MHz-5000 MHz	600	4400 MHz - 5000 MHz	600	TDD
n80	1710 MHz-1785 MHz	75	N/A		SUL
n81	880 MHz-915 MHz	35	N/A		SUL
n82	832 MHz-862 MHz	30	N/A		SUL
n83	703 MHz-748 MHz	45	N/A		SUL
n84	1920 MHz-1980 MHz	60	N/A		SUL
n86	1710 MHz-1780 MHz	70	N/A		SUL

1. From "3GPP specification series: 38series". <https://www.3gpp.org/DynaReport/38-series.htm>

FR2, or the mmWave frequency range, offers an extremely wide bandwidth up to 2 GHz in some regions. Devices or systems that intend to take advantage of this wide bandwidth require antenna designs to be fundamentally different. Because signal propagation loss is inversely proportional to signal wavelength, mmWave signals suffer severe path losses. To compensate the path loss, increasing antenna Gain through designing phased-array antennas becomes a reliable solution acknowledged by the industry. Phased-array design opens an entirely new realm of antenna design not present in 4G.

**Table 2: 5G New Radio (NR) operating bands in FR2 1**

NR Operating Band	Uplink(UL) operating band		Downlink (DL) operating band		Duplex
	BS Recieve		BS transmit		Mode
	UE Transmit		UE Receive		
	F <sub>UL_low</sub> – F <sub>UL_high</sub>	total BW	F <sub>DL_low</sub> – F <sub>DL_high</sub>	total BW	
n257	26500 MHz–29500 MHz	3000	26500 MHz–29500 MHz	3000	TDD
n258	24250 MHz–27500 MHz	3260	24250 MHz–27500 MHz	3260	TDD
n260	37000 MHz–40000 MHz	3000	37000 MHz–40000 MHz	3000	TDD
n261	27500 MHz – 28350 MHz	850	27500 MHz – 28350 MHz	850	TDD

1. From "3GPP specification series: 38series". <https://www.3gpp.org/DynaReport/38-series.htm>

## Challenging Antenna System Design Due to Co-existence

MIMO functionality requires multiple antennas to co-exist on a device and operate on the same frequency bands. The technology itself has already been used in the 4G LTE network in the form of SU-MIMO and MU-MIMO (Single-user MIMO and Multiple-user MIMO).

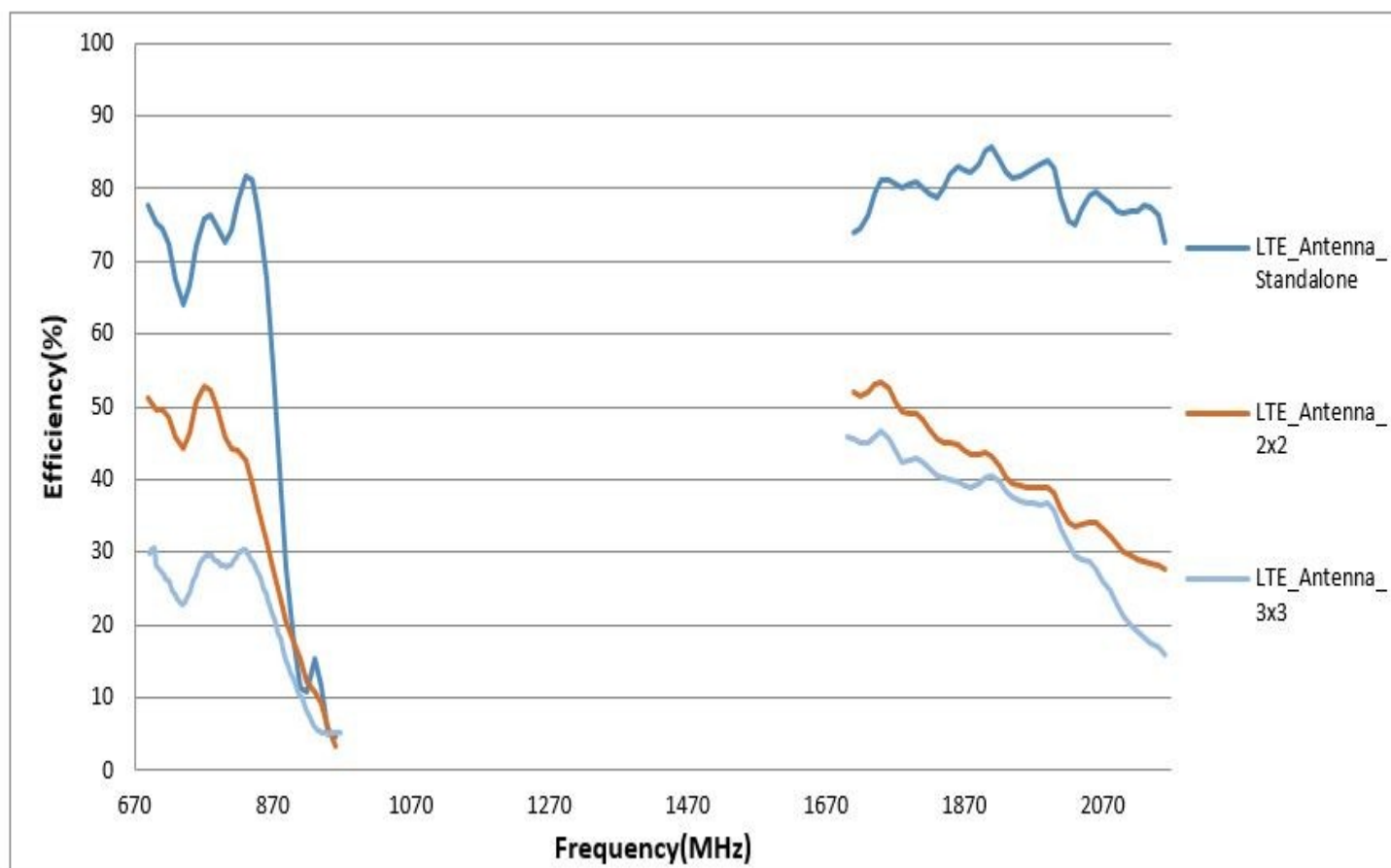
In 5G, Massive-MIMO (mMIMO) will be a necessary building block to push the cell capacity and UE downloading data rate to the next level. While most of the mMIMO antenna specifications and technology reviews nowadays focus on the base station side, where 32 or more logical antenna ports are needed, it is expected that the number of antennas on the UE is also going to increase.

Also, because of the enabling of Multiple Access technology in 5G, Bluetooth/WLAN, cellular, etc. are more often to transmit on the UE simultaneously, antenna coexistence issue can only be more complicated to solve. If not properly addressed, antenna coexistence issues can cause either communication range reduction, an unexpected blind spot, or even sporadic connectivity quality drop.

Figure 1 gives an example of antenna efficiency loss due to coexistence. Antennas must be strategically arranged in a 5G UE

to achieve the full potency of MIMO.

**Figure 1: Antenna efficiency reduction when migrating from a SISO to a MIMO system**



Design Approaches to New 5G Antenna Design Challenges  
Now that we have covered some of the challenges, let's discuss some design considerations that can help to ensure success.

## Sub-6 GHz Antenna Design Approach

5G antennas can be divided into two categories by their operating frequency: Sub-6GHz and mmWave. Comparing sub-6 GHz 5G with LTE 4G, the system RF front-end and antenna design

concepts will be very similar with the only difference being lateral complexity. This means, going from 4G to sub-6 GHz 5G, the same set of componentry will be used in the system side and the antenna will still be an omnidirectional standalone (vs. array) antenna.

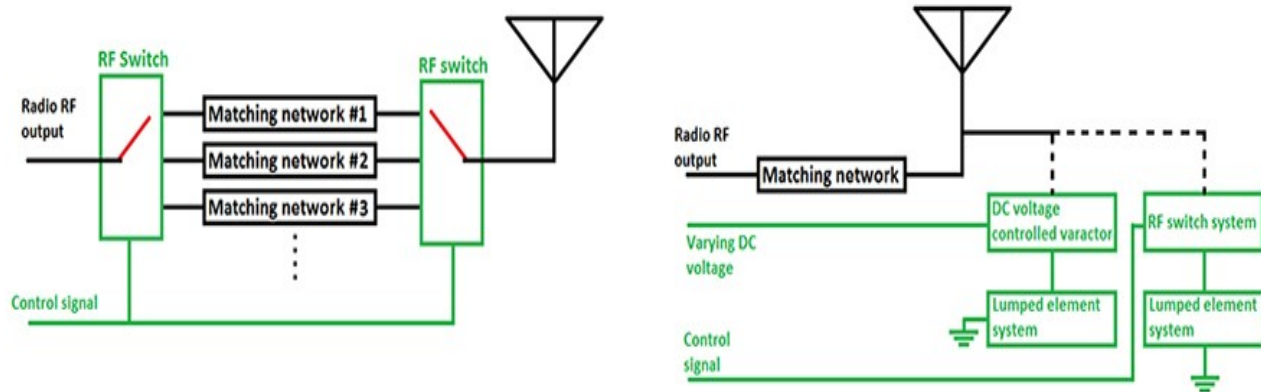
In this frequency range, common antenna types such as dipole antenna, monopole antenna, PIFA, IFA, loop antenna, etc. will still play dominating roles as they have been in 2G/3G/4G. Antenna form factors can vary from a simple printed-trace antenna to an intricate Laser Direct Structuring (LDS) antenna.

The conflict between requirements for smaller device size and larger antenna bandwidth will still be the top challenge, only much harder than before. One viable solution to this increasingly intense confrontation is to design an active antenna system.

The most commonly seen active antenna systems can be divided into two categories: active impedance matching and antenna aperture tuning. The active impedance matching technique enables the antenna system to select among different impedance-matching networks based on operating condition changes, while active aperture tuning directly changes the intrinsic characteristics of the antenna.



**Figure 2: Active matching (left) and active aperture tuning diagram (right)**



Device OEMs can also take advantages of off-the-shelf (OTS) antennas to simplify the antenna design process. However, same with 4G, the same OTS will behave differently when situated in different devices, as different PCBs provides different RF reference even if the antennas themselves are the same. At the minimum, OEMs should expect to have customized antenna matching networks for any selected OTA antennas.

## **mmWave Antenna Design Approach**

On mmWave frequencies, several signal propagation path loss greatly constraints the cell size and the bandwidth advantage can be greatly masked by connectivity coverage issues. To compensate signal path loss, phased-array antennas become necessary due to its capability of realizing very high Gain(dBi).

Designing a phased-array antenna for 5G mmWave requires significantly more upfront knowledge on fundamental antenna design concepts, array antenna design practices, mmWave signal propagation behavior, and much more. At a minimum, a phased-array antenna should be able to steer and optimize the radiation

beam to maximize the peak EIRP(dBm) towards a mobile receiving device within its cell sector. A well-designed phased-array antenna for 5G should also factor in dual polarization, minimizing array size, mitigating side lobe level, improving the beam steering angle range and resolution, suppressing system noise, improve power efficiency, and more.

mmWave antenna testing also presents engineering hurdles. Additional complexity arises with respect to calibration and setup at these high frequencies, where losses in the setup become more pronounced as compared to 4G frequencies. Conservative estimates suggest capital equipment for this testing can require investments of more than \$1 million. Choosing a testing partner who understands the specifications and procedures thus becomes critical.